COMPUTATION OF THE SPECTRA OF TURBULENT BOUNDARY LAYER SURFACE-PRESSURE FLUCTUATIONS

By

JOHN H. LINEBARGER

Bachelor of Science
United States Naval Academy
Annapolis, Maryland
1955

Master of Science
Massachusetts Institute of Technology
Cambridge, Massachusetts
1961

Submitted to the Faculty of the Graduate College
of the Oklahoma State University
in partial fulfillment of the requirements
for the Degree of
DOCTOR OF PHILOSOPHY
May, 1972

COMPUTATION OF THE SPECTRA OF TURBULENT

BOUNDARY LAYER SURFACE-PRESSURE

FLUCTUATIONS

Thesis Approved:

Ronald L. Panton

Thesis Adviser

Ladislaus J. Fila

W. B. Brooks

W. G. Tiederman, Jr.

Bennett Basore

D. Durham

Dean of the Graduate College

ACKNOWLEDGMENTS

I wish to thank the Ames Research Center of NASA for the funding under NASA Grant NGR 37-002-083 for this study. In addition, I am indebted to NASA for a traineeship furnished the first year of my work and HEW for two years of support under NDEA.

Any work, to a certain degree, is a cooperative effort. In this regard I owe particular thanks to the chairman of my committee, Dr. R. L. Panton, whose patience, insights, and encouragement made it possible for me to complete this study. To Dr. J. P. Chandler, I am indebted. Without his assistance it is doubtful that I would have been able to complete the numerical analysis necessary to achieve the major goal of this work. I am also grateful to the members of my doctoral committee for their willingness to serve in this capacity.

Thanks are also due to Mr. Darrell Haston for his drafting services, and to Mrs. E. T. Apple and Mrs. P. F. Lambert for typing the manuscript.

TABLE OF CONTENTS

LIST OF FIGURES

Figure | Page

NOMENCLATURE

Symbol	Description
A, a	constants, see context
b	constant, see context
C	a constant in the importance sampling of $\hat{r}$, computed from $C_1(\hat{y}_2)$
C_f	skin friction coefficient, $\tau_w/\frac{1}{2}\rho U_\infty^2$
C_i	a constant in the importance sampling of $\hat{y}_2$ where i = IN, MD, or OT
C_1	the non-dimensional inverse of the integral scale, δ^*/L
d	pressure transducer diameter
f(r)	longitudinal velocity correlation coefficient in isotropic turbulence
G, G_o, G_i	Green's functions
g	mean-shear, intensity product
g_o	mean value of g
i	$\sqrt{-1}$
K	Von Karman constant in mean-shear
K_i	Bessel function
k	two-dimensional wave number in k_1, k_3 plane
$\hat{k}$	$k\delta^*$
k_i	one-dimensional wave number, i = 1, 3
$\hat{k}_i$	$k_i\delta^*$
$\tilde{k}_i$	$k_i\delta$

Symbol	Description
L	integral scale of the turbulence
P	pressure
$\overline{P}$	time average of P
p	probability distribution function or fluctuating pressure as a function of x_i and t, see context
$\tilde{p}$	fluctuating pressure as a function of x_2, k_1, k_3 and t
q	dynamic pressure, $\frac{1}{2}\rho U_\infty^2$
R_{22}	experimental or isotropic velocity correlation coefficient, see context
$\hat{R}_{22}$	anisotropic velocity correlation coefficient, α = constant
$\tilde{R}_{22}$	anisotropic velocity correlation coefficient, $d = \alpha(\hat{k}_1)$
$\overset{+}{R}_{22}$	anisotropic velocity correlation coefficient with time delay, α = constant
$\check{R}_{22}$	isotropic velocity correlation coefficient with time delay
R_{pp}	two point pressure correlation coefficient
r_i	separation distance between sources points
$\check{r}_i$, $\hat{r}_i$, $\tilde{r}_i$	non-dimensional separation distance between source points, see context for non-dimensionalizing scheme
s, s'	distance between source and field points
S	area
t	time
T	non-homogeneous term in pressure equation
$\tilde{T}$	non-dimensional non-homogeneous term in pressure equation
u	dependent variable in $\hat{k}_3$ inversion equation; quasirandom number in numerical integration

Symbol	Description
v	dependent variable in $\hat{y}_2$ inversion equation; quasirandom number in numerical integration
ω	dependent variable in $\hat{y}_2$ inversion equation; quasirandom number in numerical integration
x	dependent variable in $\hat{r}$ inversion equation; quasirandom number in numerical integration
x_i, x_i'	field points, i.e. points at which measurement or calculation is being made
y_i, y_i'	source points, i.e. points in flow field contributing to calculation or measurement
$\hat{y}_2$, $\hat{y}_2'$	non-dimensional normal direction coordinate of source point
$\tilde{y}_2$	$y_2 \delta U_\tau / \nu$
z	dependent variable in $\hat{r}^2$ inversion equation; quasirandom number in numerical integration
α	anisotropy factor
β	constant in mean-shear equation
δ	Dirac delta function or boundary layer thickness, see context
$\delta *$	boundary layer displacement thickness
ζ	dummy integration variable or coordinate transformation variable, see context
θ	angle in polar coordinates
ν	kinematic viscosity, ft^2/sec
ξ_i	separation distance between field points, i.e. points at which pressure is being measured
π	3.1417
Π	constant in equation for mean-shear or non-dimensional spectrum, see context
Π_1	one-dimensional wave number spectrum
Π_2	two-dimensional wave number spectrum

Symbol	Description
$\hat{\Pi}$, $\tilde{\Pi}$	non-dimensional spectrum, see context
ρ	density
δ	standard deviation
τ	time delay
ω	frequency, radians
ω^*	non-dimensional frequency, $\omega\delta^*/U_\infty$
$\tilde{\omega}$	non-dimensional frequency, $\omega\delta/U_\infty$

CHAPTER I

INTRODUCTION

One of the inherent characteristics of a turbulent boundary layer is the presence of pressure fluctuations which extend to the surface on which the boundary layer has developed. These pressure fluctuations travel in the streamwise direction at a velocity of the order of the local mean velocity of the flow and are coherent for distances of the order of the boundary layer thickness. Sometimes they are called 'near field' noise. This 'near field' noise induces surface vibration. The flow induced vibrations can cause acoustical disturbances internal to the surface, i.e. the cabin of an aircraft, and/or structural failure. Thus, a knowledge of the pressure fluctuations at the surface is important for design purposes. In addition, the investigation of these disturbances is, as Wills (1970) stated, "important in its own right for the information it can yield on the structure of turbulence in the boundary layer."

The principle method used in studying the fluctuating components of turbulent flow is statistical in nature. Either the autocorrelation or its equivalent, the power spectral density is used. The most common experimental measurement is the single point measurement made with one pressure transducer. The signal can be processed electronically to introduce a time delay. When multiplied with the original signal, the autocorrelation results. The Fourier transform of the autocorrelation is the frequency power spectrum. A more recent method is based on the Fourier transform of experimental filtered spatial correlations (Wills, 1970).

Bies (1966) reviewed the results of wind tunnel and in-flight measurements. His composite plot of the wind tunnel data is shown in Figure 1. He concluded that there is a wide range of variation among the results of the various wind tunnel investigations even though most investigators presented self-consistent data. In one of the investigations, however, a great number of measurements were made over an extended region of the test section. These results were not self-consistent, but were within the scatter of the data of the other investigations. Flight measurements were in general agreement with wind tunnel measurements but with less scatter. When the measurements were taken in flow situations where the free stream was not uniform, the low frequency portion of the spectrum was higher. Then the spectrum approached the uniform free stream spectrum at higher frequencies.

In addition to perturbed outer flow fields, acoustical disturbances are known to contribute to the measured low frequency portion of the spectrum. Hodgson (1962) reported on a sequence of experiments designed to isolate the influence of acoustical and flow disturbances from the flow. His final experimental configuration was a microphone mounted on the upper surface of the wing of a glider. Additional glider experiments have recently been done by Panton, Lowery and Reischman (1971). The pressure transducers were installed on the fuselage of an SGS2-32 sailplane. Both of these investigations showed that the boundary layer itself contributes very little to the low frequency portion of the spectrum. Wills (1970) removed the acoustical contribution to the low frequencies from his wind tunnel measurements by calculating the contribution from correlation measurements. His findings led him to speculate that the entire contribution to the Fourier transform of the longitudinal space-time covariance below 100 Hz is acoustical. He summarized the situation when he stated that the low frequency portion of the spectrum is quite dependent on "the conditions of the experiment and not necessarily on the boundary layer itself."

At high frequencies the finite size of the transducer is a problem. It causes the measured spectrum to be underestimated. Corrections have been proposed with limited success. Perhaps the best indication of the qualitative behavior of the spectrum at high frequencies is the data taken by Hodgson in 1967 and reported by Wills (1970). Just beyond the frequency at which the spectrum peaks, the decay rate is approximately $\hat{\omega}^{-.8}$. As at frequency just a bit higher than $\hat{\omega} = 10.0$, the decay rate increases dramatically. These are the frequencies which typify the scale of the disturbances in the viscous sublayer.

Kraichnan (1956b) laid the foundation for the mathematical computation of the wall-pressure fluctuations. He used the Fourier transform method of solving the differential equation and assumed a 'mirrow flow' model of the turbulence field. He computed a family of relative wave number spectra which varied with a one-parameter model of the mean-shear gradient. Hodgson (1962) followed this procedure using an average mean-shear and computed the frequency spectrum which is shown in Figure 2. Lilley and Hodgson (1960) and

Hodgson (1962) solved the differential equation using a Green's function. Hodgson, after making a number of simplifying assumptions, computed the frequency spectrum which also is shown in Figure 2.

The level of the predicted spectra in Figure 2 must be set in some arbitrary manner because of the assumptions in each method. In both cases the isotropic form of the velocity correlation coefficient R_{22} has been used. An anisotropy model was introduced by Kraichnan (1956a), but he predicted the mean-square pressure and not the frequency spectrum. An obvious deficiency in the predicted spectra is the rapid decay at high frequencies which Hodgson (1962) attributed to a deficiency in the assumed form of R_{22}.

Because of the assumptions in each of these predictive methods, the level of the spectrum must be set in some arbitrary manner. In both cases the turbulence has been assumed isotropic. The predicted spectra decay too rapidly at high frequencies. Kraichnan (1956a) also used an anisotropy model for which he determined the mean-square pressure.

Approach and Scope of This Study

Two contributions to the calculations of pressure spectra are made in this work. First, the analysis of Hodgson is reworked to include an isotropy of the integral turbulence scales. The closed form nature of the solution is preserved and the results are presented as a one-parameter (anisotropy factor) family of curves.

The second contribution is a more complete and accurate calculation of the wave number spectra. The wave number equation for the wall-pressure fluctuations is solved with a Monte Carlo numerical integration scheme. This allows the integrand to be modeled with empirical data. The mean-shear gradient, the turbulence intensity, and certain anisotropic characteristics of the flow are allowed to vary across the boundary layer. With this technique a one-parameter family of wave number spectra is computed, Figure 15. Kraichnan's scale anisotropy model is used and the magnitude of the parameter, α, is allowed to be a function of the streamwise wave number $\tilde{k}_1$. Using α $(\tilde{k}_1)$, a wave number spectrum is constructed, Figure 16. Then Taylor's hypothesis is applied to the result to predict the frequency power spectrum, Figure 17.

CHAPTER II

GENERAL MATHEMATICAL FORMULATION AND PREVIOUS WORK

In this chapter the problem is posed and general methods for mathematical solution discussed. The two different methods of solution are a Green's function solution by Lilley and Hodgson (1960) and Hodgson (1962) and a Fourier transform solution proposed by Kraichnan (1956b). The general formulations reviewed here are background for the work presented in later chapters.

The Problem

The problem concerns the pressure fluctuations produced by a turbulent boundary layer on the surface of an infinite flat plate. The flow is assumed incompressible and without a pressure gradient. The governing equations are the continuity equation,

$$\frac{\partial U_j}{\partial x_j} = 0 \tag{2-1}$$

and the momentum equation,

$$\frac{\partial U_j}{\partial t} + \frac{\partial}{\partial x_k}(U_j U_k) = -\frac{1}{\rho}\frac{\partial P}{\partial x_j} + \nu\frac{\partial^2 U_j}{\partial x_k \partial x_k} \tag{2-2}$$

An equation for the pressure is derived by taking the divergence of equation (2-2) and using equation (2-1).

$$\frac{\partial^2 P(x_i,t)}{\partial x_j \partial x_j} = -\rho \frac{\partial^2}{\partial x_j \partial x_k} U_j(x_i,t) U_k(x_i,t) \tag{2-3}$$

If the right hand side is known, this is a linear non-homogeneous equation called 'Poisson's equation'. Next, the mean flow is considered parallel and two-dimensional while the fluctuating components are unrestricted.

$$\begin{aligned} U_1(x_i,t) &= \overline{U}_1(x_2) + u_1(x_i,t) \\ U_2(x_i,t) &= u_2(x_i,t) \\ U_3(x_i,t) &= u_3(x_i,t) \\ P(x_i,t) &= \overline{P}(x_i,t) + p(x_i,t) \end{aligned} \tag{2-4}$$

The subscript '1' stands for the streamwise direction, '2' stands for the direction normal to the plate, and '3' stands for the spanwise direction. Substituting equations (2-4) into equation (2-3) and subtracting the time-average of equation (2-3) yields an equation for the fluctuating pressure.

$$\frac{\partial^2 p}{\partial x_j \partial x_j} = -2\rho \frac{d\overline{U}_1}{d x_2} \frac{\partial u_2}{\partial x_1} - \rho \frac{\partial^2}{\partial x_j x_k}(u_j u_k - \overline{u_j u_k}) \tag{2-5}$$

The first term on the right hand side of equation (2-5) is called the linear source term or the 'mean-shear:turbulence' term (M-T term). The second is called the 'turbulence:turbulence' term (T-T term) and is actually the sum of a number of terms. Both Kraichnan (1956b) and Hodgson (1962) estimated the relative magnitude of these terms. For uniform shear in a homogeneous turbulence field, Kraichnan calculated that $\overline{p}^2_{T-T}/\overline{p}^2_{M-T} \simeq 1.5\%$. Hodgson computed the power spectral density contribution of the T-T term using Kraichnan's 'mirror-flow' turbulence model and the assumption that the turbulence intensity has Gaussian distribution. He found that $\overline{p}^2_{T-T}/\overline{p}^2_{M-T} \simeq 4.0\%$ and that the contribution of the T-T term to the power spectral density was negligible over the important frequency range. For these reasons and for mathematical simplicity, the T-T term is neglected leaving

$$\frac{\partial^2 p(x_i,t)}{\partial x_j \partial x_j} = -2\rho \frac{d\overline{U}_1}{d x_2}(x_2)\frac{\partial u_2}{\partial x_1}(x_i,t) = -T(x_i,t) \qquad (2\text{-}6)$$

This is the basic equation to be solved. It's worth noting that the solution of equation (2-6) represents the contribution of the M-T term to the fluctuation pressure, and because the problem is linear the T-T contribution could, in principle, be added later.

The boundary conditions are that the derivative of the pressure fluctuations in the normal direction vanish at the plate and that the fluctuations die out far from the plate. The first boundary condition is approximate. It has been substantiated by order of magnitude arguments due to Townsend (1956).

Green's Function Solution

Equation (2-6) can be solved by using the appropriate Green's function considering the boundary conditions. This solution is given in detail in Appendix A. The resulting equation for the fluctuating pressure at a point on the plate is

$$p(x_1,0,x_3,t) = \frac{\rho}{\pi}\int_V \left[\frac{d\overline{U}_1(y_2)}{dy_2}\frac{\partial u_2(y_i,t)}{\partial y_1}\Big/ s(x_i,y_i)\right] dV(y_i) \tag{2-7}$$

where $dV(y_i)$ is a volume element at y_i and $s(x_i,y_i)$ is the distance from x_i to y_i. The integration extends over all space above the plate.

The pressure covariance between two points on the plate, x_i and x_i' with $x_2 = x_2' = 0$, is

$$R_{pp}(x_i,x_i',\tau) = \overline{p(x_1,0,x_3,t)\,p(x_1',0,x_3',t+\tau)} \tag{2-8}$$

Then,

$$R_{pp}(x_i,x_i',\tau) = \frac{\rho^2}{\pi^2}\int_V\int_{V'} \frac{\langle u_2(y_2)\rangle\langle u_2(y_2')\rangle}{s(x_i,y_i)\,s'(x_i',y_i')}\frac{d\overline{U}_1(y_i)}{dy_2}\frac{d\overline{U}_1(y_i')}{dy_2'}\frac{\partial^2 R_{22}}{\partial y_1\,\partial y_1'}(y_i,y_i',\tau)\,dV'(y_i')\,dV(y_i)$$

(2-9)

where $$R_{22}(y_i,y_i',\tau) = \frac{\overline{u_2(y_i,t)\,u_2(y_i',t+\tau)}}{\langle u_2(y_2)\rangle\langle u_2(y_2')\rangle}, \tag{2-10}$$

$$\langle u_2(y_2)\rangle = \left[\overline{u_2^2(y_2)}\right]^{1/2}$$

Equation (2-9) is simplified by noting that R_{22} and its derivatives vanish at infinity in the y_2 direction and by assuming that the flow is homogeneous in planes parallel to the plate. The last assumption is justified as follows. Both R_{pp} and R_{22} are known to approach zero in a distance of the order of a few boundary layer thicknesses. Over this distance the boundary layer growth is very small, especially when the pressure gradient is zero. This assumption, however, will be least applicable to the large-scale disturbances in the flow. The homogeneity assumption allows R_{pp} to be a function of $\xi_i = x_i - x_i'$ in lieu of x_i and x_i'.

The mathematical details of the simplification of equation (2-9) are in Appendix B. The result is the two-point pressure correlation,

$$R_{pp}(\xi_1,0,\xi_3,\tau) = \frac{2\rho^2}{\pi}\frac{\partial}{\partial\xi_1}\int_0^{\infty}\int_{-\infty}^{\infty}\int_{-y_2}^{\infty}\int_{-\infty}^{\infty}\frac{\langle u_2(y_2)\rangle\langle u_2(y_2,r_2)\rangle\frac{d\overline{U}_1}{dy_2}(y_2)\frac{d\overline{U}_1}{dr_2}(y_2,r_2)\,R_{22}(y_2,r_i,\tau)(\xi_1-r_1)\,dr_3\,dr_2\,dr_1\,dy_2}{\sqrt{(2y_2+r_2)^2+(\xi_1-r_1)^2+(\xi_3-r_3)^2}\left[2y_2+r_2+\sqrt{(2y_2+r_2)^2+(\xi_1-r_1)^2+(\xi_3-r_3)^2}\right]} \qquad (2\text{-}11)$$

The autocorrelation is obtained from equation (2-11) by differentiating with respect to ξ_1 and letting $\xi_1 = \xi_3 = 0$. The frequency power spectrum is the Fourier transform of the autocorrelation.

$$\Pi(\omega) = \frac{1}{2\pi}\int_{-\infty}^{\infty} R_{pp}(0,0,0,\tau)\exp(-i\omega\tau)\,d\tau \qquad (2\text{-}11a)$$

Equation (2-11) is the key in Hodgson's formulation. Because of its importance, consider the terms in the integrand. There are four: the mean-shear distribution, $d\overline{U}_1/dy_2$, the turbulence intensity distribution, $\langle u_2' \rangle$, the velocity correlation coefficient, R_{22}, and a weighting term which depends on the geometry of the positions on the plate and in the flow. Of the four terms, the correlation coefficient, R_{22} is the most difficult to determine because of the paucity of experimental information of turbulent flows. The mean-shear distribution and the turbulence intensity distribution are known empirically except for the viscous sublayer region.

Hodgson (1962) continued to solve for the frequency power spectrum from equation (2-11). He used isotropic turbulence and average values of mean-shear and intensity. The details of this work are a special case of an anisotropic model which will be given in Chapter III.

Fourier Transform Solution

Another method of solving equation (2-6) uses the Fourier transform. By doubly transforming the equation with respect to two space variables, an ordinary differential equation evolves for which the solution is known. A more rigorous approach follows the same methodology but uses the Fourier-Stieltjes integrals (Lilley, 1960 or Hodgson, 1962).

The double Fourier transform of equation (2-6) with respect to x_1 and x_3 is

$$\frac{d^2\tilde{\beta}}{dx_2^2}(x_2,k_1,k_3,t) - k^2\tilde{\beta}(x_2,k_1,k_3,t) = -\tilde{T}(x_2,k_1,k_3,t) \qquad (2\text{-}12)$$

where

$$k^2 = k_1^2 + k_3^2 \;, \qquad (2\text{-}13)$$

$$\tilde{p}(x_2,k_1,k_3,t) = \frac{1}{4\pi^2}\int_{-\infty}^{\infty}\int_{-\infty}^{\infty} p(x_1,x_2,x_3,t)\, exp[-i(k_1x_1 + k_3x_3)]dx_1dx_3 \qquad (2\text{-}14)$$

and

$$\tilde{T}(x_2,k_1,k_3,t) = \frac{1}{4\pi^2}\int_{-\infty}^{\infty}\int_{-\infty}^{\infty} T(x_1,x_2,x_3,t)\, exp[-i(k_1x_1 + k_3x_3)]dx_1dx_3 \qquad (2\text{-}15)$$

Equation (2-12) is a linear inhomogeneous ordinary differential equation with constant coefficients. Its general solution is

$$\tilde{p}(x_2,k_1,k_3,t) = A\,exp(kx_2) + B\,exp(-kx_2) + \frac{1}{2}k^{-1}\int_{-\infty}^{\infty} exp(-k|y_2-x_2|)\tilde{T}(y_2,k_1,k_3,t)dy_2 \qquad (2\text{-}16)$$

After applying the boundary conditions,

$$\begin{aligned}\tilde{p}(x_2,k_1,k_3,t) = \frac{1}{2}k^{-1}\int_0^{\infty} exp(-k|y_2-x_2|)\,\tilde{T}(y_2,k_1,k_3,t)\,dy_2 \; + \cdots \\ \cdots \frac{1}{2}k^{-1}exp(-kx_2)\int_0^{\infty} exp(-ky_2)\tilde{T}(y_2,k_1,k_3,t)dy_2\end{aligned} \qquad (2\text{-}17)$$

On the plate $x_2 = 0$, so the surface-pressure transform is

$$\tilde{p}(0,k_1,k_3,t) = k^{-1}\int_0^{\infty} exp(-ky_2)\,\tilde{T}(y_2,k_1,k_3,t)\,dy_2 \qquad (2\text{-}18)$$

The two-dimensional wave number spectrum function is found by multiplying equation (2-18) by its complex conjugate and taking the time average with zero time delay.

$$\Pi_2(0,k_1,k_3) = \overline{\tilde{p}(0,k_1,k_3,t)\,\tilde{p}^*(0,k_1,k_3,t)}$$

$$\Pi_2'(0,k_1,k_3) = \frac{4\rho^2 k_1^2}{k^2}\int_0^\infty\int_0^\infty \exp[-k(y_2+y_2')]\frac{d\bar{U}_1(y_2)}{dy_2}\frac{dU_1(y_2')}{dy_2'}\Phi_{22}(y_2,y_2',k_1,k_3)\,dy_2'\,dy_2 \tag{2-19}$$

Φ_{22} is the two-dimensional wave number spectrum function of u_2 velocity.

Equation (2-11) and Hodgson's equation (2-19) are quite similar in that essentially the same assumptions have been made in their derivations. Equation (2-11) has the advantage of giving two-point correlation information. Equation (2-19) has the advantage of producing power spectrum information as a function of the size of the disturbances, i.e. wave number.

The one-dimensional wave number power spectrum is obtained from π_2 by integrating the k_3 dependence.

$$\Pi_1'(k_1) = \int_{-\infty}^{\infty} \Pi_2'(0,k_1,k_3)\,dk_3 \tag{2-20}$$

Then the frequency power spectrum may be obtained by substituting for k_1

$$\omega = k_1 U_c \tag{2-21}$$

Equation (2-21) is Taylor's hypothesis which means that all of the time dependence in the flow arises by convection of a relatively slow changing spatial pattern. It is possible in this formulation to let U_c be a function of wave number.

Equations (2-19) and (2-20) are the key equations in the Fourier transform formulation. Essentially the same physical information is needed to solve these equations as is required in the Green's function approach. In this regard, note that Φ_{22} is the two-dimensional Fourier transform of R_{22} .

Previous Fourier Transform Solutions

Kraichnan (1956b) represented the turbulence field by a 'mirror-flow' model. The details concerning this model are found in Appendix C. Essentially, this model represents the turbulence field by mirroring two homogeneous fields in the wall. If $\overline{\overline{\Phi}}_{22}$ is the two-dimensional wave number spectrum function of a homogeneous flow field, then

$$\overline{\Phi}_{22}(y_2, y_2', k_1, k_3) = \overline{\overline{\Phi}}_{22}(y_2 - y_2', k_1, k_3) - \overline{\overline{\Phi}}_{22}(y_2 + y_2', k_1, k_3) \quad (2\text{-}22)$$

The negative features of this model are that u_1 and u_3 do not vanish at the plate and that the intensity of the turbulence is finite at infinity. Kraichnan contends that the model is viable in that the viscous sublayer makes little contribution to the surface-pressure field and that the finite intensity at infinity is not unreasonable considering experimental results. It can also be argued that the indefinite extent of the intensity should not seriously affect the answer as the mean-shear term goes to zero in the far field.

Kraichnan (1956b) computed a family of relative wave number power spectra for various mean-shear profiles. He called $k^2 = k_1^2 + k_3^2$ the relative wave number and so the convective assumption $\omega = k_1 U_c$ cannot directly be applied. Later Hodgson

(1962) calculated a frequency spectrum with the mirror flow model. He used equations (2-19) and (2-20) to predict the frequency power spectrum. Following Kraichnan, he modeled the mean-shear gradient by

$$\frac{d\overline{U}_1(y_2)}{dy_2} = \frac{d\overline{U}_1(0)}{dy_2} \exp(-\beta y_2) \tag{2-23}$$

This, along with equation (2-22), is substituted into equation (2-19).

$$\Pi_2(0,k_1,k_3) = \frac{4\rho^2 k_1^2 [d\overline{U}_1(0)/dy_2]^2}{k^2} \int_0^\infty \left[\frac{1}{k+\beta} - y_2\right] \exp[-(k+\beta)y_2]\, \Phi_{22}(y_2,k_1,k_3)\, dy_2 \tag{2-24}$$

The interim mathematical steps between equations (2-21) and (2-24) are reviewed in Appendix D. $\Phi_{22}(y_2, k_1, k_3)$ must be an even function of y_2. Next let

$$\frac{d\overline{U}_1(0)}{dy_2} = 3.7\, U_r/\delta^* , \qquad \beta = 0.31/\delta^* \tag{2-25}$$

and assume that the turbulence field is isotropic. This assumption will be considered in more detail in Chapter III. It allows $\Phi_{22}(y_2, k_1, k_3)$ to be represented analytically with the following relationships:

$$\Phi_{22}(y_2,k_1,k_3) = \int_{-\infty}^{\infty} \Phi_{22}^*(k_1,k_2,k_3) \exp(iy_2k_2)\, dk_2 , \tag{2-26}$$

$$\Phi^{*}_{22}(k_i) = \mathcal{S}^2 E(\mathcal{S})/4\pi \qquad (2\text{-}27)$$

where $\mathcal{S}^2 = k_1^2 + k_2^2 + k_3^2$

and $$E(\mathcal{S}) = \frac{1}{\pi}\int_0^\infty \overline{u_2^2}\, f(r)\, \mathcal{S}^2 r^2 [\sin(\mathcal{S}r)/\mathcal{S}r - \cos(\mathcal{S}r)]\,dr \qquad (2\text{-}28)$$

where $f(r) = \exp(-r/L)$.

In principle, substituting equations (2-25), and (2-27) into equation (2-24) determines the two-dimensional wave number power spectrum, $\pi_2\ (0, k_1, k_3)$. Then the frequency spectrum is computed with the aid of equations (2-20) and (2-21). Hodgson used $L = 1.5\delta^*$ and $U_c(k_1) = .8U_\infty$ for this computation.

Hodgson is very vague about the details of this calculation and at what stage numerical estimates were made. His result, the frequency power spectrum, is shown in Figure 2. This figure has been reproduced from Hodgson (1962). It is important to note that the dependent variable has been normalized with τ_w^2 and that Hodgson fixed the level of the theoretical curves by using his experimental value of $\sqrt{\overline{p^2}}/q^2$ as $2.2C_f$.

Lilley and Hodgson (1960) also compared their simplified isotropic calculation of the relative wave number spectrum with Kraichnan's 'mirror flow' model simplified in the same manner. They concluded that no substantial differences existed. Also, in the same paper they made an estimate for the 'big-eddie' contribution.

This used a scale anisotropy model similar to Townsend and Grant. Their estimating expression lead them to conclude that the 'big eddie' contributions would be sensitive to the different integral scales.

CHAPTER III

ANISOTROPIC GREEN'S FUNCTION SOLUTION

The method of Hodgson (1962) and Lilley and Hodgson (1960) for determining the power spectrum is modified to include anisotropy. The anisotropy model assumes the integral scale of the turbulence is largest in the streamwise direction. A family of frequency spectra is derived showing the effect of various degrees of anisotropy.

Simplified Frequency Spectrum Problem

The method of obtaining the frequency spectrum from the correlation equation, (2-11), is to perform the ξ_2 differentiation and then let ξ_1 and ξ_3 go to zero. The resulting autocorrelation can be Fourier transformed giving the frequency spectrum. Hodgson simplified the integrand to the point that analytic integration was possible. The simplifications neglect variations of quantities across the boundary layer. His hope was that the computed spectrum would be qualitatively correct.

The first step is to remove the y_2 dependence from all the terms in the integrand except the weighting function. Therefore, let

$$g(y_2) = \frac{d\overline{U}_1}{dy_2}(y_2)\langle u_2(y_2)\rangle \tag{3-1}$$

and take g_o as a mean value. Then remove the y_2 dependence from R_{22} which means that the flow is assumed homogeneous in the normal direction. The correlation equation, (2-11), reduces to

$$R_{pp}(\xi_1, 0, \xi_3, \tau) = \frac{2\rho^2 g_o^2}{\pi^2} \frac{\partial}{\partial \xi_1} \int_0^\infty \int_{-\infty}^\infty \int_{-y_2}^\infty \int_{-\infty}^\infty \frac{R_{22}(r_i, \tau)(\xi_1 - r_1)\, dr_3\, dr_2\, dr_1\, dy_2}{\sqrt{(2y_2+r_2)^2+(\xi_1-r_1)^2+(\xi_3-r_3)^2}\left[2y_2+r_2+\sqrt{(2y_2+r_2)^2+(\xi_1-r_1)^2+(\xi_3-r_3)^2}\right]} \tag{3-2}$$

By rearranging the limits in equation (3-2), it can be integrated with respect to y_2. Then it is necessary to take an average value of the integrand with respect to r_2 prior to differentiating with respect to ξ_1. Taking ξ_1 and ξ_3 as zero gives the autocorrelation of the pressure fluctuations at a point on the plate. The details are found in Appendix E.

$$R_{pp}(\tau) = \frac{\rho^2 g_o^2}{\pi} \int_{-\infty}^\infty \int_0^\infty \int_{-\infty}^\infty \left(\frac{r_2^2 + r_3^2}{r^3}\right) \check{R}_{22}(r_i, \tau)\, dr_3\, dr_2\, dr_1 \tag{3-3}$$

R_{22} must be even in r_2.

In order to obtain an analytical expression for R_{22}, assume that the turbulence is isotropic. An isotropic field is one in which the turbulence is invariant with respect to coordinate system rotations and reflections. This assumption is considered good on a 'local' basis for the fine-scale turbulence structure and a first approximation to the large-scale turbulence structure (Hinze, 1959). The form of the isotropic velocity correlation coefficient with zero time delay is

$$\check{R}_{22}(r_i, 0) = f(r) + \left(\frac{r_1^2 + r_3^2}{2r}\right)\frac{df(r)}{dr} \tag{3-4}$$

where $r^2 = r_1^2 + r_2^2 + r_3^2$.

Equation (3-4) must be modified to include a time delay and also an explicit relationship for f(r). Hodgson assumed that

$$f(r) = exp(-r^2/L^2) \tag{3-5}$$

where L is defined as $\int_0^\infty f(r)\,dr$, the integral scale of the turbulence. The time delay is introduced by Taylor's hypothesis. The velocity correlation in a moving reference frame is separated into the product of a spatially dependent term and a time dependent term. By assuming the flow is 'frozen', i.e. Taylor's hypothesis, the correlation is transformed into a fixed reference frame (see Appendix F).

$$\check{R}_{22}(r_i, \tau) = exp[-(r_2^2 + r_3^2)/L^2]exp[-(r_1 - U_c\tau)^2/L^2][1 - r_3^2/L^2 - (r_1 - U_c\tau)^2/L^2] \tag{3-6}$$

The convective velocity U_c is assumed a constant.

Equation (3-6) is substituted into equation (3-3) and then non-dimensionalized according to

$$\check{r}_i = r_i/L, \quad \check{\tau} = U_c\tau/L \tag{3-7}$$

Noting that the integrand is even in r_3, the autocorrelation is

$$R_{pp}(\tau) = \frac{2\rho^2 q_0^2 L^2}{\pi} \int_{-\infty}^{\infty}\int_{0}^{\infty}\int_{-\infty}^{\infty} \left[\frac{\check{r}_2^2 + \check{r}_3^2}{\check{r}^3}\right]\left[1 - \check{r}_3^2 - (\check{r}_1 - \check{\tau})^2\right] \exp\left[-\check{r}_2^2 - \check{r}_3^2 - (\check{r}_1 - \check{\tau})^2\right] d\check{r}_3\, d\check{r}_2\, d\check{r}_1 \tag{3-8}$$

The Fourier transform of equation (3-8) is the frequency power spectrum

$$\Pi(\check{\omega}) = \frac{1}{2\pi}\frac{L}{U_c}\int_{-\infty}^{\infty} R_{pp}(\tau) \exp(-i\check{\omega}\check{\tau})\, d\check{\tau} \tag{3-9}$$

where $\check{\omega} = \omega L/U_c$. Performing the substitution and expanding as in Appendix E yields

$$\Pi(\check{\omega}) = \frac{2\rho^2 q_0^2 L^3}{\pi^2 U_c}\int_0^{\infty} \exp(-\check{\tau}^2)\cos(\check{\omega}\check{\tau})\, d\check{\tau} \int_0^{\infty}\int_0^{\infty}\int_0^{\infty} \left[\frac{\check{r}_2^2 + \check{r}_3^2}{\check{r}^3}\right]\left[(1 - \check{r}_2^2 - \check{r}_1^2 - \check{\tau}^2)\cosh(2\check{r}_1\check{\tau}) + \ldots \right.$$

$$\left. \ldots\, 2\check{r}_1\check{\tau}\sinh(2\check{r}_1\check{\tau})\right]\exp(-\check{r}^2)\, d\check{r}_3\, d\check{r}_2\, d\check{r}_1 \tag{3-10}$$

Equation (3-10) is for isotropic turbulence and was integrated by Hodgson (1962). It is a special case of the anisotropic case which will be introduced next.

Scale Anisotropy

The 'eddy' model of turbulent flow envisages regions in the boundary layer of various scales within which the properties such as velocity and pressure are correlated. The larger the scale of the 'eddy', the greater the region of correlation. The larger eddies are the size of the boundary layer and are greatly influenced by both the wall and the free stream. Experimental evidence shows that the large-scale structure is more anisotropic in nature than the small-scale structure. It is generally accepted that this large-scale structure is the major contributor to the lower frequencies in the spectrum. Thus, the anticipated change with an anisotropic model would be to improve the prediction at the lower frequencies.

Kraichnan (1956a) proposed a simple scale anisotropy model of the velocity correlations. This is motivated by the difference in the integrals scales as seen in Figure 3. This data, taken from Grant (1958), shows the integral scale to be larger in the streamwise direction than in the other directions. The analytical form of the isotropic velocity correlation component is

$$R_{ii}(r_i) = f(r_i) \; ; \; i = 1,2, \text{ or } 3 \; ; \text{ no sum on } i. \qquad (3\text{-}11)$$

If the turbulence were isotropic, all of the data points of Figure 3 would collapse and lie along a single curve.

The elongation of the integral scale in the streamwise direction was modeled by letting R_{22} have the isotropic form in stretched coordinates, r_i'.

$$\begin{aligned} r_1' &= r_1/\alpha \\ r_2' &= r_2 \\ r_3' &= r_3 \end{aligned} \qquad (3\text{-}12)$$

In equations (3-12) $\alpha \geq 1.0$. Kraichnan demonstrated that the new correlation coefficient $R_{jk}'(r_i')$ satisfies the continuity equation.

Power Spectrum Equation

The effect of the anisotropy model on the power spectrum is elevated by substituting equation (3-12) into (3-6).

$$\overset{+}{R}_{22}(\check{r}_i,\check{\tau};\alpha) = \exp[-(\check{r}_2^2+\check{r}_3^2)/L^2]\exp[-(\check{r}_1-U_c\check{\tau})^2/\alpha^2L^2][1-\check{r}_3^2/L^2-(\check{r}_1-U_c\check{\tau})^2/\alpha^2L^2] \tag{3-13}$$

When equation (3-13) is processed through equations (3-7), (3-8), and (3-9), the equivalent of equation (3-10) is the frequency power spectrum equation,

$$\check{\Pi}(\check{\omega};\alpha) = \frac{2\rho_\infty^2 q_0^2 L^3}{\pi^2 U_c}\int_0^\infty\int_0^\infty\int_0^\infty\left[\frac{\check{r}_2^2+\check{r}_3^2}{\check{r}^3}\right]\exp(-\check{r}_1^2/\alpha^2)\exp[-(\check{r}_2^2+\check{r}_3^2)]\,d\check{r}_3\,d\check{r}_2\,d\check{r}_1 \cdots$$

$$\cdots\int_0^\infty \exp(-\check{\tau}^2/\alpha^2)\cos(\check{\omega}\check{\tau})\{[1-\check{r}_3^2-\check{r}_1^2/\alpha^2-\check{\tau}^2/\alpha^2]\cosh(2\check{r}_1\check{\tau}/\alpha)+\cdots \tag{3-14}$$

$$\cdots(2\check{r}_1\check{\tau}/\alpha)\sinh(2\check{r}_1\check{\tau}/\alpha^2)\}\,d\check{\tau}$$

Integration of this equation follows the procedure outlined by Lilley and Hodgson (1960). The details of this work are found in Appendix H. The final result is a closed form solution.

$$\check{\Pi}(\check{\omega};\alpha) = \frac{\rho^2 L^3 q_0^2 \alpha}{4\pi^{1/2} U_c}\left\{\frac{\check{\omega}^2}{4}\left[\frac{\check{\omega}^2}{4}-\frac{\check{\omega}^2}{2\alpha^2}+\frac{1}{\alpha^4}\right]E_1(\check{\omega}^2/4)+\cdots\right.$$

$$\left.\cdots\exp(-\check{\omega}^2/4)\left[\frac{\check{\omega}^2}{4}(2/\alpha^2-1)+1-1/\alpha^4\right]\right\} \tag{3-15}$$

where E_1 is the exponential integral,

It is common to plot the spectrum as a function of ω^*, defined as

$$\omega^* = \omega\,\delta^*/U_\infty \tag{3-16}$$

The following constants are defined:

$$C_1 = \delta^*/L, \qquad (3\text{-}17)$$

$$C_2 = U_c/U_\infty\,, \qquad (3\text{-}18)$$

$$C_3 = (\delta^*/L)(U_c/U_\infty)\,. \qquad (3\text{-}19)$$

Also the independent variable is normalized so that

$$\hat{\pi} = \frac{\check{\pi}}{\rho^2 L^3 g_0^2 / 4\pi^{1/2}\, U_c} \qquad (3\text{-}20)$$

The final equation is

$$\hat{\pi}(\omega^*;\alpha) = \alpha\left\{\left(\frac{\omega^*}{2C_3}\right)^2\left[\left(\frac{\omega^*}{2C_3}\right)^2 - \frac{1}{2}\left(\frac{\omega^*}{C_3\alpha}\right)^2 + \frac{1}{\alpha^4}\right]E_1\left[\left(\frac{\omega^*}{2C_3}\right)^2\right] + \cdots\cdots\right.$$
$$\left.\cdots \exp\left[-\left(\frac{\omega^*}{2C_3}\right)^2\right]\left[\left(\frac{\omega^*}{2C_3}\right)^2\left(2/\alpha^2 - 1\right) + 1 - 1/\alpha^2\right]\right. \qquad (3\text{-}21)$$

Figure 4 is a plot of equation (3-21) for various values of alpha. The value of C_3 as defined in equation (3-19) and used to compute these curves is 1.0. Except for the difference in normalizing and the value of C_3 , the $\alpha = 1$ curve of Figure 4 and Hodgson's (or Lilley and Hodgson (1960)) Green's function solution of Figure 2 are equivalent.

The curves are very sensitive to small changes in alpha with the larger values of alpha increasing the spectrum at the lower frequencies. Now the zero frequency value $\hat{\pi}(0;\alpha)$ is the mean-square value of the fluctuating pressure p', which is, of course, 0. Equation (3-21) gives $\hat{\pi}(0;\alpha) = 1-1/\alpha^2$. The reason for this anomaly is not known.

CHAPTER IV

FORMULATION OF THE ONE-DIMENSIONAL WAVE NUMBER PROBLEM

In this chapter the one-dimensional wave number equation to be numerically integrated is developed. The calculation incorporates realistic variations across the boundary layer of the mean-shear, turbulence scale, and turbulence intensity. The anisotropic turbulence model of Chapter III is also retained.

When deciding which of the two methods, the Fourier transform method or the Green's function method, to integrate numerically, the inherent singularity in the Green's function solution makes it the least likely candidate. Essentially the same assumptions have been made in the developments of each method. However, there is one difference which proves to be important. The Fourier transform method is expressed in the wave number domain. This allows the anisotropy factor and the convective velocity to be considered as functions of the wave number and assumed after the integration is completed.

The Non-Dimensional Equation

It is desired to non-dimensionalize the problem so that the answer is as independent of Reynolds number as possible. Starting point for the procedure is $\pi_1(k_1)$, the one-dimensional wave number spectrum of the wall-pressure fluctuations.

$$\Pi_1'(k_1) = 4\rho^2 \int_{-\infty}^{\infty}\int_0^{\infty}\int_0^{\infty} \frac{k_1^2}{k^2} \exp[-k(y_2+y_2')] \frac{d\overline{U}_1}{dy_2} \frac{d\overline{U}_1}{dy_2'} \Phi_{22}\, dy_2'\, dy_2\, dk_3 \tag{4-1}$$

This is the integration over k_3 of the two-dimensional spectrum given in equation (2-19).

In equation (4-1), Φ_{22} is the Fourier transform of the velocity correlation function.

$$\Phi_{22}(y_2, y_2', k_1, k_3) = \frac{u_2(y_2)\, u_2(y_2')}{4\pi^2} \int_{-\infty}^{\infty}\int_{-\infty}^{\infty} R_{22}(y_2, y_2', r_1, r_3) \exp(-ik_1 r_1) \exp(-ik_3 r_3)\, dr_3\, dr_1 \tag{4-2}$$

where $u_2 = \sqrt{\overline{u_2^2}(y_2)}$ and $u_2' = \sqrt{\overline{u_2^2}(y_2')}$. It will include the effect of anisotropic structure. Philosophically, it is important to note that it is Φ_{22} and not R_{22} which is assumed. An expression for R_{22} will be integrated and the result motivates an assumption for Φ_{22} . This procedure is masked because, for computational purposes, equation (4-2) is substituted into equation (4-1).

The correlation coefficient R_{22} is an even function of r_1 and r_3 . Substituting equation (4-2) into equation (4-1) and noting that the result is even in k_1 yields

$$\Pi_1'(k_1) = \frac{8\rho^2}{\pi^2} \int_0^{\infty}\int_0^{\infty}\int_0^{\infty}\int_0^{\infty}\int_0^{\infty} \frac{k_1^2}{k^2} \exp[-k(y_2+y_2')] \frac{d\overline{U}_1}{dy_2} \frac{d\overline{U}_1}{dy_2'} u_2 u_2' R_{22} \cdots$$

$$\cdots \cos(k_1 r_1) \cos(k_3 r_3)\, dr_3\, dr_1\, dy_2'\, dy_2\, dk_3 \tag{4-3}$$

Empirical forms of the mean-shear and the intensity are fairly independent of Reynolds number when the length scale is $\delta *$, the displacement thickness, and the velocity scale is U_{τ}^{*}, the friction velocity. This aspect is discussed more fully later on. On the other hand, the customary form used for experimental frequency spectra requires the non-dimensional dependent variable, $\hat{\Pi}_1 = \Pi_1 / q^2 \delta^*$. In non-dimensional variables the problem reduces to

$$\hat{\Pi}_1(\hat{k}_1) = \frac{32}{\pi^2}\left(\frac{U_\tau}{U_\infty}\right)^4 \int_0^\infty\int_0^\infty\int_0^\infty\int_0^\infty\int_0^\infty \frac{\hat{k}_1^2}{\hat{k}^2} \exp[-\hat{k}(\hat{y}_2+\hat{y}_2')] \frac{dU^*}{d\hat{y}_2}\frac{dU^*}{d\hat{y}_2'} \hat{a}_2 \hat{a}_2' R_{22} \cdots$$

$$\cdots \cos(\hat{k}_1 \hat{r}_1) \cos(\hat{k}_3 \hat{r}_3)\, d\hat{r}_3\, d\hat{r}_1\, dy_2'\, dy_2\, dk_3 \tag{4-4}$$

where $$(U_\tau / U_\infty)^4 = (C_f/2)^2$$

The Reynolds number dependence of the wave number spectrum will be discussed in Chapter VI.

Mean-Shear Expression

Bull (1969) studied expressions for the mean-shear in a zero pressure gradient boundary layer. He divided the boundary layer into three regions and concluded that the following equations best represent the experimental information.

Inner region: Limits, $0 \leq y_2 < 32.2\, \nu/\delta^* U_\tau$

$$\frac{dU^*}{d\hat{y}_2} = \frac{U_\tau \delta^*}{\nu}\left[1 + (\tilde{y}_2/a) + \frac{1}{2}(\tilde{y}_2/a)^2 + \frac{1}{6}(\tilde{y}_2/a)^6\right]\exp(-\tilde{y}_2/a) \tag{4-5}$$

where $\tilde{y}_2 = \hat{y}_2\, \delta^* U_\tau / \nu$

Middle region: Limits, $\frac{32.2\nu}{\delta^* U_\tau} \le \hat{y}_2 < \alpha_c \delta/\delta^*$

$$\frac{dU^*}{d\hat{y}_2} = \frac{\delta^*}{K\delta}\left[\frac{\delta}{\delta^*\hat{y}_2} + \frac{\pi\Pi}{\alpha_c}\sin\left(\frac{\pi\delta^*\hat{y}_2}{\alpha_c\delta}\right)\right] \tag{4-6}$$

where $K = .41$, $\pi = .60$, and $\alpha_c = .837$

Outer region: Limits, $\alpha_c \delta/\delta^* < \hat{y}_2 < \delta/\delta^*$

$$\frac{dU^*}{d\hat{y}_2} = \frac{\delta^*}{\delta\alpha_c K}\left[(1 - \hat{y}_2\delta^*/\delta)/(1 - \alpha_c\delta/\delta^*)\right]^{m-1} \tag{4-7}$$

where $m = 1.67$

The inner region consists of the viscous sublayer and the buffer layer. The extent and the profile in this region depend upon Reynolds number. For the majority of calculations a Reynolds number of $U_\infty \delta^*/\nu = 6000$ was assumed. The middle region is the customary 'log law' plus the 'law of the wake'. The constant K is universal while π, and α_c depend on pressure gradient. The shape factor, δ/δ^*, also depends somewhat on the Reynolds number. Bull proposed the outer region equation to compensate for the failure of the 'law of the wake' at the edge of the boundary layer. These equations are valid for a wide range of Reynolds numbers.

Turbulence Intensity

Klebanoff (1954) measured the intensity, $\hat{u}_2$ ($\hat{y}_2$) in the boundary layer. He extrapolated the data further toward the wall using the pipe flow results of Laufer (1954). In the region of overlap these data agreed very well when plotted in wall layer variables. More recently, Kim et al. (1968) measured the intensity near the wall of a low Reynolds number boundary layer. This data is also in good agreement when plotted in wall layer variables.

However, for $y^* < 8$ (viscous sublayer) there are no measurements. The data were extrapolated to the wall as follows. The continuity equation, when evaluated at the wall, shows that $\hat{u}_2$ increases at least as $\hat{y}_2^2$. Thus, it is assumed that $\hat{u}_2$ is parabolic out to $y^* = 8$ where $y^* = y_2 U_\tau/\nu$. This defines the outer boundary of the viscous sublayer. From that point the experimental data are used. The equations fit the data with an error of less than 5%.

$$\hat{u}_2 = 27(\hat{y}_2^2/A) , \qquad 0 \leq \hat{y}_2 < \frac{8\nu}{U_\tau \delta *} \tag{4-8}$$

$$\hat{u}_2 = 27(.3\hat{y}_2^{\frac{1}{2}} - 1.63\hat{y}_2^2) , \qquad \frac{8\nu}{U_\tau \delta *} \leq \hat{y}_2 < \frac{.017\delta}{\delta *} \tag{4-9}$$

$$\hat{u}_2 = 27[.0395 - (\hat{y}_2 - 1)^2/1.24] , \qquad \frac{.017\delta}{\delta *} \leq \hat{y}_2 < \frac{.1\delta}{\delta *} \tag{4-10}$$

$$\hat{u}_2 = 27[.0394 - (\hat{y}_2 - .14)^2/21.5] , \qquad \frac{.1\delta}{\delta *} \leq \hat{y}_2 < \frac{.575\delta}{\delta *} \tag{4-11}$$

$$\hat{u}_2 = 27(.0638 - .057\hat{y}_2) , \qquad \frac{.575\delta}{\delta *} \leq \hat{y}_2 < \frac{.9\delta}{\delta *} \tag{4-12}$$

$$\hat{u}_2 = 27[.0068 + (\hat{y}_2 - 1)^2/1.25] , \qquad \frac{.9\delta}{\delta *} \leq \hat{y}_2 \leq \frac{\delta}{\delta *} \tag{4-13}$$

In equation (4-8), A is determined by solving equations (4-8) and (4-9) at $y^* = 8$.

$$A = \hat{y}_2^{\,2} / (.3\,\hat{y}_2^{\,1/2} - 16.3\,\hat{y}_2^{\,2})\Big|_{\hat{y}_2 = \frac{8\nu}{U_\tau^*}} \tag{4-14}$$

$$A = .0306$$

The equations above depend upon Reynolds number in the innermost layers, i.e. equations (4-8) and (4-9). Calculations were first run with a low Reynolds number. When a check was run at a larger Reynolds number a surprisingly large effect was observed. This effect was thought to result from the fact that the equations above are actually valid only for the large Reynolds number $Re_{\delta *} = 9.9 \cdot 10^3$. They must be modified in the region $0 < y^* < 32$ for any other Reynolds number. Calculations were rerun at the proper $Re_{\delta *} = 9.9 \cdot 10^3$. At this time the innermost equation was modified to the form $a\hat{y}^2 + b\hat{y}^3$. The addition of the cubic term allows the slope of the data to be matched at $y^* = 8$. This modification was included because the inner layers contributed much more to the spectrum (at high wave numbers) than anticipated. The values of a and b were $4.17 \cdot 10^3$ and $-7.9 \cdot 10^5$ respectively.

The value of the boundary layer thickness, δ, in Klebanoff's (1954) data had to be changed to be consistent with the form of the mean-shear, particularly equation (4-6). Klebanoff's mean velocity profile was matched to the 'law of the wall and wake'. A value of $\delta = 2.76$ inches was computed to replace the value $\delta = 3$ inches reported by Klebanoff. Figures 5 and 6 are plots of the scaled intensity equations. Figure 12 shows the variation of the product of the velocity intensity and mean-shear across the boundary layer.

This variation proves to be important in devising a technique for numerically integrating the spectrum equation.

Turbulence Correlation

The turbulence correlation information enters the problem through $\Phi_{22}(\hat{y}_2, \hat{y}_2', \hat{k}_1, \hat{k}_3)$. This is the Fourier transform on $\hat{r}_1$ and $\hat{r}_3$ of the two point correlation, $R_{22}(\hat{y}_2, \hat{y}_2', \hat{r}_1, \hat{r}_3)$, with zero time delay, equation (4-2). As previously emphasized, it is Φ_{22} and not R_{22} which is assumed. The theoretical procedure is to Fourier transform the scale anisotropic model of R_{22} given in Chapter II. The anisotropy factor α is taken as constant in this integration. This would be the exact value of Φ_{22} if all of the disturbances in the flow had the same anisotropy factor. Next alpha is allowed to be a function of wave number. Thus, it no longer can be claimed that the original R_{22} is proper for the flow field. For the numerical calculation, the procedure is to substitute equation (4-2) into equation (4-1) and use an analytic expression for R_{22}.

The isotropic form of R_{22} is given in equation (3-4). It involves the longitudinal correlation function, f(r). For the calculations it is assumed that f(r) = exp (-r/L), in lieu of $f(r) = \exp(-r^2/L^2)$. Hodgson (1962) showed that the former representation more adequately represents the experimental data, particularly at the higher frequencies. Substituting the apropos non-dimensional variables into equation (3-4), R_{22} is

$$R_{22}(\hat{r}_k) = \left[1 - \frac{C_1}{2}\left(\frac{\hat{r}_1^2 + \hat{r}_3^2}{\hat{r}}\right)\right]\exp(-C_1\hat{r}) \qquad (4\text{-}15)$$

where $C_1 = \delta^*/L$ and $\hat{r}^2 = \hat{r}_1^2 + \hat{r}_2^2 + \hat{r}_3^2$.

Grant's (1958) velocity correlation data motivate two modifications to equation (4-15). The first is the dependence of the integral scale across the boundary layer, as seen in Figure 7. The second is the increase in the streamwise direction of the integral scale as modeled previously by α, Figure 3. A third modification would be in the orientation of the turbulence vorticity vector. Townsend found a preferred orientation of 45° for large scale boundary layer disturbances. Kraichnan found that scale anisotropy had the greater influence on the mean-square pressure.

The R_{22} dependence on $\hat{y}_2$ can be modeled by making C_1 in equation (4-15) dependent on $\hat{y}_2$. The value of C_1 is found at various values of y_2/δ by a least squares fit to the data in Figure 7. Then a least squares fit of these values to an exponential is used to determine $C_1(\hat{y}_2)$. The details are found in Appendix I, and the result is plotted in Figure 8. As before, the streamwise stretching in the integral scale is accounted for by changing the definition of $\hat{r}$ to

$$\hat{r}^2 = \hat{r}_1^2/\alpha^2 + \hat{r}_2^2 + \hat{r}_3^2 \tag{4-16}$$

With these two modifications and by noting that $\hat{r}_2 = \hat{y}_2' - \hat{y}_2$, the expression for $\hat{R}_{22}$ is

$$\hat{R}_{22}(\hat{y}_2, \hat{y}_2', \hat{r}_1, \hat{r}_3; \alpha) = \left\{1 - \left[\frac{C_1(\hat{y}_2)}{2}\right]\left[\frac{\hat{r}_1^2 + \hat{r}_3^2}{\hat{r}}\right]\right\} \exp\left[-C_1(\hat{y}_2)\,\hat{r}\right] \tag{4-17}$$

where $\hat{r}^2 = \hat{r}^2/\alpha^2 + (\hat{y}_2' - \hat{y}_2)^2 + \hat{r}_3^2$.

Since the small-scale structure of the turbulence is more isotropic in character than the large-scale structure, it is reasonable to let alpha be a function of $\hat{k}_1$, the streamwise wave number. This functional relationship need not be chosen until it is desired to convert the wave number spectra into a frequency spectrum. This will be done in Chapter VI.

Final Problem Statement

The equation to be solved is obtained by substituting equation (4-17) into equation (4 -4).

$$\hat{\Pi}(\hat{k}_1) = \frac{8}{\pi^2} C_f^2 \int_0^\infty \int_0^{\delta/\delta^*} \int_0^{\delta/\delta^*} \int_0^\infty \int_0^\infty \frac{\hat{k}_1^2}{\hat{k}^2} \exp[-\hat{k}(\hat{y}_2 + \hat{y}_2')] \cdots$$

$$\cdots \frac{dU^*}{d\hat{y}_2} \frac{dU^*}{d\hat{y}_2'} u_2 u_2' \left[1 - \left(\frac{C_1}{2}\right)\left(\frac{\hat{r}_1^2 + \hat{r}_3^2}{\hat{r}}\right)\right] \exp(-C_1 \hat{r}) \cdots \tag{4-18}$$

$$\cdots \cos(\hat{k}_1 \hat{r}_1) \cos(\hat{k}_3 \hat{r}_3)\, d\hat{r}_3\, d\hat{r}_1\, d\hat{y}_2'\, d\hat{y}_2\, d\hat{k}_3$$

The finite limits on $\hat{y}_2$ and $\hat{y}_2'$ are due to the mean-shear going to zero at the outer edge of the boundary layer. It will be convenient at a later stage to have transformed $\hat{r}_1$ and $\hat{r}_3$ to polar coordinates. Then equation (4-18) becomes

$$\hat{\Pi}(\hat{k}_1) = \frac{8\alpha}{\pi^2} C_f^2 \int_0^\infty \int_0^{\delta/\delta^*} \int_0^{\delta/\delta^*} \int_0^\infty \int_0^{2\pi} \frac{\hat{k}_1^2}{\hat{k}^2} \exp[-\hat{k}(\hat{y}_2 + \hat{y}_2')] \cdots$$

$$\cdots \frac{dU^*}{d\hat{y}_2}\frac{dU^*}{d\hat{y}_2'}\hat{u}_2\hat{u}_2'\left\{\hat{r} - \left(\frac{C_1}{2}\right)\left(\frac{\hat{r}^3}{[\hat{r}^2+(\hat{y}_2'-\hat{y}_2)^2]^{1/2}}\right)\right\}\cdots \tag{4-19}$$

$$\cdots \exp\left\{-C_1\left[\hat{r}^2+(\hat{y}_2'-\hat{y}_2)^2\right]^{1/2}\right\}\cos(\alpha\hat{k}_1\hat{r}\cos\theta)\cos(\hat{k}_3\hat{r}\sin\theta)\,d\theta\, d\hat{r}\, d\hat{y}_2'\, d\hat{y}_2\, d\hat{k}_3$$

where $\hat{r}^2 = \hat{\rho}_1^2 + \hat{r}_3^2$, $\theta = \sin^{-1}(\hat{r}_3/\hat{r})$, and $\hat{\rho}_1 = \hat{r}_1/\alpha$. Equation (4-19) is the final statement of the problem. The method used to integrate it is the subject of the next chapter.

CHAPTER V

THE MONTE CARLO NUMERICAL INTEGRATION

This chapter will describe how the wave number spectrum equation, equation (4-19), was prepared for computer programming and evaluation by a Monte Carlo technique.

Numerical evaluation of one-dimensional integrals is a well perfected art. When these schemes are generalized to multidimensional problems, the number of points required increases exponentially. If M points are required on each variable, then M^5 points are required for a five-dimensional integral. Take M as a modest 50 points, then M^5 is 1,562,500,000. The Monte Carlo technique is based on principles which are independent of the space dimension. The number of points required to apply the method increases with the variance of the function. For this reason the Monte Carlo technique was chosen and 5000 iterations or 25,000 non-zero producing points gave acceptable results.

The Monte Carlo Method

Integration by a sampling technique for a Monte Carlo method is an unbiased, iterative, numerical method based on the 'Strong Law of Large Numbers' (Davis and Rabinowitz, 1967). To illustrate this consider a one-dimensional example. Let the integral be

$$I = \int_a^b f(x)dx \tag{5-1}$$

From the 'Mean-Value Theorem', an estimator for I would be

$$I \simeq \frac{b-a}{N} \sum_{i=1}^{N} f(x_i) = (b-a)\cdot \text{Mean-value of } f(x) \tag{5-2}$$

The values of x_i are chosen from a set of random numbers which are uniformly distributed on the interval (a, b). The 'Strong Law of Large Numbers' says that

$$\text{Probability}\left[\lim_{N\to\infty} \frac{1}{N} \sum_{i=1}^{N} f(x_i) = I/(b-a)\right] = 1 \tag{5-3}$$

Thus, as the number of samples, N, becomes infinite, the technique converges to an exact, i.e. unbiased, answer.

Instead of selecting random numbers from a stored list, it is more convenient to calculate a sequence of numbers which passes the statistical tests for randomness. Such a sequence is called pseudo-random. It is even more desirable to use a sequence of numbers which is quasirandom. A quasirandom sequence is non-random. It passes only those statistical tests for randomness necessary for the application. The quasirandom sequences used in this work are Halton sequences obtained from the Fortran subroutine CORPUT written by Professor J. P. Chandler of Oklahoma State University. The quasi-random sequence has two distinct advantages. Firstly, the numbers are generated serially in the same sequence each time the subroutine is used. This is useful in comparing the answers from separate computer runs. Secondly, the statistical error from a fixed sample size is less than that resulting from the use of a random or pseudo-random sequence.

If f(x) in equation (5-2) were a constant, only one sample would be required to find its mean-value. If f(x) has large variations, it may take many samples to compute its mean-value. It turns out that the rms or variance measures the difficulty of computing an integral by the Monte Carlo technique. The successful application of Monte Carlo integration employs various tricks known as variance reduction techniques. They reduce the statistical error for a fixed sample size or more important, reduces the sample size for an acceptable statistical error.

Importance sampling is a variance reduction technique where more samples are taken from the 'important' region of the interval. This is accomplished by changing the independent variable in such a way that the new integrand is flatter. As an example, consider the previous problem and introduce a function p(x),

$$I = \int_a^b f(x)\,dx = \int_a^b \frac{f(x)}{p(x)}\,p(x)\,dx \tag{5-4}$$

with the conditions that

$$p(x) > 0 \tag{5-5}$$

and

$$\int_a^b p(x)\,dx = 1 \tag{5-6}$$

From a statistical viewpoint the function, p(x), is called the probability density function.

Let a new variable, u(x), be defined by the inversion equation,

$$u(x) = \int_0^u du = \int_a^x p(\xi)\,d\xi \tag{5-7}$$

Another important condition is that p(x) possess a closed form integral so that equation (5-7) can be evaluated, otherwise there is another numerical integration. Since p(x) > 0 is the Jacobian, u(x) will be single valued and may be inverted either explicitly or numerically to obtain

$$x = x(u) \tag{5-8}$$

Substituting the change of variable into equation (5-4) gives the new problem

$$I = \int_0^1 \frac{f[x(u)]}{p[x(u)]}\,du \simeq \frac{1}{N}\sum_{i=1}^{N} \frac{f[x_i(u_i)]}{p[x_i(u_i)]} \tag{5-9}$$

The new integrand has less variance on the new interval (0, 1) than f(x) had on the interval (a, b). In the limit, as the variance approaches zero, the new integrand would approach a constant value on the interval (0, 1). If this were true, then the integral I would be known after sampling one value of u_i. This result is trivial as the value of I would be known 'a priori' to within a constant and there would be no need to use the Monte Carlo technique. However, the moral of the preceeding story is that p(x) should mimic f(x) on the interval (a, b). This causes each point on the new interval (0, 1) to be relatively as important as any other point. In a multidimensional integrand $p(x_1, \ldots x_n)$ is chosen to mimic the dominant behavior of the independent variables in $f(x_1, \ldots x_n)$. Often $p(x_1, \ldots x_n)$ is chosen to be a product of functions, $p = p_1(x_1) \ldots p_n(x_n)$, for simplicity. This implies that the variance reduction on x_1 is independent of the variance reduction on the other variables. In truly complicated problems this would not be expected.

Variance Reduction of the Problem

In order to apply the importance sampling technique to the current problem, the probability density functions must be chosen and the inversion equations deduced. Taking the variables one at a time, the integrand is inspected to find the dominant role of that variable. Then the probability density function can be chosen to mimic that behavior.

Consider first the θ variable in equation (4-19). It appears in a complex oscillatory manner in the argument of both sine and cosine functions. Its behavior is very difficult to mimic. Fortunately, it is unnecessary since the variance is relatively small and the computation worked well without any reduction.

The variable $\hat{r}$ appears in the expression

$$\left\{\hat{r} - \frac{\hat{r}^3}{[\hat{r}^2 + (\hat{y}_2' - y_2)^2]^{1/2}}\right\} \exp\left\{-C_1[\hat{r}_1^2 + (\hat{y}_2' - \hat{y}_2)^2]^{1/2}\right\} \tag{5-10}$$

This term goes to zero at the origin and as $\hat{r}$ approaches infinity it tends toward

$$\left(\hat{r} - \frac{C_1}{2}\hat{r}^2\right)\exp(-C_1\hat{r}) \tag{5-11}$$

This would be a likely candidate for the probability density function except that it is not always greater than zero. This problem was circumvented by separating equation (4-19) into two integrals at the minus sign between the $\hat{r}$ and $\hat{r}^2$ dependencies. Then the wave number spectrum is

$$\hat{\Pi}(\hat{k}_1) = \frac{8\alpha}{\pi^2} C_f^2 (I_1 - I_2) \tag{5-12}$$

$$I_1 = \int_0^\infty \int_0^{\delta/\delta^*} \int_0^{\delta/\delta^*} \int_0^\infty \int_0^{2\pi} \hat{r}\, f(\hat{k}_3, \hat{y}_2, \hat{y}_2', \hat{r}, \theta)\, d\theta\, d\hat{r}\, d\hat{y}_2'\, d\hat{y}_2\, d\hat{k}_3 \tag{5-13}$$

$$I_2 = \int_0^\infty \int_0^{\delta/\delta^*} \int_0^{\delta/\delta^*} \int_0^\infty \int_0^{2\pi} \frac{\hat{r}^3}{[\hat{r}^2 + (\hat{y}_2' - \hat{y}_2)^2]^{1/2}}\, f(\hat{k}_3, \hat{y}_2, \hat{y}_2', \hat{r}, \theta)\, d\theta\, d\hat{r}\, d\hat{y}_2'\, d\hat{y}_2\, d\hat{k}_3 \tag{5-14}$$

where

$$f(\hat{k}_3, \hat{y}_2, \hat{y}_2', \hat{r}, \theta) = \frac{\hat{k}_1}{\hat{k}^2} \exp[-\hat{k}(\hat{y}_2 + \hat{y}_2')] \frac{d\hat{U}^*}{d\hat{y}_2} \frac{d\hat{U}^*}{d\hat{y}_2'} \hat{u}_2 \hat{u}_2' \ldots \tag{5-15}$$

$$\ldots \exp\{-C_1[\hat{r}^2 + (\hat{y}_2' - \hat{y}_2)^2]^{1/2}\} \cos(\alpha \hat{k}_1 \hat{r} \cos\theta) \cos(\hat{k}_3 \hat{r} \sin\theta)$$

The dominant $\hat{r}$ dependence in I_1 is

$$r \exp(-Cr) \tag{5-16}$$

where C is used in lieu of $C_1 = C_1(\hat{y}_2)$ and C must be constant. Let p_1, the probability density function for $\hat{r}$ in I_1, be proportional to term (5-16). Applying condition (5-6) where a is zero and b is infinite,

$$p_1(r) = C\hat{r}\exp(-C\hat{r}) \tag{5-17}$$

From equation (5-7) the inversion equation is

$$x = (C\hat{r}+1)\exp(-C\hat{r}) \tag{5-18}$$

In this instance equation (5-18) must be inverted numerically to obtain

$$\hat{r} = \hat{r}(x) \tag{5-19}$$

The Fortran subroutine XMEAX developed by Professors J. P. Chandler performs the inversion.

Following steps similar to those used to determine the $\hat{r}$ dependence in I_1, the probability density function for $\hat{r}$ in I_2 is

$$p_2(\hat{r}) = \frac{C^3}{2}\hat{r}^2\exp(-C\hat{r}) \tag{5-20}$$

and the inversion equation is

$$z = \left(\frac{C^2\hat{r}^2}{2} + C\hat{r}+1\right)\exp(-C\hat{r}) \tag{5-21}$$

Equation (5-21) also is inverted numerically by subroutine XMEAX.

Having selected the probability density functions and the resulting inversion equations for $\hat{r}$ in I_1 and I_2, the same must be done for $\hat{k}_3$, $\hat{y}_2$, $\hat{y}_2'$ variables. These variables can not be isolated as was $\hat{r}$. They play a dominant and symmetric role in the expression

$$\frac{\hat{k}_1^2}{\hat{k}^2} \exp[-\hat{k}(\hat{y}_2+\hat{y}_2')] \frac{dU^*}{d\hat{y}_2}(\hat{y}_2) \frac{dU^*}{d\hat{y}_2'}(\hat{y}_2') \hat{u}_2(\hat{y}_2) \hat{u}_2(\hat{y}_2') \tag{5-22}$$

However, $\hat{k}_3$ also enters the first exponential and the multiplier $\hat{k}_1^2/\hat{k}^2$.

A closer examination of the term $\hat{u}_2 \, dU^*/d\hat{y}_2$ reveals that it changes considerably over the range $0 \le \hat{y}_2 \le \delta/\delta^*$ (see Figure 12). The $\hat{y}_2$ variables were importance sampled in different ways on each of three regions. This technique is known as stratified sampling (Hammersley and Handscomb, 1967). The computational regions are divided as follows:

1. Inner: $0 \le \hat{y}_2 \le .025$; denoted by IN.
2. Middle: $.025\,\delta/\delta^* < \hat{y}_2 < .2\delta/\delta^*$; denoted by MD.
3. Outer: $.2\delta/\delta^* \le \hat{y}_2 \le \delta/\delta^*$; denoted by OT.

Because of the symmetry in $\hat{y}_2$ and $\hat{y}_2'$, the stratified sampling separates both I_1 and I_2 in equation (5-12) into nine integrals each. Symbolically I_1 and I_2 are composed of

$$\begin{aligned} I_j = \int_0^\infty \Big[& \int_{IN}\int_{IN}\int_0^\infty\int_0^{2\pi} + \int_{IN}\int_{MD}\int_0^\infty\int_0^{2\pi} + \int_{IN}\int_{OT}\int_0^\infty\int_0^{2\pi} + \int_{MD}\int_{IN}\int_0^\infty\int_0^{2\pi} + \int_{MD}\int_{MD}\int_0^\infty\int_0^{2\pi} + \int_{MD}\int_{OT}\int_0^\infty\int_0^{2\pi} + \cdots \\ & \cdots \int_{OT}\int_{IN}\int_0^\infty\int_0^{2\pi} + \int_{OT}\int_{MD}\int_0^\infty\int_0^{2\pi} + \int_{OT}\int_{OT}\int_0^\infty\int_0^{2\pi} (\cdots\cdots) \, d\theta \, d\hat{r} \, d\hat{y}_2' \, d\hat{y}_2 \Big] d\hat{k}_3 \end{aligned} \tag{5-23}$$

In a five-dimensional format, a typical integral in I_1 which includes the probability distribution function is expressed as

$$I_{1i} = \int_0^d \int_a^b \int_e^f \int_0^\infty \int_0^{2\pi} \frac{f_1(\hat{k}_3, \hat{y}_2, \hat{y}_2', \hat{r}, \theta)}{p_{3i}(\hat{k}_3, \hat{y}_2, \hat{y}_2', \hat{r}, \theta) p_1(r)} p_{3i}(\hat{k}_3, \hat{y}_2, \hat{y}_2') p_1(\hat{r}) \, d\theta \, d\hat{r} \, d\hat{y}_2' \, d\hat{y}_2 \, d\hat{k}_3 \tag{5-24}$$

Likewise a typical integral in I_2 is

$$I_{2i} = \int_0^d \int_a^b \int_e^f \int_0^\infty \int_0^{2\pi} \frac{f_2(\hat{k}_3, \hat{y}_2, \hat{y}_2', \hat{r}, \theta)}{p_{3i}(\hat{k}_3, \hat{y}_2, \hat{y}_2') p_2(\hat{r})} p_{3i}(\hat{k}_3, \hat{y}_2, \hat{y}_2') p_2(\hat{r}) \, d\theta \, d\hat{r} \, d\hat{y}_2' \, d\hat{y}_2 \, d\hat{k}_3 \tag{5-25}$$

In equations (5-24) and (5-25) the upper limit d on $\hat{k}_3$ is finite but large enough not to change the value of the integral. The limits a, b and e, f on $\hat{y}_2$ and $\hat{y}_2'$ are permuted to correspond to the regions IN, MD, and OT.

The probability density function p_{3_i} must satisfy conditions analogous to equations (5-5) and (5-6).

$$\int_0^d \int_a^b \int_e^f p_{3i}(\hat{k}_3, \hat{y}_2, \hat{y}_2') \, d\hat{y}_2' \, d\hat{y}_2 \, d\hat{k}_3 = 1 \tag{5-26}$$

$$p_{3i}(\hat{k}_3, \hat{y}_2, \hat{y}_2') > 0 \tag{5-27}$$

The apropos probability density function which satisfies these conditions is

$$p_{3i}(\hat{k}_3, \hat{y}_2, \hat{y}_2') = \left\{ \frac{\hat{k}_1}{\hat{k}^2 \tan^{-1}(d/\hat{k}_1)} \right\} \cdots$$

$$\cdots \left\{ \frac{(\hat{k}+C_i)^2 \exp[-(\hat{k}+C_i)(\hat{y}_2+\hat{y}_2')]}{\{\exp[-(\hat{k}+C_i)a] - \exp[-(\hat{k}+C_i)b]\}\{\exp[-(\hat{k}+C_i)e] - \exp[-(\hat{k}+C_i)f]\}} \right\} \tag{5-28}$$

In equation (5-28) the constants C_i are determined by the region that is being sampled. In the inner region $C_i = C_I = 14.0$, in the middle region $C_i = C_M = 1.6$, and $C_i = C_M = 0.3$. The constants were selected to allow $p_{3\,i}$ to mimic the behavior of the product $\hat{u}_2 \; dU^*/d\hat{y}_2$ in each of the regions. The inversion equations $u(\hat{k}, \hat{y}_2, \hat{y}_2')$, $v(\hat{k}_3, \hat{y}_2, \hat{y}_2')$ and $w(\hat{k}_3, \hat{y}_2, \hat{y}_2')$ must be compatible with the Jacobian of the three-dimensional transformation. Two of the inversion equations can be selected arbitrarily. The third is computed from the first two and the selected probability density function (the Jacobian of the transformation). The mathematical details of this work and some additional comments on the selection of $p_{3\,i}$ are found in Appendix K. The inversion equations for $\hat{k}_3$, $\hat{y}_2$, and $\hat{y}_2'$ are

$$u = \tan^{-1}(\hat{k}_3/\hat{k}_1)/\tan^{-1}(d/\hat{k}_1) \tag{5-29}$$

$$v = \{1 - \exp[-(\hat{k}+c_i)\hat{y}_2]\} / \{\exp[-(\hat{k}+c_i)a] - \exp[-(\hat{k}+c_i)b]\} \tag{5-30}$$

$$w = \{1 - \exp[-(\hat{k}+c_i)\hat{y}_2']\} / \{\exp[-(\hat{k}+c_i)e] - \exp[-(\hat{k}+c_i)f]\} \tag{5-31}$$

They can be inverted explicitly to obtain

$$\hat{k}_3 = \hat{k}_1 \tan[u \tan^{-1}(d/\hat{k}_1)] \tag{5-32}$$

$$\hat{y}_2 = -\ln[1 - v\{\exp[-(\hat{k}+c_i)a] - \exp[-(\hat{k}+c_i)b]\}] / (\hat{k}+c_i) \tag{5-33}$$

$$\hat{y}_2' = -\ln[1 - w\{\exp[-(\hat{k}+c_i)e] - \exp[-(\hat{k}+c_i)f]\}] / (\hat{k}+c_i) \tag{5-34}$$

All of the elements of the problem are now defined such that it is ready to be programmed for the computer.

Program Operation

The computer program executes the following steps in sequence for a multidimensional integral each iteration:

1. Select M quasirandom numbers on the interval (0, 1). M is the number of variables in the problem. If the variable is not being importance sampled, the random variable M is the value of the variable used in the integrand. In this program, θ is not being importance sampled.

2. Compute the value of the variables which are being importance sampled using the explicit inversion equations or numerical

inversion schemes. In this problem, one of the quasirandom numbers is used to compute two values of $\hat{r}$ from equations (5-18) and (5-21). Two of the other numbers are used to compute three values of the variables $\hat{y}_2$ and $\hat{y}_2'$ from equations (5-33) and (5-34). A value is needed for each of the regions IN, MD, and OT. The final number is used to compute the value of $\hat{k}_3$ using equation (5-32).

3. The variables are then substituted into the original integrands, equations (5-13) and (5-14), and the probability distribution functions, equations (5-17), (5-20), and (5-28), to compute their values.

4. The value of the integrands are divided by the product of the probability distribution functions to produce the integrands of equations (5-24) and (5-25). This is analogous to equation (5-9) for one-dimension. This quotient is the contribution to the iteration to the integral.

5. As in equation (5-9) the value of the iteration is added to the sum of the previous iterations. When the desired number of samples is reached, the accumulated sum is divided by the total number of samples or iterations.

Appendix K is a listing of the integration program and Appendix L is a detailed discussion of the program chronology. Included is a list of the definitions of the program pseudonyms.

It is important that the contribution of each iteration be non-zero. If no contribution is made to the integral on a particular iteration and the iteration is counted as a sample, an erroneous answer results. In the program for this problem, 5000 non-zero producing samples were desired. It took approximately 5500 iterations to reach the stated goal. Dividing the smaller number by the larger yields an efficiency of 90%. But note that the integral value is determined by dividing the accumulated sum of contributions to the integrand by 5000, not 5500. Efficiency is an important feature of the Monte Carlo technique. It indicates that the proper importance sampling technique is employed.

The Monte Carlo technique is unbiased, thus a finite number of samples will not guarantee an exact answer. It is desirable to estimate how close the computed answer is to the exact answer. The measure of this closeness is called the statistical error and is measured in terms of the statistical quantities variation and standard deviation.

The standard deviation for 5000 iterations using quasirandom numbers is

$$\sigma_{5000} = \frac{K}{J-1}\sqrt{VAR_{100}} \tag{5-35}$$

where K is unknown. Had random or pseudorandom numbers been used, the standard deviation would be

$$\sigma_{5000} = \sqrt{VAR_{100}/(J-1)} \tag{5-36}$$

VAR_{100}, the variation for 100 samples, and J are obtained by dividing the 5000 iteration blocks into fifty, one-hundred iteration blocks. Then J is 50. The variance of these small blocks can be computed by

$$VAR_{100} = \sum_{i=1}^{50}\left(\hat{I}_{100,i} - \hat{I}_{5000}\right)^2 \tag{5-37}$$

In equation (5-37), $\hat{I}_{100,i}$ is the value of the integral calculated independently for each small block, and $\hat{I}_{5000}$ is the value of the integral after 5000 iterations. The standard deviation, σ_{100}, is defined by

$$\sigma_{100} = \sqrt{VAR_{100}} \tag{5-38}$$

In order to estimate the order of magnitude of K in equation (5-35), σ_{5000} was computed using the procedure used to compute σ_{100}.

$$\sigma_{5000} = \sqrt{VAR_{5000}} \tag{5-39}$$

where

$$VAR_{5000} = \sum_{i=1}^{5} \left(\hat{I}_{5000,i} - \hat{I}_{25,000} \right)^2 \tag{5-40}$$

The results are the three data points shown in Figure 20. In this case J was limited to 5 because it took 16 minutes of IBM 360/65 computer time to compute five, 5000 iteration blocks. The value of K turned out to be about 1. This is considered an order of magnitude estimate in that only five blocks were computed. Had this number been increased, K would have been a bit larger. The error is about 1% and is plotted in Figure 20 as computed by equation (5-35) with K = 1.

Figures 18 and 19 are plots of the regional contributions of the boundary layer to the wave number spectra. The division of the boundary layer into three regions in $\hat{y}_2$ and $\hat{y}_2'$ causes the total integral to be the sum of nine integrals. The contributions of three of these integrals were used to obtain the data for Figures 18 and 19. Figure 18 is a plot of the relative contribution of each of these integrals relative to the contribution of the sum of the three. Figure 19 is a plot of the ratio of the contribution of the integral representing the inner region to the total value of the spectrum at that wave number. The three integrals are

$$I_{IN} = \int_0^{\infty}\int_{IN}\int_{IN}\int_0^{\infty}\int_0^{2\pi}(\ldots\ldots)\,d\theta\,d\hat{r}\,d\hat{y}_2'\,d\hat{y}_2\,d\hat{k}_3 \tag{5-41}$$

$$I_{MD} = \int_0^{\infty}\int_{IN}\int_{IN}\int_0^{\infty}\int_0^{2\pi}(\ldots\ldots)\,d\theta\,d\hat{r}\,d\hat{y}_2'\,d\hat{y}_2\,d\hat{k}_3 \tag{5-42}$$

$$I_{OT} = \int_0^{\infty}\int_{OT}\int_{OT}\int_0^{\infty}\int_0^{2\pi}(\ldots\ldots)\,d\theta\,d\hat{r}\,d\hat{y}_2'\,d\hat{y}_2\,d\hat{k}_3 \tag{5-43}$$

The symbolic integrand in these equations is the integrand in equation (4-19). In the figures, I_{IN} is referred to as the INNER-INNER integral and likewise with I_{MD} and I_{OT}. Figure 19 gives a better picture of the contribution of the inner region of the boundary layer, $y_2/\delta \leq .025$, to the spectrum. The data in Figure 18 tends to overestimate the contribution of the inner region at moderate to high wave numbers in the region of the peak of the wave number spectrum. It also tends to overestimate the contribution of the inner region to the low wave numbers. The results will be discussed in more detail in the next chapter.

CHAPTER VI

DISCUSSION OF RESULTS

The final chapter contains discussions of the wave number spectra, anisotropy, and the frequency spectra. Following these discussions, the conclusions are summarized.

Wave Number Spectra

The principle results of this study are the wave number spectra given in Figures 14 and 15. A family of curves for a value of the anisotropy parameter from 1 to 4 is presented. The advantage of presenting the data as a function of wave number is that the spectra can be computed without introducing the convective velocity assumption or a particular anisotropy factor assumption. These assumptions are determined as a function of wave number and are added subsequently in order to predict the frequency spectrum.

The spectrum behaves about like $\tilde{k}_1^{-2}$ in the low wave number region with alpha simply shifting the level of the curves. The wave number at which the spectrum peaks decreases with increasing alpha. The opposite is true of the peak magnitude. It increases with increasing alpha. Just beyond the peak, the constant slope region decays at a rate equal to about $\tilde{k}_1^{-.75}$ for $\alpha = 1$. This compares with Bradshaw's (1967) prediction of $\tilde{k}_1^{-1}$. This initial constant slope region spans the values of $\tilde{k}_1$ from 5.5 to 34.5.

At that point the spectrum transitions to another constant slope region with slope equal to -1.1. This region terminates at $\tilde{k}_1 \cong 140$. From that point the spectrum decays at a much faster rate approaching $\tilde{k}_1^{-5.0}$. Wills (1970) predicted that the k_1^{-1} region is bounded by $\omega\delta^*/U_\infty = 0.6$ and $\omega\nu/U_\tau^2 = 0.5$. He proposed these limits on the basis of the 'eddy' scales being comparable with the spatial limits of the wall similarity region. In these computations, the lower limit is $\tilde{k}_1 = 5.5$ and the upper limit is $\tilde{k}_1 = 85.5$.

Recall that the computation of the spectrum was broken into nine regional contributions. Three of these integrals, inner-inner, middle-middle, and outer-outer are purely single region contributions while the remainder are cross contributions. Figure 18 plots the relative contributions of the single region integrals as a function of wave number. To get a more complete story Figure 19 should be considered where the contribution of inner-inner integral as a percentage of the total integration is displayed. Physically the inner region is the viscous layer plus the buffer region out to $y^* = 40$ for the Reynolds number of these computations. The middle region is the log region and the outer region is the last 80% of the boundary layer.

The middle and outer regions are responsible for the spectrum at low wave numbers up to and slightly over the peak. The inner contribution begins to pick up in the $\tilde{k}_1^{-.75}$ section and is 50% at $\tilde{k}_1 = 27.6$ ($\hat{k}_1 = 4$). At $\tilde{k}_1 = 138$ ($\hat{k}_1 = 20$) and beyond the inner region is solely responsible for the spectrum.

The spectra are strictly applicable to only one Reynolds number, $Re_{\delta^*} = 9.9 \cdot 10^3$. This is dictated by Klebanoff's intensity data. The mean-shear equations compensate for changes in Reynolds number but the intensity equations do not.

$$\tilde{\pi} = \pi_1 / \delta q^2 C_f^2 = (\delta^*/\delta)\hat{\pi}(\delta^*\tilde{k}_1/\delta)/C_f^2 \qquad (6\text{-}1)$$

and the independent variable is

$$\tilde{k}_1 = k_1 \delta = \hat{k}_1 \delta/\delta^* \qquad (6\text{-}2)$$

Since the program computes $\hat{\pi}$ $(\hat{k}_1)$ and $\hat{\pi}(\hat{k}_1)/C_f^2$, the independent and dependent variables must be scaled as shown in equation (6-1). It is anticipated that this selection of variables will remove most of the Reynolds number sensitivity from the spectrum, especially at low wave numbers.

It can be justified in the following manner. Assume that equation (4-3) is non-dimensionalized with length scale δ instead of $\delta*$, and that the intensity and mean-shear are the most sensitive terms in the integrand to Reynolds number. In the middle and outer regions these terms will be essentially free of Reynolds number dependence, when normalized with U_τ and δ. From Figure 18, it can be seen that the inner-inner region relative contribution is less than 3% below $\hat{k}_1 = .25$. Since the region beyond the buffer layer contributes the greatest portion of the spectrum at low wave numbers, the integrand and thus $\tilde{\pi}$ $(\tilde{k}_1)$ as defined in equation (6-1) will be relatively Reynolds number independent. This is not the case at high wave numbers. $\tilde{\pi}$ $(\tilde{k}_1)$ will depend on Reynolds number but it is not anticipated that the dependence at high wave numbers is strong. In order to test this hypothesis by computation, the modification of the intensity equations, mentioned earlier, is necessary.

Anisotropy

Two kinds of anisotropy are accounted for in the calculations. The first is actually a local isotropy which changes through the boundary layer by allowing the integral scale to be a function of $\hat{y}_2$. It is incorporated in the wave number spectrum calculation. The second kind of anisotropy is the scale anisotropy where α measures the elongation of the integral scale in the flow direction compared to the other directions. Alpha as a function of wave number can be assumed after the spectrum is calculated (but before the frequency spectrum is obtained).

The variation of the integral scale ($C_1(\hat{y}_2) = \delta^*/L(\hat{y}_2)$) across the boundary layer has a profound effect on the magnitude of the wave number spectrum. Prior to the inclusion of $C_1(\hat{y}_2)$, the program was run with constant C_1 . The value used was that proposed by Hodgson (1962), $C_1 = 2/3$. Selected points of the spectrum had values one to two orders of magnitude too high. The $C_1(\hat{y}_2)$ curve is one of the weakest points in the analysis since there is not much experimental data to determine this curve.

Scale anisotropy dramatically changes the spectrum at low frequencies when it was used in Hodgson's simplified solution (Figure 4). As previously mentioned, this result is deemed qualitatively correct, but of questionable quantitative value. The qualitative effect of alpha on the wave number spectra is similar to its effect on the frequency spectra. It is generally agreed that low wave number disturbances have a high alpha and should tend to isotropy at the higher wave numbers. Considering the experimental data from several angles , Figure 9 has been produced as a best guess for $\alpha(\tilde{k}_1)$. The wave number spectrum in Figure 16 was constructed using this functional form of $\alpha(\tilde{k}_1)$.

When alpha is allowed to be a function of $\hat{k}_1$ it is incorrect to consider the correlation R_{22} used in the calculation procedure as the actual assumption. $R_{22}(\hat{r}_1, \hat{r}_2, \hat{r}_3, \hat{y}_2)$ and $\Phi_{22}(\hat{k}_1, \hat{r}_2, \hat{k}_3, \hat{y}_2)$ are a Fourier transform pair and R_{22} should not be a function of $\hat{k}_1$. The numerical analysis used the following calculation procedure to determine Φ_{22} .

$$\Phi_{22}(\hat{k}_1, \hat{r}_2, \hat{k}_3, \hat{y}_2) = \frac{1}{4\pi^2}\int_{-\infty}^{\infty}\int_{-\infty}^{\infty} R_{22}(\hat{r}_1, \hat{r}_2, \hat{r}_3, \hat{y}_2, \alpha(\hat{k}_1)) \cdots$$

$$\cdots \exp[-i(\hat{k}_1\hat{r}_1 + \hat{k}_3\hat{r}_3)]\, d\hat{r}_1\, d\hat{r}_3 \tag{6-3}$$

The scale anisotropy form of R_{22} was integrated and then an assumption for $\alpha(\hat{k}_1)$ introduced. The correct R_{22} could be found by the inverse transform

$$\tilde{R}_{22}(\hat{r}_1, \hat{r}_2, \hat{r}_3, y_2) = \int_{-\infty}^{\infty}\int_{-\infty}^{\infty} \Phi_{22}(\hat{k}_1, \hat{r}_2, \hat{k}_3, y_2) \cdots$$

$$\cdots \exp[i(\hat{k}_1\hat{r}_1 + \hat{k}_3\hat{r}_3)]\, d\hat{k}_1\, d\hat{k}_3 \tag{6-4}$$

One might say that the $\hat{k}_1$ dependence of Φ_{22} has been defined by a procedure. The procedure can be checked against experimental data for $\tilde{R}_{22}$ ($\hat{r}_1$, 0, 0, $\hat{y}_2$) and $\tilde{R}_{11}$ ($\hat{r}_1$, 0, 0, $\hat{y}_2$).

Consider the inner integral in equation (6-3) and define the one-dimensional transform

$$\mathcal{R}_{22}(\hat{k}_1, \hat{r}_2, \hat{r}_3, \hat{y}_2) \equiv \frac{1}{2\pi}\int_{-\infty}^{\infty} R_{22}(\hat{r}_1, \hat{r}_2, \hat{r}_3, \hat{y}_2, \alpha(\hat{k}_1)) \cdots \tag{6-5}$$

$$\cdots \exp(-i\hat{k}_1\hat{r}_1)\, d\hat{r}_1$$

This can be computed for $\hat{r}_2 = \hat{r}_3 = 0$ with the scale anisotropy model, equation (4-17), for R_{22}.

$$\mathcal{R}_{22}(\hat{k}_1, 0, 0, \hat{y}_2) = \frac{C_1^3\alpha + 3C_1\alpha^3\hat{k}_1^2}{2\pi(C_1^2 + \alpha^2\hat{k}_1^2)^2} \tag{6-6}$$

with $\alpha = \alpha(\hat{k}_1)$ given in Figure 9. The correct $\tilde{R}_{22}$ was found by numerically performing the Fourier transform

$$\tilde{R}_{22}(\hat{r}_1, 0, 0, \hat{y}_2) = \int_{-\infty}^{\infty} \mathcal{R}_{22}(\hat{k}_1, 0, 0, \hat{y}_2)\exp(i\hat{k}_1 r_1)\, d\hat{k}_1 \tag{6-7}$$

The results are compared to the experimental data of Grant (1958) in Figure 10.

Comparison with Grant's $\tilde{R}_{11}$ (r_1/δ_0, 0, 0) data was also made. R_{11} is defined by an equation similar to (6-5), the analogue of equation (6-6) is produced, and $\tilde{R}_{11}$ calculated numerically by the Fourier transform. Figure 11 gives the results. Results for constant alphas of 1 and 2 are shown for reference.

The model assumed for $\alpha(\hat{k}_1)$ succeeds rather well in bringing

$\tilde{R}_{11}$ $(r_1/\delta_o, 0, 0)$ at $y_2/\delta = .45$ in coincidence with the data. This is more apparent when it is remembered that for isotropy, i.e. $\alpha_o = 1$,

$$\tilde{R}_{11}(\hat{r}_1/\delta_o, 0, 0) = \hat{R}_{22}(0, r_1/\delta_o, 0) \tag{6-8}$$

The model does not do as well in matching $\tilde{R}_{22}$ $(r_1/\delta_o, 0, 0)$ to the data. It does have the proper qualitative behavior and does match well for small values of r_1/δ_o.

Frequency Spectra

The predicted frequency spectrum in Figure 17 was constructed from the wave number spectrum of Figure 16 using Taylor's hypothesis. In this instance Taylor's hypothesis means that the spatial correlation pattern with zero time delay, $\pi(k_1)$, is convected past a fixed point producing a frequency spectrum. The frequency is given by $\omega = U_c(k_1)\cdot k_1$. The convective velocity data of Wills (1970), Figure 13 was used. Wills' data was extrapolated at the high and low wave number portions of the curve. Wills, himself, questions the downward trend at low wave numbers since it is based on limited data. Bradshaw (1967) observed a similar behavior and attributed it to boundary layer growth. The growth of the boundary layer was not a factor in Wills' data.

Landahl (1967) computed the convective velocity from a wave-guide model of turbulence. His results were slightly Reynolds number dependent but this would have negligible effect. However, it would be well to note that Wills' data was obtained at

$Re_{\delta *} = 13.5 \cdot 10^3$. The trend of Landahl's data showed a general decrease in convective velocity with Reynolds number.

Favre, et al. (1958) found that Taylor's hypothesis is a good approximation from $y_2/\delta = .06$ to $y_2 = \delta$. From Figure 19 it can be seen that at $\hat{k}_1 = 4.0$ or $\tilde{k}_1 = 27.6$ and above, 50% or more of the contribution to the spectrum originates well below this region ($y_2/\delta < .025$). If Favre's findings are assumed accurate, the practice of using Taylor's hypothesis at high frequencies or wave numbers is questionable.

Three types of experimental data are shown for comparative purposes. Hodgson's (1962) and Panton's et al. (1971) glider data are best for comparison at low frequencies. Serafini's (1963) data is shown for comparison at high frequencies. Hodgson's wind tunnel data is shown for qualitative comparison at high frequencies. Note that in Figure 17 Hodgson's data is plotted on a different scale from the other data both in the ordinate and abscissa. His boundary layer data was not available to allow the simple conversion to the coordinate system of the other data. Since Hodgson has not as yet published this data, permission was obtained to plot only the outline of the curve. No effort has been made to smooth the result.

The predicted spectrum is in good qualitative agreement with the measured results, but quantitatively it is high in the mid to high frequency region. Transducer size corrections and measurements are most difficult in this region. If the computed results are greater than the true power spectrum, the most probable cause is the function used for the variation of the integral scale ($1/C_1$) across the boundary layer. Close to the wall $C_1(y_2/\delta)$ becomes infinite. The function modeling it does not. The data does not give a clear picture of how the curve should approach this limit. Since the region close to the wall dominates the high frequency portion of the spectrum, an increase in C_1 near the wall will lower the prediction in that portion of the spectrum only. More data at higher Reynolds numbers is needed to formulate a better model for C_1 (y_2/δ) than was used in this study. Such work may prove that C_1 has a significant Reynolds number dependence similar to that of the mean-shear and intensity at small values of y_2/δ.

Statement of Conclusions

The major conclusions of this study are as follows:

1. It is feasible to numerically integrate the five dimensional integral for the 'M-T' contribution to the wave number spectrum. This evolves from the Fourier transform solution of the governing differential equation. The technique used is a Monte Carlo scheme using quasirandom numbers and a variance reduced integrand. The statistical error for 5000 non-zero producing iterations is about 1%, and a non-zero contribution is made to the integrand about 90 out of every 100 iterations.

2. The 'M-T' contribution to the spectrum thus computed is the major one, particularly at high frequencies. This is consistent with the findings of Kraichnan (1956b), Lilley and Hodgson (1960), and Hodgson (1962). It does not appear that the contribution at low frequencies can be other than a spectrum which approaches zero as k_1^{-2} even when anisotropic effects are considered.

3. The predicted frequency spectrum is in good qualitative

and quantitative agreement at low frequencies with those spectra measured in an experimental environment uncontaminated at low frequencies. It is in good qualitative agreement with the measured spectra most representative of the high frequency contribution but is quantitatively high. In general it is superior to previous computed spectra, particularly at high frequencies.

4. Anisotropic characteristics of the flow which effect the integral scale of the turbulence have a strong influence on the magnitude of the spectrum and a lesser influence on its shape.

5. The region of the boundary layer from the wall to y_2/δ = .025 contributes at least 50% of the spectrum at wave numbers $\hat{k}_1$ = 4.0 or $\tilde{k}_1$ = 27.6 and above. This, coupled with the work of Favre et al. (1958) causes the use of Reynolds analogy at high frequencies or wave numbers to be questionable.

6. The same region of the boundary layer discussed in item number 5 accounts for about 2% or less of the spectrum at wave numbers $\hat{k}_1$ = .2 or $\tilde{k}_1$ = 13.8.

7. It is postulated that the proper variables in which to plot the wave number spectrum to free the low wave number portion from Reynolds number dependence are $\pi(\tilde{k}_1) = \overline{p}^2(\tilde{k}_1)/\tau_w^2$ and $\tilde{k}_1 = k_1\delta$. It is thought that the high wave number dependence on Reynolds number in these variables will not be strong.

BIBLIOGRAPHY

Bies, D. A. "A Review of Flight and Wind Tunnel Measurements of Boundary Layer Pressure Fluctuations and Induced Structural Response." NASA CR-626, 1966.

Bradshaw, P. " 'Inactive' Motion and Pressure Fluctuations in Turbulent Boundary Layers." Journal of Fluid Mechanics, Vol. 30, 1967, 241.

Bull, M. K. "Mean Shear in a Constant Pressure Turbulent Boundary Layer." AIAA Journal, Vol. 7, 1969, 359.

Davis, P. J. and P. Rabinowitz. Numerical Integration. Blaisdell Publishing Co., Waltham, 1967.

Favre, A. J., J. J. Gaviglio, and R. Dumas. "Further Space-Time Correlations of Velocity in a Turbulent Boundary Layer." Journal of Fluid Mechanics, Vol. 3, 1958, 344.

Grant, H. L. "The Large Eddies of Turbulent Motion." Journal of Fluid Mechanics, Vol. 4, 1958, 149.

Hammersley, J. M. and D. C. Handscomb. Monte Carlo Methods. Methuen and Company, Ltd., London, 1967.

Hinze, J. O. Turbulence. McGraw-Hill Book Co., New York, 1959.

Hodgson, T. H. "Pressure Fluctuations in Shear Flow Turbulence." (unpublished Ph.D. Thesis, University of London, 1962).

Kim, H. T., S. J. Kline, and W. C. Reynolds. "An Experimental Study of Turbulence Production Near a Smooth Wall in a Turbulent Boundary Layer with Zero Pressure-Gradient." Thermosciences Division, Dept. of Mechanical Engineering, Stanford University, Report MD-20, 1968.

Klebanoff, P. S. "Characteristics of Turbulence in a Boundary Layer with Zero Pressure Gradient." NACA TN 3178, 1954.

Kraichnan, R. H. "Pressure Field Within Homogeneous Anisotropic Turbulence." Journal of the Acoustical Society of America, Vol. 28, 1956a, 64.

Kraichnan, R. H. "Pressure Fluctuations in Turbulent Flow Over a Flat Plate." Journal of Acoustical Society of America, Vol. 28, 1956b, 378.

Landahl, M. T. "A Wave-Guide Model for Turbulent Shear Flow." Journal of Fluid Mechanics, Vol. 29, 1967, 441.

Laufer, J. "The Structure of Fully Developed Pipe Flow." NACA Rept. 1174, 1954.

Lilley, G. M. and T. H. Hodgson. "On Surface Pressure Fluctuations in Turbulent Boundary Layers." AGARD Rept. 276, 1960.

Lilley, G. M. "Pressure Fluctuations in an Incompressible Turbulent Boundary Layer." College of Aeronautics, Cranfield, Rept. 133, 1960.

Panton, R. L., R. L. Lowery, and M. Reischman. "A Theoretical and Flight Test Study of Pressure Fluctuations Under a Turbulent Boundary Layer." Part Two, 1971. (Final Report on NASA Grant NGR 37-002-083, to be published).

Serafini, J. S. "Wall-Pressure Fluctuations and Pressure-Velocity Correlations in Turbulent Boundary Layers." AGARD Rept. 453, 1963.

Townsend, A. A. The Structure of Turbulent Shear Flow. Cambridge University Press, Cambridge, 1956.

Wills, J. A. B. "Measurements of the Wave-Number/Phase Velocity Spectrum of Wall Pressure Beneath a Turbulent Boundary Layer." Journal of Fluid Mechanics, Vol. 45, 1970, 65.

APPENDIX A

GREEN'S FUNCTION SOLUTION OF EQUATION (2-6)

One method of solving Poisson's equation is to use Poisson's formula which evolves from Green's second identity. This Appendix reviews the material presented by Lilley and Hodgson (1960) and Hodgson (1962). The governing partial differential equation is

$$\frac{\partial^2 p(x_i,t)}{\partial x_j \partial x_j} = -T(x_i,t) \tag{A-1}$$

where

$$T(x_i,t) = 2\rho\left[\frac{d\bar{U}_1}{dx_2}(x_2)\frac{\partial u_2}{\partial x_1}(x_i,t)\right] \tag{A-2}$$

Its attendant boundary conditions are

$$\left.\frac{\partial p}{\partial x_2}\right|_{x_2=0} = 0 \tag{A-3}$$

and

$$\left. p\right|_{x_2=0} = 0 \tag{A-4}$$

Boundary condition (A-3), though not exact, has been substantiated by previous authors on the basis of some experimental measurements by Townsend (1956).

The solution of equation (A-1) is given by Poisson's formula as

$$p(x_i, t) = \int_V G(x_i, y_i)\,T(y_i, t)\,dV(y_i) + \int_S \Big[G(x_i, y_i)\frac{\partial p}{\partial n}(y_i, t) \cdots$$

$$\cdots - p(y_i, t)\frac{\partial G}{\partial n}(x_i, y_i)\Big]dS(y_i) \qquad \text{(A-5)}$$

where the Green's function $G(x_i, y_i)$ satisfies the equation

$$\frac{\partial}{\partial y_i}\frac{\partial}{\partial y_i} G(x_i, y_i) = \delta[s(x_i, y_i)] \qquad \text{(A-6)}$$

In equation (A-6), s is the length

$$s(x_i, y_i) = \sqrt{(x_1-y_1)^2 + (x_2-y_2)^2 + (x_3-y_3)^2} \qquad \text{(A-7)}$$

and δ is the Dirac delta function. In equation (A-5), V is the semi-infinite volume bounded by the surface of the plate, $y_2 = 0$, and S is the surface of the volume.

The conditions on G are that it must satisfy the boundary conditions and not introduce any more singularities in the region of the integration. These requirements are met by the linear combination

$$G = G_o + G_i \qquad \text{(A-8)}$$

In equation (A-8), G_o is the solution to the unbounded problem and G_i is the solution to the unbounded problem in an image plane described by

$$y_1' = y_1$$

$$y_2' = -y_2 \qquad \text{(A-9)}$$

$$y_3' = y_3$$

Since the solution to G_o is

$$G_0(x_i, y_i) = \frac{1}{4\pi\, s(x_i, y_i)} \qquad \text{(A-10)}$$

from the symmetry in equations (A-9)

$$G_i(x_i, y_i) = \frac{1}{4\pi\, s'(x_i', y_i')} \qquad \text{(A-11)}$$

Substituting equations (A-10) and (A-11) into equation (A-8), the function G and its normal derivative on the plate are

$$G\Big|_{x_2=0} = 2\, G_0 \qquad \text{(A-12)}$$

$$\frac{\partial G}{\partial n}\Big|_{x_2=0} = 0 \qquad \text{(A-13)}$$

The pressure fluctuations on the plate can be computed from equation (A-5) by setting x_2 to zero and substituting equations (A-12) and (A-13)

$$p(x_1, 0, x_3, t) = 2\int_V G_0(x_1, 0, x_3, y_i)\, T(y_i, t)\, dV(y_i) + \cdots$$

$$\cdots 2\int_S G_0(x_1, 0, x_3, y_i)\, \frac{\partial p}{\partial n}(y_i, t)\, dS(y_i) \qquad \text{(A-14)}$$

The surface integral in equation (A-14) vanishes because of the boundary conditions. The final form is determined by substituting the values of $T(y_i, t)$ from equation (A-2) and G_o from equation (A-10) into equation (A-14).

$$p(x_1, 0, x_3, t) = \frac{\rho}{\pi} \int_V \left[\frac{d\overline{U}_1}{dy_2}(y_2) \frac{\partial u_2}{\delta y_2}(y_i, t) \Big/ s(x_i, y_i) \right] dV(y_i) \qquad \text{(A-15)}$$

APPENDIX B

INTEGRATION OF EQUATION (2-9)

Equation (2-9) as given in Chapter II is

$$R_{pp}(x_i, x_i', \tau) = \frac{\rho^2}{\pi^2} \int_{-\infty}^{\infty}\int_{0}^{\infty}\int_{-\infty}^{\infty}\int_{-\infty}^{\infty}\int_{0}^{\infty}\int_{-\infty}^{\infty} \frac{\langle u_2(y_2)\rangle \langle u_2(y_2')\rangle \frac{d\bar{U}_1(y_i)}{d y_2}\frac{d\bar{U}_1(y_i')}{d y_2'}}{s(x_i, y_i)\, s'(x_i', y_i')} \cdots$$

$$\cdots \frac{\partial}{\partial y_1}\frac{\partial}{\partial y_1'} R_{22}(y_i, y_i', \tau)\, dy_i\, dy_i' \qquad \text{(B-1)}$$

Experimental evidence confirms that R_{22} and its derivatives vanish at infinity in the longitudinal direction. Thus equation (B-1) can be simplified by integrating by parts twice.

$$R_{pp} = \frac{\rho^2}{\pi^2} \int_{-\infty}^{\infty} \frac{1}{s} \frac{\partial}{\partial y_1}\left(\frac{\partial}{\partial y_1'} R_{22}\right) dy_1 \int_{0}^{\infty}\int_{-\infty}^{\infty} \cdots \qquad \text{(B-2)}$$

$$R_{pp} = \frac{\rho^2}{\pi^2} \left\{ \left[\frac{1}{s}\frac{\partial}{\partial y_1'} R_{22}\right]_{-\infty}^{\infty} - \int_{-\infty}^{\infty} \frac{\partial}{\partial y_1'} R_{22} \frac{\partial}{\partial y_1}\left(\frac{1}{s}\right) dy_1 \right\} \int_{0}^{\infty}\int_{-\infty}^{\infty} \cdots$$

The first term on the right hand side of equation (B-3) is zero. A similar integration is carried out with respect to y_1' , leaving

$$R_{pp}(x_i, x_i', \tau) = \frac{\rho^2}{\pi^2} \int_{-\infty}^{\infty}\int_{0}^{\infty}\int_{-\infty}^{\infty}\int_{-\infty}^{\infty}\int_{0}^{\infty} \langle u_2(y_2)\rangle \langle u_2(y_2')\rangle \frac{d\overline{U}_1(y_2)}{dy_2} \frac{d\overline{U}_1(y_2')}{dy_2'} \cdots \tag{B-4}$$

$$\cdots \frac{\partial}{\partial y_1}(1/s) \frac{\partial}{\partial y_1'}(1/s')\, R_{22}(y_i, y_i', \tau)\, dy_i\, dy_i'$$

Using the homogeneity in x_1 and x_3 and

$$r_1 = y_1' - y_1 \,,$$

and

$$r_2 = y_2' - y_2 \tag{B-5}$$

$$r_3 = y_3' - y_3 \,,$$

equation (B-4) becomes

$$R_{pp}(\xi_1, 0, \xi, \tau) = \frac{\rho^2}{\pi^2} \int_{-\infty}^{\infty}\int_{0}^{\infty}\int_{-\infty}^{\infty}\int_{-\infty}^{\infty}\int_{-y_2}^{\infty}\int_{-\infty}^{\infty} \langle u_2(y_2)\rangle \langle u_2(y_2, r_2)\rangle \frac{d\overline{U}_1}{dy_2}(y_2) \frac{d\overline{U}_1}{dr_2}(y_2, r_2) \cdots$$

$$\cdots \frac{\partial}{\partial y_1}\left(s(x_i, y_i)\right) \frac{\partial}{\partial r_1}\left(s'(x_i', y_i')\right) R_{22}(y_2, r_i, \tau)\, dr_i\, dy_i \tag{B-6}$$

The subsequent y_1 and y_3 partial integrations of equation (B-6) follow Hodgson (1962). Define I_1 as

$$I_1 = \int_{-\infty}^{\infty}\int_{-\infty}^{\infty} \frac{\partial}{\partial y_1}\left[\frac{1}{s(x_i, y_i)}\right] \frac{\partial}{\partial r_1}\left[\frac{1}{s(x_i, y_i, r_i)}\right] dy_1\, dy_3 \tag{B-7}$$

Hodgson's vector notation will be adopted for simplicity.

$$s(x_i, y_i) = |\underline{x} - \underline{y}|$$
$$s(x_i', y_i, r_i) = |\underline{x}' - \underline{y} - \underline{r}| \tag{B-8}$$

Then,

$$I_1 = \int_{-\infty}^{\infty}\int_{-\infty}^{\infty} \frac{\partial}{\partial y_1} \frac{1}{|\underline{x} - \underline{y}|} \quad \frac{\partial}{\partial r_1} \frac{1}{|\underline{x}' - \underline{y} - \underline{r}|} \, dy_1 \, dy_3 \tag{B-9}$$

Since $\frac{1}{|\underline{x} - \underline{y}|}$ is not a function of $\underline{r}$ and $\underline{r}$ is constant in the integration,

$$I_1 = \frac{\partial}{\partial r_1} \int_{-\infty}^{\infty}\int_{-\infty}^{\infty} \frac{1}{|\underline{x}' - \underline{y} - \underline{r}|} \frac{\partial}{\partial y_1} \frac{1}{|\underline{x} - \underline{y}|} \, dy_1 \, dy_3 \tag{B-10}$$

$$I_1 = \frac{\partial}{\partial r_1} \int_{-\infty}^{\infty}\int_{-\infty}^{\infty} \frac{\partial}{\partial y_1} \left\{ \left| \frac{1}{\underline{x}' - \underline{y} - \underline{r}} \right| \left| \frac{1}{\underline{x} - \underline{y}} \right| \right\} dy_1 \, dy_3 - \ldots$$

$$\ldots \frac{\partial}{\partial r_1} \int_{-\infty}^{\infty}\int_{-\infty}^{\infty} \frac{1}{|\underline{x} - \underline{y}|} \frac{\partial}{\partial y_1} \frac{1}{|\underline{x}' - \underline{y} - \underline{r}|} \, dy_1 \, dy_3 \tag{B-11}$$

The first integral in equation (B-11) is zero and the differentiation, $\frac{\partial}{\partial y_1}$, in the second integral can be replaced by $\frac{\partial}{\partial r_1}$ which can be confirmed by mechanically performing the operations. Then $\frac{\partial}{\partial r_1}$ can be taken outside the integral.

$$I_1 = -\frac{\partial^2}{\partial r_1^2}\int_{-\infty}^{\infty}\int_{-\infty}^{\infty}\frac{1}{|\underline{x}-\underline{y}|}\;\frac{1}{|\underline{x}'-\underline{y}-\underline{r}|}\,dy_1\,dy_3 \qquad \text{(B-12)}$$

Remembering the relationships,

$$\underline{\xi} = \underline{x}' - \underline{x}$$

$$\underline{r} = \underline{y}' - \underline{y} \qquad \text{(B-13)}$$

a change of variable will be made which is a change in origin in an infinite integral.

$$\underline{\zeta} = \underline{x} - \underline{y}$$

$$\underline{z} = \underline{r} - \underline{\xi} \qquad \text{(B-14)}$$

Use the notation $|\underline{\zeta}| = \zeta$,

$$I_1 = -\frac{\partial^2}{\partial r_1^2}\int_{-\infty}^{\infty}\int_{-\infty}^{\infty}\frac{1}{\zeta}\;\frac{1}{|\underline{\zeta}-\underline{z}|}\,d\zeta_1\,d\zeta_3 \qquad \text{(B-15)}$$

Introduce the integral identity,

$$\frac{1}{|\underline{a}|\cdot|\underline{b}|} = \frac{2}{\pi}\int_0^{\infty}\frac{1}{a^2+b^2\lambda^2}\,d\lambda \qquad \text{(B-16)}$$

where $a^2 = |\underline{\zeta} - \underline{z}|^2$ and $b^2 = \zeta^2$. Change the integration variable to

$$\underline{\zeta}' = \underline{\zeta} - \frac{\underline{z}}{1+\lambda^2} \qquad \text{(B-17)}$$

and substitute equations (B-16) and (B-17) into (B-15) and assuming the order of integration can be changed,

$$I_1 = -\frac{2}{\pi}\frac{\partial^2}{\partial r_1^2}\left\{\int_0^\infty \frac{d\lambda}{1+\lambda^2}\int_{-\infty}^{\infty}\int_{-\infty}^{\infty}\frac{d\zeta_1' \, d\zeta_3'}{\left[\rho^2 + \frac{\lambda^2 z^2}{(1+\lambda^2)^2}\right]^2}\right\} \quad \text{(B-18)}$$

Let $\frac{\partial^2}{\partial r_1^2} = \frac{\partial}{\partial r_1}\left(\frac{\partial}{\partial z_1}\right)$ from equation (B-14) and perform the differentiation with respect to z_1 inside the integrals.

$$I_1 = \frac{\partial}{\partial \xi_1}\left\{\frac{4z_1}{\pi}\int_0^\infty \frac{\lambda^2 d\lambda}{(1+\lambda^2)^3}\int_{-\infty}^{\infty}\int_{-\infty}^{\infty}\frac{d\zeta_1' \, d\zeta_3'}{\left[\rho^2 + \frac{\lambda^2 z^2}{(1+\lambda^2)^2}\right]^2}\right\} \quad \text{(B-19)}$$

where $\frac{\partial}{\partial \xi_1}$ has entered from equation (B-14). The double integration with respect to ζ_1' and ζ_3' can be performed by using polar coordinates.

$$I_1 = \frac{\partial}{\partial \xi_1}\left\{4z_1\int_0^\infty \frac{\lambda^2 d\lambda}{(1+\lambda^2)\left[(1+\lambda^2)^2\rho^2 + \lambda^2 z^2\right]}\right\} \quad \text{(B-20)}$$

However, $x_2 = x_2' = \xi_2 = 0$ on the surface of the plate. Hence, $\zeta_2 = -y_2$ and $z_2 = r_2$ from equations (B-14) and

$$\zeta_2' = -\left[y_2 + r_2/(1+\lambda^2)\right] \quad \text{(B-21)}$$

from equation (B-17). Therefore,

$$I_1 = \frac{\partial}{\partial \xi_1}\left\{4z_1\int_0^\infty \frac{\lambda^2 d\lambda}{(1+\lambda^2)\left\{\left[(1+\lambda^2)y_2 + r_2\right]^2 + z^2\lambda^2\right\}}\right\} \quad \text{(B-22)}$$

Noting that the denominator in equation (B-22) is the sixth power in λ, define I_2 as

$$I_2 = \int_0^\infty \frac{\lambda^2 d\lambda}{(1+\lambda^2)\{[(1+\lambda^2)y_2 + r_2]^2 + z^2\lambda^2\}} \tag{B-23}$$

$$I_2 = \int_0^\infty \frac{\lambda^2 d\lambda}{\lambda^6 + p\lambda^4 + q\lambda^2 + r} \tag{B-24}$$

which when evaluated is

$$I_2 = \frac{\pi}{\alpha(\alpha^2 - p) - 2r^{1/2}} \tag{B-25}$$

where α is the largest root of

$$(x^2 - p)^2 - 8xr^{1/2} - 4q = 0 \tag{B-26}$$

Solving for α,

$$\alpha = 1 + \sqrt{(Z/y_2)^2 + 4r_2/y_2 + 4} \tag{B-27}$$

Now I_2 is

$$I_2 = \frac{\pi}{2(4y_2^2 + 4r_2y_2 + z^2)^{1/2}\left[2y_2 + r_2 + (4y_2^2 + 4r_2y_2 + z^2)^{1/2}\right]} \tag{B-28}$$

Substituting equation (B-28) into equation (B-20) and finally into equation (B-6,

$$R_{pp}(\xi_1, 0, \xi_3, \tau) = \frac{2\rho^2}{\pi}\int_0^\infty\int_{-\infty}^\infty\int_{-y_2}^\infty\int_{-\infty}^\infty \langle u_2(y_2)\rangle\langle u_2(y_2, r_2)\rangle \frac{d\bar{U}_1(y_2)}{dy_2}\frac{d\bar{U}_1(y_2, r_2)}{dr_2}\ldots$$

$$\cdots \frac{R_{22}(y_2, r_i, \tau)\,(\xi_1 - r_1)\, dr_3\, dr_2\, dr_1\, dy_2}{\left[(2y_2 + r_2)^2 + (\xi_1 - r_1)^2 + (\xi_3 - r_3)^2\right]^{1/2} \left\{2y_2 + r_2 + \left[(2y_2 + r_2)^2 + (\xi_1 - r_1)^2 + (\xi_3 - r_3)\right]^{1/2}\right\}} \tag{B-29}$$

APPENDIX C

THE MIRROR-FLOW MODEL

The motivation for the 'mirror-flow' model is the desire to obtain a functional representation for $\Phi_{22}(y_2, y_2', k_1, k_3)$ which will be characteristic of the turbulence velocity field and simplify the mathematics. By using this model the y_2' integration in equation (2-19) can be performed. Let $y_i{}^*$ be the mirror image with respect to the $y_2 = 0$ plane, i.e.

$$y_1{}^* = y_1 \ , \ y_2{}^* = -y_2 \ , \ y_3{}^* = y_3 \qquad \text{(C-1)}$$

Then the turbulence velocity field is described by

$$u_1(y_i,t) = 1/\sqrt{2}\left[\bar{\bar{u}}_1(y_i,t) + \bar{\bar{u}}_1(y_i^*,t)\right], \qquad \text{(C-2)}$$

$$u_2(y_i,t) = 1/\sqrt{2}\left[\bar{\bar{u}}_2(y_i,t) - \bar{\bar{u}}_2(y_i^*,t)\right] \qquad \text{(C-3)}$$

and

$$u_3(y_i,t) = 1/\sqrt{2}\left[\bar{\bar{u}}_3(y_i,t) + \bar{\bar{u}}_3(y_i^*,t)\right] \qquad \text{(C-4)}$$

The velocity, $u_i(y_i, t)$, satisfies continuity if $\bar{\bar{u}}_i(y_i, t)$ does and the boundary conditions on the plate

$$u_2 = 0 \ , \ \frac{\partial^2 u_2}{\partial y_2^2} = 0 \quad \text{and} \quad \frac{\partial p}{\partial y_2} = 0 \qquad \text{(C-5)}$$

are satisfied. However u_1 and u_3 do not vanish at the plate nor does the turbulence vanish at large distances from the plate in the normal direction.

Equations (C-3) cause the velocity correlation coefficient, R_{22}, to be given by

$$R_{22}(y_2, y_2', r_1, r_3) = \overline{\overline{R}}_{22}(y_2 - y_2', r_1, r_3) - \overline{\overline{R}}_{22}(y_2 + y_2', r_1, r_3) \quad \text{(C-6)}$$

The two dimensional Fourier transformation of equation (C-6) is

$$\Phi_{22}(y_2, y_2', k_1, k_3) = \overline{\overline{\Phi}}_{22}(y_2 - y_2', k_1, k_3) - \overline{\overline{\Phi}}_{22}(y_2 + y_2', k_1, k_3) \quad \text{(C-7)}$$

APPENDIX D

INTEGRATION OF EQUATION (2-19)

When equations (2-22) and (2-23) are substituted into equation (2-19), the result is

$$\Pi_2'(0,k_1,k_3) = \frac{4\rho^2 k_1^2}{k^2}\left[\frac{d\bar{U}_1(0)}{dy_2}\right]^2 \int_0^\infty\int_0^\infty \exp[-k(y_2+y_2')]\exp[-\beta(y_2+y_2')]\cdots$$

$$\cdots\left\{\bar{\bar{\Phi}}_{22}(y_2-y_2',k_1,k_3) - \bar{\bar{\Phi}}_{22}(y_2+y_2',k_1,k_3)\right\}dy_2\,dy_2' \tag{D-1}$$

Let I be defined as the double integral with its integrand in equation (D-1) and show only the functional dependence of the integration variable in y_2 and y_2'.

$$I = \int_0^\infty\int_0^\infty \exp[-(k+\beta)(y_2+y_2')]\left\{\bar{\bar{\Phi}}_{22}(y_2-y_2') - \bar{\bar{\Phi}}_{22}(y_2+y_2')\right\}dy_2\,dy_2' \tag{D-2}$$

Changing the integration variable in equation (D-2), it becomes

$$I = \int_0^\infty \exp[-2(k+\beta)y_2]\,dy_2 \int_{-\infty}^{y_2} \exp[(k+\beta)\xi]\,\bar{\Phi}(\xi)\,d\xi - \cdots$$

$$\cdots\int_0^\infty dy_2 \int_{y_2}^\infty \exp[-(k+\beta)\xi]\,\bar{\Phi}(\xi)\,d\xi \tag{D-3}$$

After integrating equation (D-3) by parts,

$$I = \frac{1}{k+\beta}\int_{-\infty}^{0} \exp[(k+\beta)y_2]\,\Phi(y_2)\,dy_2 - \int_{0}^{\infty} y_2 \exp[-(k+\beta)y_2]\,\Phi(y_2)\,dy_2 \tag{D-4}$$

Change the integration variable in the first of the two integrals in equation (D-4) so that

$$I = \frac{1}{k+\beta}\int_{0}^{\infty} \exp[-(k+\beta)y_2]\,\Phi(-y_2)\,dy_2 - \int_{0}^{\infty} y_2 \exp[-(k+\beta)y_2]\,\Phi(y_2)\,dy_2 \tag{D-5}$$

Then if $\Phi(-y_2) = \Phi(y_2)$, i.e. if Φ is an even function of y_2,

$$I = \int_{0}^{\infty}\left[\frac{1}{k+\beta} - y_2\right] \exp[-(k+\beta)y_2]\,\Phi(y_2)\,dy_2 \tag{D-6}$$

With equation (D-6), equation (D-1) becomes

$$\pi_2'(0,k_1,k_3) = \frac{4\rho^2 k_1^2}{k^2}\left[\frac{d\overline{U}_1(0)}{dy_2}\right]^2 \int_{0}^{\infty}\left[\frac{1}{k+\beta} - y_2\right] \exp[-(k+\beta)y_2]\,\Phi_{22}(y_2,k_1,k_3)\,dy_2 \tag{D-7}$$

APPENDIX E

SIMPLIFICATION OF EQUATION (3-2)

From Chapter III, equation (3-2) is

$$R_{pp}(\xi_1,0,\xi_3,\tau) = \frac{2\rho^2 g_0^2}{\pi}\frac{\partial}{\partial \xi_1}\int_0^{\infty}\int_{-\infty}^{\infty}\int_{-y_2}^{\infty}\int_{-\infty}^{\infty}\left\{\frac{\check{R}_{22}(r_i,\tau)}{\left[(2y_2+r_2)^2+(\xi_1-r_1)^2+(\xi_3-r_3)^2\right]^{1/2}}\right\}\cdots$$

$$\cdots\left\{\frac{dr_3\,dr_2\,dr_1\,dy_2}{2y_2+r_2+\left[(2y_2+r_2)^2+(\xi_1-r_1)+(\xi_3-r_3)\right]^{1/2}}\right\} \qquad \text{(E-1)}$$

Equation (E-1) can be integrated with respect to y_2 by changing the limits and sequence of integration on the y_2 and r_2 integrals. The area of the y_2 and r_2 integrations, $\int_0^{\infty} dy_2 \int_{-y_2}^{\infty} dr_2$, is shown below.

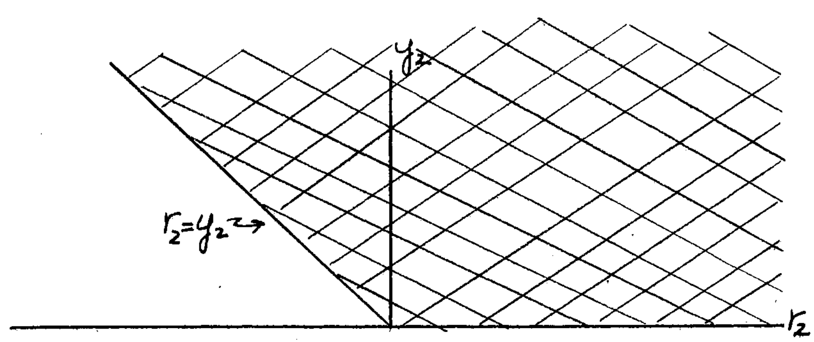

The same area of integration is represented by the sum

$$\int_0^{\infty} dr_2 \int_0^{\infty} dy_2 + \int_{-\infty}^{0} dr_2 \int_{-r_2}^{\infty} dy_2 \qquad \text{(E-2)}$$

First perform the y_2 integrations indicated in (E-2). The integrand from equation (E-1) is

$$\frac{1}{(4y_2^2+4r_2y_2+A^2)^{1/2}\left[2y_2+r_2+(4y_2^2+4r_2y_2+A^2)^{1/2}\right]} \tag{E-3}$$

where $A^2 = (\xi_1 - r_1)^2 + r_2^2 + (\xi_3 - r_3)^2$. Multiply numerator and denominator of (E-3) by $2y_2 + r_2 - \sqrt{4y_2^2 + 4r_2 y_2 + A^2}$.

$$\frac{1}{r_2^2 - A^2}\left[\frac{2y_2 - r_2}{(4y_2^2+4r_2y_2+A^2)^{1/2}} - 1\right] \tag{E-4}$$

Let the two y_2 integrals in (E-2) be split so that

$$I_1 = \frac{1}{r_2^2 - A^2}\left[\int_0^{\infty}\frac{2y_2+r_2}{(4y_2^2+4r_2y_2+A^2)^{1/2}} - \int_0^{\infty} dy_2\right] \tag{E-5}$$

and

$$I_2 = \frac{1}{r^2 - A^2}\left[\int_{-r_2}^{\infty}\frac{2y_2+r_2}{(4y_2^2+4r_2y_2+A^2)^{1/2}} - \int_{-r_2}^{\infty} dy_2\right] \tag{E-6}$$

Subsequent to the integration of equation (E-5) and (E-6),

$$I_1 = -\frac{1}{2}\,\frac{A}{r_2^2 - A^2} \tag{E-7}$$

and

$$I_2 = \frac{1}{2}\left(\frac{2r_2 - A}{r_2^2 - A^2}\right) \tag{E-8}$$

Substitute equations (E-7) and (E-8) into equation (E-2).

$$I = -\frac{A}{2}\int_{0}^{\infty} \frac{\check{R}_{22}(r_i, \tau)}{r_2^2 - A^2}\, dr_2 \quad + \cdots$$

$$\cdots \frac{1}{2}\int_{-\infty}^{0} \frac{\check{R}_{22}(r_i, \tau)(2r_2 - A)}{r_2^2 - A^2}\, dr_2 \tag{E-9}$$

By changing the limits of integration on the second integral in equation (E-9),

$$I = \int_{0}^{\infty} \frac{\check{R}_{22}(r_i, \tau)}{A - r_2}\, dr_2 \tag{E-10}$$

with the condition that R_{22} is an even function of r_2. Substituting equation (E-10) into (E-1),

$$R_{pp}(\xi_1, 0, \xi_3, \tau) = \frac{2\rho^2 g_0^2}{\pi}\frac{\partial}{\partial \xi_1}\int_{-\infty}^{\infty}\int_{0}^{\infty}\int_{-\infty}^{\infty} \frac{(\xi_1 - r_1)\;\check{R}_{22}(r_i, \tau)}{[(\xi_1 - r_1)^2 + r_2^2 + (\xi_3 - r_3)^2]^{1/2} - r_2}\, dr_3\, dr_2\, dr_1 \tag{E-11}$$

If it is assumed that equation (E-11) can be approximated by averaging in r_2,

$$R_{pp}(\xi_1, 0, \xi_3, \tau) = \frac{\rho^2 g_0^2}{\pi}\frac{\partial}{\partial \xi_1}\int_{-\infty}^{\infty}\int_{0}^{\infty}\int_{-\infty}^{\infty} \frac{(\xi_1 - r_1)\,\check{R}_{22}(r_i, \tau)}{[(\xi_1 - r_1)^2 + r_2^2 + (\xi_3 - r_3)^2]^{1/2}} \tag{E-12}$$

Differentiate the integrand with respect to ξ_1 and let ξ_1 and ξ_3 go to zero.

APPENDIX F

DEVELOPMENT OF $\check{R}_{22}(r_i,\tau)$

The spatially dependent isotropic velocity correlation, $\check{R}_{22}(r_i)$, is given in equation (3-4) as

$$\check{R}_{22}(r_i,0) = f(r) + \left(\frac{r_1^2 + r_3^2}{2r}\right)\frac{df(r)}{dr} \tag{F-1}$$

With this relationship, consider a field of turbulence which is homogeneous in parallel planes as seen from a reference frame moving with a constant mean velocity U_c in a direction parallel to the planes of homogeneity. The two point correlation coefficient that is measured in this moving frame is $\check{R}'_{jk}(r'_i, \tau)$ where $r'_i = (r'_1, r'_2, r'_3)$ is the separation vector between the two points in the moving coordinate frame. Assume that the spatially dependent portion of $\check{R}'_{jk}(r'_i, \tau)$ can be separated from the time dependent portion in the following manner.

$$\check{R}'_{jk}(r_i,\tau) = R^*_{jk}(r'_i)\, R'_{jk}(\tau) \tag{F-2}$$

In a stationary reference frame the turbulence appears to be convected past at a speed U_c in the r_1 direction. The correlation coefficient in this frame is

$$\check{R}_{jk}(r_i,\tau) = R^*_{jk}(r_1 - U_c\tau, r_2, r_3)\, R'_{jk}(\tau) \tag{F-3}$$

where $(r_1', r_2', r_3', \tau) = (r_1 - U_c\tau, r_2, r_3, \tau)$. Since the spatial structure of the turbulence is the same in either reference frame, the functional form of the spatial variation does not change from equation (F-2) to equation (F-3), however the independent variables are modified by the mean velocity in the r_1 direction.

In equation (F-3) time enters explicitly in two ways, the convective time effect and the 'true' time effect. Taylor's hypothesis says that the flow essentially is frozen, i.e. the convective time effect is much greater than the 'true' time effect. Favre's space-time correlation experiments showed this to be a valid approximation in all but that 6% of the boundary layer next to the plate. With this assumption,

$$\check{R}_{jk}(r_i,\tau) = R^*_{jk}(r_1 - U_c\tau, r_2, r_3) \tag{F-4}$$

Since equation (F-1) is the correlation coefficient in the moving frame, if we let $f(r') = \exp(-r'^2/L^2)$

$$\check{R}_{22}(r_i,\tau) = \left[1 - r_3^2/L^2 - (r_1 - U_c\tau)^2/L^2\right]\exp\left[-(r_1 - U_c\tau)^2/L^2\right]\exp\left[-(r_3^2 + r_2^2)/L^2\right] \tag{F-5}$$

APPENDIX G

FOURIER TRANSFORMATION OF EQUATION (3-8)

Represent the $\check{\tau}$ and $\check{r}_1$ integrals obtained from substituting equation (3-8) into equation (3-9) by

$$I = \int_{-\infty}^{\infty} \exp(-i\check{\omega}\check{\tau})\, d\check{\tau} \int_{-\infty}^{\infty} \phi(\check{r}_1 - \check{\tau})^2\, d\check{r}_1 \qquad \text{(G-1)}$$

Express equation (G-1) as a sum

$$\begin{aligned} I = &\int_{0}^{\infty} \exp(-i\check{\omega}\check{\tau})\, d\check{\tau} \int_{0}^{\infty} \phi(\check{r}_1 - \check{\tau})^2\, d\check{r}_1 + \cdots \\ &\cdots \int_{0}^{\infty} \exp(-i\check{\omega}\check{\tau})\, d\check{\tau} \int_{-\infty}^{0} \phi(\check{r}_1 - \check{\tau})^2\, d\check{r}_1 + \cdots \\ &\cdots \int_{-\infty}^{0} \exp(-i\check{\omega}\check{\tau})\, d\check{\tau} \int_{0}^{\infty} \phi(\check{r}_1 - \check{\tau})^2\, d\check{r}_1 + \cdots \\ &\cdots \int_{-\infty}^{0} \exp(-i\check{\omega}\check{\tau}) \int_{-\infty}^{0} \phi(\check{r}_1 - \check{\tau})^2\, d\check{r}_1 \end{aligned} \qquad \text{(G-2)}$$

Define I in equation (G-2) as

$$I = I_1 = I_2 = I_3 = I_4 \qquad \text{(G-3)}$$

respectively.

$$I_2 = \int_{0}^{\infty} \exp(-i\check{\omega}\check{\tau})\, d\check{\tau} \int_{-\infty}^{0} \phi(\check{r}_1 - \tau)^2\, d\check{r}_1 \qquad \text{(G-4)}$$

By rearranging limits and with appropriate changes in the integration variable,

$$I_2 = \int_0^\infty \exp(-i\check{\omega}\check{\tau})\,d\check{\tau}\int_0^\infty \phi(\check{r}_1+\check{\tau})^2\,d\check{r}_1 \tag{G-5}$$

Likewise,

$$I_3 = \int_0^\infty \exp(i\check{\omega}\check{\tau})\,d\check{\tau}\int_0^\infty \phi(\check{r}_1+\check{\tau})^2\,d\check{r}_1 \tag{G-6}$$

and

$$I_4 = \int_0^\infty \exp(i\check{\omega}\check{\tau})\,d\check{\tau}\int_0^\infty \phi(\check{r}_1-\check{\tau})^2\,d\check{r}_1 \tag{G-7}$$

Therefore,

$$I = 2\int_0^\infty \cos(\check{\omega}\check{\tau})\,d\check{\tau}\left[\int_0^\infty \phi(\check{r}_1+\check{\tau})^2\,d\check{r}_1 + \int_0^\infty \phi(\check{r}_1-\check{\tau})^2\,d\check{r}_1\right] \tag{G-8}$$

The Fourier transformation of equation (3-8) is then

$$\Pi'(\check{\omega}) = \frac{2\varphi^2 q_0^2 L^3}{\pi^2\, U_c}\int_0^\infty \cos(\check{\omega}\check{\tau})\left\{\int_0^\infty\int_0^\infty\int_0^\infty [1-\check{r}_3^2-(\check{r}_1-\check{\tau})^2]\cdots\right.$$

$$\exp[-\check{r}_2^2-\check{r}_3^2-(\check{r}_1-\check{\tau})^2]\,d\check{r}_3\,d\check{r}_2\,d\check{r}_1 + \int_0^\infty\int_0^\infty\int_0^\infty [1-\check{r}_3^2-(\check{r}_1+\check{\tau})^2]\cdots \tag{G-9}$$

$$\left.\exp[-\check{r}_2^2-\check{r}_3^2-(\check{r}_1+\check{\tau})^2]\,d\check{r}_3\,d\check{r}_2\,d\check{r}_1\right\}$$

Expanding the exponents and using the hyperbolic identity,

$$\exp(\pm 2\check{r}_1\check{r}) = \cosh(2\check{r}_1\check{r}) \pm \sinh(2\check{r}_1\check{r}) \qquad \text{(G-10)}$$

equation (G-9) becomes

$$\Pi'(\check{\omega}) = \frac{2\varphi^2 g_0^2 L^3}{r^2 v_c}\int_0^\infty \exp(-\check{r}^2)\cos(\check{\omega}\check{r})\,d\check{r}\ldots.$$

$$\ldots\int_0^\infty\int_0^\infty\int_0^\infty\left[\frac{\check{r}_2^{\,2}+\check{r}_3^{\,2}}{\check{r}_3}\right]\left[(1-\check{r}_3^{\,2}-\check{r}_1^{\,2}-\check{r}^2)\cosh(2\check{r}_1\check{r})+\ldots\right. \qquad \text{(G-11)}$$

$$\left.\ldots 2\check{r}_1\check{r}\sinh(2\check{r}_1\check{r})\right]\exp(-r^2)\,d\check{r}_3\,d\check{r}_2\,d\check{r}_1$$

APPENDIX H

INTEGRATION OF EQUATION (3-14)

Equation (3-14) is

$$\check{\Pi}(\check{\omega};\alpha) = \frac{2\rho^2 g_0^2 L^3}{\pi^2 U_c}\int_0^\infty\int_0^\infty\int_0^\infty\left[\frac{\check{r}_2^2+\check{r}_3^2}{\check{r}^3}\right]\exp(-\check{r}_1^2/\alpha^2)\exp[-(\check{r}_2^2+\check{r}_3^2)]\cdots$$

$$\cdots d\check{r}_3\, d\check{r}_2\, d\check{r}_1 \int_0^\infty \exp(-\tau^2/\alpha^2)\cos(\check{\omega}\check{\tau})\left\{\left[1-\check{r}_3^2-\check{r}_1^2/\alpha^2-\check{\tau}^2/\alpha^2\right]\cdots\right. \tag{H-1}$$

$$\left.\cdots\cosh(2\check{r}_1\check{\tau}/\alpha^2)+(2\check{r}_1\check{\tau}/\alpha^2)\sinh(2\check{r}_1\check{\tau}/\alpha^2)\right\}d\check{\tau}$$

First, perform the time integral, I_1 .

$$I_1 = (1-\check{r}_3^2-\check{r}_1^2/\alpha^2)\, I_{1,1} - (1/\alpha^2)\, I_{1,2} + (2\check{r}_1/\alpha^2)\, I_{1,3} \tag{H-2}$$

where

$$I_{1,1} = \int_0^\infty \cos(\check{\omega}\check{\tau})\exp(-\check{\tau}^2/\alpha^2)\cosh(2\check{r}_1\check{\tau}/\alpha^2)\, d\check{\tau}\ , \tag{H-3}$$

$$I_{1,2} = \int_0^\infty \cos(\check{\omega}\check{\tau})\exp(-\check{\tau}^2/\alpha^2)\,\check{\tau}^2\cosh(2\check{r}_1\check{\tau}/\alpha^2)\, d\check{\tau} \tag{H-4}$$

and

$$I_{1,2} = \int_{0}^{\infty} \cos(\check{\omega}\check{\tau}) \exp(-\check{\tau}^2/\alpha^2)\, \check{\tau} \sinh(2\check{r}_1\check{\tau}/\alpha^2)\, d\check{\tau} \qquad \text{(H-5)}$$

The procedure for evaluating equations (H-3), (H-4), and (H-5) is the same. Equation (H-3) will be integrated to demonstrate the procedure. Because the integrand is even in $\check{\tau}$,

$$I_{1,1} = \frac{1}{2}\int_{-\infty}^{\infty} \cos(\check{\omega}\check{\tau}) \exp(-\check{\tau}^2/\alpha^2) \cosh(2\check{r}_1\check{\tau}/\alpha^2)\, d\check{\tau} \qquad \text{(H-6)}$$

Use the identity,

$$\cosh(2\check{r}_1\check{\tau}/\alpha^2) = \frac{1}{2}\left[\exp(2\check{r}_1\check{\tau}/\alpha^2) + \exp(-2\check{r}_1\check{\tau}/\alpha^2)\right] \qquad \text{(H-7)}$$

and substitute it in equation (H-6).

$$I_{1,1} = \frac{1}{4}\int_{-\infty}^{\infty} \cos(\check{\omega}\check{\tau}) \exp[-(\check{\tau}^2 - 2\check{r}_1\check{\tau})/\alpha^2]\, d\check{\tau} + \cdots$$

$$\text{(H-8)}$$

$$\cdots \frac{1}{4}\int_{-\infty}^{\infty} \cos(\check{\omega}\check{\tau}) \exp[-(\check{\tau}^2 + 2\check{r}_1\check{\tau})/\alpha^2]\, d\check{\tau}$$

Define the first integral in equation (H-8) as I_A and the second as I_B. To evaluate I_A, complete the square in the exponent.

$$I_A = \frac{1}{4}\exp(\check{r}_1^2/\alpha^2)\int_{-\infty}^{\infty} \cos(\check{\omega}\check{\tau}) \exp[-(\check{\tau} - \check{r}_1)^2/\alpha^2]\, d\check{\tau} \qquad \text{(H-9)}$$

Let $\lambda = \check{\tau} - \check{r}_1$ in equation (H-9).

$$I_A = \frac{1}{4}\exp(\check{r}_1^2/\alpha^2)\int_{-\infty}^{\infty} \cos[\check{\omega}(\lambda + \check{r}_1)] \exp(-\lambda^2/\alpha^2)\, d\lambda \qquad \text{(H-10)}$$

Expand the double angle cosine in terms of a single angle identity.

$$I_A = \frac{1}{4}\exp(\check{r}_1^2/\alpha^2)\cos(\check{\omega}\check{r}_1)\int_{-\infty}^{\infty}\cos(\check{\omega}\lambda)\exp(-\lambda^2/\alpha^2)d\lambda \quad - \quad \cdots$$

(H-11)

$$\cdots \frac{1}{4}\exp(\check{r}_1^2/\alpha^2)\sin(\check{\omega}\check{r}_1)\int_{-\infty}^{\infty}\sin(\check{\omega}\lambda)\exp(-\lambda^2/\alpha^2)d\lambda$$

The second integral in equation (H-11) vanishes as the integrand is odd in λ. Now equation (H-11) can be integrated.

$$I_A = \frac{1}{4}\exp(\check{r}_1^2/\alpha^2)\cos(\check{\omega}\check{r}_1)\left[\alpha\sqrt{\pi}\exp(-\alpha^2\check{\omega}^2/4)\right] \qquad \text{(H-12)}$$

If I_B is integrated, the result is identical to equation I_A. Thus,

$$I_{1,1} = (\alpha\sqrt{\pi}/2)\cos(\check{\omega}\check{r}_1)\exp(\check{r}_1^2/\alpha^2)\exp(-\alpha^2\check{\omega}^2/4) \qquad \text{(H-13)}$$

Using the same integration procedure,

$$I_{1,2} = \frac{\sqrt{\pi}}{2}\exp(\check{r}_1^2/\alpha^2)\exp(-\alpha^2\check{\omega}^2/4)\left\{\cos(\check{\omega}\check{r}_1)\left[\frac{1}{2\alpha} - \frac{\alpha\check{\omega}^2}{4} + \alpha\check{r}_1^2\right] - \left(\frac{\check{\omega}\check{r}_1}{2}\right)\sin(\check{\omega}\check{r}_1)\right\}$$

(H-14)

and

$$I_{1,3} = \frac{\sqrt{\pi}}{2}\exp(\check{r}_1^2/\alpha^2)\exp(-\alpha^2\check{\omega}^2/4)\left[\alpha\check{r}_1\cos(\check{\omega}\check{r}_1) - (\check{\omega}/2\alpha)\sin(\check{\omega}\check{r}_1)\right] \qquad \text{(H-15)}$$

Now substitute equations (H-13), (H-14), and (H-15) into equation (H-2).

$$I_1 = \left(\frac{\alpha\sqrt{\pi}}{2}\right)\exp(\check{r}_1^2/\alpha^2)\exp(-\alpha^2\check{\omega}^2/4)\cos(\check{\omega}\check{r}_1)\left[1 - \frac{1}{2\alpha^4} + \frac{\check{\omega}^2}{4\alpha^2} - \check{r}_3^2\right] \qquad \text{(H-16)}$$

$$\check{\Pi}'(\check{\omega};\alpha) = \frac{\alpha \rho^2 L \check{g}_0^{3\,2}}{\pi^{3/2}\, \tau/c} \exp(-\alpha^2 \check{\omega}^2/4) \int_0^\infty \int_0^\infty (\check{r}_2^2 + \check{r}_3^2) \exp(\check{r}_2^2 + \check{r}_3^2) \cdots$$

(H-17)

$$\cdots \left[1 - \frac{1}{2\alpha^4} + \frac{\check{\omega}^2}{4\alpha^2} - \check{r}_3^2\right] d\check{r}_3\, d\check{r}_2 \int_0^\infty \frac{\cos(\check{\omega}\check{r}_1)}{\check{r}^3}\, d\check{r}_1$$

where $\check{r}^3 = (\check{r}_1^2 + \check{r}_2^2 + \check{r}_3^2)^{\frac{3}{2}}$

Define I_2 as

$$I_2 = \int_0^\infty \frac{\cos(\check{\omega}\check{r}_1)}{\check{r}^3}\, d\check{r}_1 \qquad \text{(H-18)}$$

From the integral identity,

$$\int_0^\infty \frac{\cos x\, dx}{(x^2 + \rho^2)^{3/2}} = \frac{K_1(\rho)}{\rho} \qquad \text{(H-19)}$$

$$I_2 = \check{\omega}\; K_1\left(\check{\omega}\sqrt{\check{r}_2^2 + \check{r}_3^2}\right) \Big/ \sqrt{\check{r}_2^2 + \check{r}_3^2} \qquad \text{(H-20)}$$

where K_1 is a modified Bessel function. Put equation (H-20) back into equation (H-17).

$$\check{\Pi}'(\check{\omega};\alpha) = \frac{\alpha \rho^2 g_0^2 L^3}{\pi^{3/2}\, \tau/c} \left[\check{\omega} \exp(-\alpha^2 \check{\omega}^2/4)\right] \int_0^\infty \int_0^\infty \sqrt{\check{r}_2^2 + \check{r}_3^2}\, \exp(\check{r}_2^2 + \check{r}_3^2) \cdots$$

(H-21)

$$\cdots \left[1 - \frac{1}{2\alpha^4} + \frac{\check{\omega}^2}{4\alpha^2} - \check{r}_3^2\right] K_1\left(\check{\omega}\sqrt{\check{r}_2^2 + \check{r}_3^2}\right) d\check{r}_3\, d\check{r}_2$$

The symmetry in r_2 and r_3 suggests the use of cylindrical coordinates. Thus, let

$$\rho^2 = \check{r}_2^2 + \check{r}_3^2 \tag{H-22a}$$

and

$$\cos\varphi = \check{r}_3/\rho \tag{H-22b}$$

Now define I_3 as

$$I_3 = \check{\omega}\exp(-\alpha^2\check{\omega}^2/4)\int_0^{\pi/2} d\varphi \int_0^{\infty} \rho^2 \exp(\rho^2) K_1(\check{\omega}\rho) \cdots$$

$$\cdots \left(1 - \frac{1}{2\alpha^4} + \frac{\check{\omega}^2}{4\alpha^2} - \rho^2\cos\varphi\right) d\rho \tag{H-23}$$

Divide equation (H-23) into two integrals and perform the φ integration.

$$I_3 = (\pi/2)\,\check{\omega}\exp(-\alpha^2\check{\omega}^2/4)(1 - 1/2\alpha^4 + \check{\omega}^2/4\alpha^2)\cdots$$

$$\cdots\int_0^{\infty} \rho^2 K_1(\check{\omega}\rho)\exp(-\rho^2)\,d\rho - (\pi/4)\,\check{\omega}\exp(-\alpha^2\check{\omega}^2/4)\cdots \tag{H-24}$$

$$\cdots\int_0^{\infty} \rho^4 K_1(\check{\omega}\rho)\exp(-\rho^2)\,d\rho$$

Let $\zeta^2 = \lambda$.

$$I_3=\left(\frac{\pi}{4}\right)\breve{\omega}\exp(-\alpha^2\breve{\omega}^2/4)\left(2-\frac{1}{\alpha^4}+\frac{\breve{\omega}^2}{2\alpha^2}\right)\int_0^\infty\sqrt{\lambda}\,K_1(\breve{\omega}\lambda^{1/2})\exp(-\lambda)d\lambda\ - \cdots$$

$$\cdots\left(\frac{\pi}{4}\right)\breve{\omega}\exp(-\alpha^2\breve{\omega}^2/4)\int_0^\infty\lambda^{3/2}K_1(\breve{\omega}\lambda^{1/2})\exp(-\lambda)\,d\lambda \tag{H-25}$$

Define I_A and I_B from equation (H-25) as

$$I_A=\int_0^\infty\exp(-\lambda)\,\lambda^{1/2}K_1(\breve{\omega}\lambda^{1/2})d\lambda \tag{H-26}$$

and

$$I_B=\int_0^\infty\exp(-\lambda)\lambda^{3/2}K_1(\breve{\omega}\lambda^{1/2})d\lambda \tag{H-27}$$

The following identities and relationships will be useful in integrating equations (H-26) and (H-27).

$$\int_0^\infty\exp(-t)\,t^{-a/2}K_a\left[2(z\,t)^{1/2}\right]dt=\frac{\Gamma(a,z)\Gamma(1-a)}{2z^{a/2}\exp(-z)} \tag{H-28}$$

where the real part of a is less than 1 and $\Gamma(a, z)$ is the incomplete Gamma function.

$$K_{-a}(z)=K_a(z) \tag{H-29}$$

$$K_{a-1}(z)\exp[(a-1)\pi i]-K_{a+1}(z)\exp[(a+1)\pi i]=\frac{2a}{z}K_a(z)\exp(a\pi i) \tag{H-30}$$

where $i = \sqrt{-1}$.

Integrate equation I_A by letting $a = -1$, $z = \check{\omega}^2/4$, and $t = \lambda$ in equation (H-28) and using equation (H-29).

$$I_A = (\check{\omega}/4)\exp(\check{\omega}^2/4)\,\Gamma(-1, \check{\omega}^2/4) \tag{H-31}$$

$\Gamma(-1, \check{\omega}^2/4)$ can be evaluated from

$$\Gamma(-n, z) = \left[(-1)^n/n!\right]\left[E_1(z) - \exp(-z)\sum_{j=0}^{n-1}\frac{(-1)^j\, j!}{z^{j+1}}\right] \tag{H-32}$$

where $E_1(x) = \int_1^\infty [\exp(-x\lambda)/\lambda]\,d\lambda$.

$$I_A = (\check{\omega}/4)\exp(\check{\omega}^2/4)\left[-E_1(\check{\omega}^2/4) + (4/\check{\omega}^2)\exp(-\check{\omega}^2/4)\right] \tag{H-33}$$

To integrate I_B, first express $K_1(z)$ in terms of $K_2(z)$ and $K_3(z)$ using equation (H-30).

$$K_1(\check{\omega}\lambda^{1/2}) = K_3(\check{\omega}\lambda^{1/2}) - (4/\check{\omega}\lambda^{1/2})\,K_2(\check{\omega}\lambda^{1/2}) \tag{H-34}$$

Then,

$$I_B = \int_0^\infty \exp(-\lambda)\lambda^{3/2} K_3(\check{\omega}\lambda^{1/2})\,d\lambda - (4/\check{\omega})\int_0^\infty \exp(-\lambda)\lambda\, K_2(\check{\omega}\lambda^{1/2})\,d\lambda \tag{H-35}$$

Each of the integrals in equation (H-35) can be integrated in a manner similar to I_A.

$$I_B = -(\check{\omega}/4)\exp(\check{\omega}^2/4)\left\{(2 + \check{\omega}^2/4)\,E_1(\check{\omega}^2/4) - \left[(\check{\omega}^2+4)/\check{\omega}^2\right]\exp(-\check{\omega}^2/4)\right\} \tag{H-36}$$

Combining equations (H-24), (H-33), and (H-35) and substituting them into equation (H-21), the final result is

$$\check{\Pi}'(\check{\omega};\alpha) = \frac{\alpha \rho^2 L^3 g_0^2}{4\pi^{1/2} U_c}\left\{\frac{\check{\omega}^2}{4}\left[\frac{\check{\omega}^2}{4} - \frac{\check{\omega}^2}{2\alpha^2} + \frac{1}{\alpha^4}\right]E_1(\check{\omega}^2/4) + \cdots\right. \tag{H-37}$$

$$\left.\cdots \exp(-\check{\omega}^2/4)\left[(\check{\omega}^2/4)(2/\alpha^2 - 1) + 1 - 1/\alpha^4\right]\right\}$$

APPENDIX I

DETERMINATION OF C_1 ($\hat{y}_2$)

The integral scale, $C_1 = \delta^*/L$ in equation (4-15), is a strong function of $\hat{y}_2$. This is shown in Grant's (1958) data, Figure 7. This figure is a plot of the velocity correlation components at various values of y_2/δ_o. δ_o is defined as the value of y_2 where $\bar{U}_2 = U_\infty - U_\tau$ and is equal to .69 δ. For this data $Re_{\delta^*} = 3\cdot10^3$ and $\delta^*/\delta = .158$.

The scale anisotropy model of these components are from (4-17)

$$\hat{R}_{22}(\hat{r}_1, 0, 0; \alpha) = \left(1 - \frac{C_1}{2}\frac{\hat{r}_1}{\alpha}\right)exp(-C_1\hat{r}_1/\alpha) \tag{I-1}$$

$$\hat{R}_{22}(0, \hat{r}_2, 0) = exp(-C_1\hat{r}_2) \tag{I-2}$$

$$\hat{R}_{22}(0, 0, \hat{r}_3) = \left(1 - \frac{C_1}{2}\hat{r}_3\right)exp(-C_1\hat{r}_3) \tag{I-3}$$

The values of C_1 ($\hat{y}_2$) can be computed by fitting any equation (I-1) through (I-3) to Grant's data. This was done using the method of least squares and a minimization routine to optimize the value of C_1. The values are plotted in Figure 8.

When equation (I-1) was used an iteration scheme was necessary.

First $\alpha = 1$ was used and C_1 determined. This C_1 was employed to find $\alpha(\hat{r})$ to improve the fit. $\alpha(r)$ varied from .9 to 2.1. Finally the new C_1 was found. There was not much difference between the last C_1 and the first so the iteration was stopped.

The equation chosen to fit the variation of C_1 was

$$C_1(y_2/\delta) = 1 + \frac{A}{(1 + By_2/\delta)^C} \tag{I-4}$$

The constants A, B, and C were computed by the method of least squares using the multidimensional, numerical, minimization Fortran subroutine STEPIT developed by Professor J. P. Chandler. The final result in terms of the non-dimensional variables of the problem is

$$C_1(\hat{y}_2) = 1 + .111/(.748 \cdot 10^{-7} + \hat{y}_2 \delta^*/\delta)^{.937} \tag{I-5}$$

This curve is plotted in Figure 8 with the independent variable y_2/δ.

APPENDIX J

PROBABILITY DISTRIBUTION FUNCTION $p_{3_i}(\hat{k}_3, \hat{y}_2, \hat{y}'_2)$

AND ITS INVERSION EQUATIONS

The method used to obtain $p_{3_i}(\hat{k}_3, \hat{y}_2, \hat{y}'_2)$ was 'stumbled upon' after attempting to importance sample each of the three variables separately, i.e.

$$p_{3i}(\hat{k}_3, \hat{y}_2, \hat{y}_2') = p_4(\hat{k}_3)\, p_{5i}(\hat{y}_2)\, p_{6i}(\hat{y}_2') \tag{J-1}$$

In this case,

$$p_4(\hat{k}_3) \propto 1/\hat{k}^2 \tag{J-2}$$

$$p_{5i}(\hat{y}_2) \propto \exp[-(\hat{k}_1 + C_i)\hat{y}_2] \tag{J-3}$$

$$p_{6i}(\hat{y}_2') \propto \exp[-(\hat{k}_1 + C_i)\hat{y}_2'] \tag{J-4}$$

These function were derived after looking at the function format of (5-22). Later it was realized that the three one-dimensional probability density functions of equation (J-1) can be combined into one three-dimensional probability density function. From equation (5-24) or (5-25),

$$p_{3i}(\hat{k}_3, \hat{y}_2, \hat{y}_2')\, d\hat{k}_3\, d\hat{y}_2\, d\hat{y}_2' = du\, dv\, dw \tag{J-5}$$

Since (5-22) is symmetric in the variables $\hat{y}_2$ and $\hat{y}'_2$, $p'_{3_i}(\hat{k}_3, \hat{y}_2)$ will be used in the derivation in lieu of p_{3_i}. Thus,

$$p_{3i}'(\hat{k}_3, \hat{y}_2)\, d\hat{k}_3\, d\hat{y}_2 = du\, dv \tag{J-6}$$

Motivated by equations (J-2) and J-1), let

$$P_{3i}'(\hat{k}_3,\hat{y}_2)=\left\{\frac{\hat{k}_1}{\hat{k}^2\tan^{-1}(d/k_1)}\right\}\left\{\frac{(\hat{k}+C_i)\exp[-(\hat{k}+C_i)\hat{y}_2]}{\exp[-(\hat{k}+C_i)a]-\exp[-(\hat{k}+C_i)b]}\right\} \qquad \text{(J-7)}$$

This form satisfies the necessary conditions for the probability density function

$$\int_0^d\int_a^b P_{3i}'(\hat{k}_3,\hat{y}_2)\,d\hat{k}_3\,d\hat{y}_2 = 1 \qquad \text{(J-8)}$$

and

$$P_{3i}'(\hat{k}_3,\hat{y}_2) > 0 \qquad \text{(J-9)}$$

Equations (J-8) and (J-9) are not sufficient to get the inversion equations for u and v. One of the inversion equations can be selected arbitrarily in conjunction with the form of equation (J-7). The other is computed from the choice of the first, equation (J-6), noting that it is Jacobian of the two-dimensional transformation. Compute the equation for u by assuming $u = u(\hat{k}_3)$ and

$$du = \left[\hat{k}_1/\tan^{-1}(d/\hat{k}_1)\right]d\hat{k}_3 \qquad \text{(J-10)}$$

Then

$$u(\hat{k}_3) = \tan^{-1}(\hat{k}_3/\hat{k}_1)\Big/\tan^{-1}(d/\hat{k}_1) \qquad \text{(J-11)}$$

is one of the inversion equations from which

$$\hat{k}_3 = \hat{k}_1\tan\left[u\tan^{-1}(d/\hat{k}_1)\right] \qquad \text{(J-12)}$$

To obtain the other inversion equation, $v = v(\hat{k}_3, \hat{y}_2)$, use the Jacobian of the two-dimensional transformation which is equal to $p'_{3_i}(\hat{y}_2, \hat{k}_3)$ in equation (J-6).

$$p'_{3i}(\hat{k}_3, \hat{y}_2) = \frac{\partial v}{\partial \hat{y}_2}\frac{\partial u}{\partial \hat{k}_3} - \frac{\partial u}{\partial \hat{y}_2}\frac{\partial v}{\partial \hat{k}_3} \tag{J-13}$$

From equation (J-11),

$$\partial u/\partial \hat{k}_3 = \left[\frac{\hat{k}_1}{\tan^{-1}(d/\hat{k}_1)}\right]\left[1/\hat{k}^2\right] \tag{J-14}$$

and

$$\frac{\partial v}{\partial \hat{k}_3} = 0 \tag{J-15}$$

Substituting equations (J-14) and (J-15) into equation (J-13),

$$p'_{3i}(\hat{k}_3, \hat{y}_2) = \left[\hat{k}_1/\tan^{-1}(d/\hat{k}_1)\right]\left[1/\hat{k}^2\right]\frac{\partial v}{\partial \hat{y}_2} \tag{J-16}$$

After substituting equation (J-7) into equation (J-16) and integrating

$$v = g(\hat{k}_3) + \int_{\substack{a \\ \hat{k}_3 = \text{const.}}}^{\hat{y}_2} \frac{(\hat{k} + C_i)\exp[-(\hat{k} + C_i)\Upsilon]\,d\Upsilon}{\exp[-(\hat{k}+C_i)a] - \exp[-(\hat{k}+C_i)b]} \tag{J-17}$$

Let $g(\hat{k}_3) = 0$, then

$$v = \frac{1 - \exp[-(\hat{k} + C_i)\hat{y}_2]}{\exp[-(\hat{k}+C_i)a] - \exp[-(\hat{k}+C_i)b]} \tag{J-18}$$

When inverted,

$$\hat{y}_2 = -\ln\left[1 - v\{\exp[-(\hat{k}+C_i)a] - \exp[-(\hat{k}+C_i)b]\}\right]/(\hat{k}+C_i) \quad \text{(J-19)}$$

Because of the symmetry in $\hat{y}_2$ and $\hat{y}_2'$,

$$P_{3i}(\hat{k}_3, \hat{y}_2, \hat{y}_2') = \left\{\frac{\hat{k}_1}{\hat{k}^2 \tan^{-1}(d/k_i)}\right\}\left\{\frac{(\hat{k}+C_i)^2}{\{\exp[-(\hat{k}+C_i)a] - \exp[-(\hat{k}+C_i)b]\}}\right\} \cdots$$

(J-20)

$$\cdots\left\{\frac{\exp[-(\hat{k}+C_i)(\hat{y}_2+\hat{y}_2')]}{\{\exp[-(\hat{k}+C_i)e] - \exp[-(\hat{k}+C_i)f]\}}\right\}$$

$$w = \frac{1 - \exp[-(\hat{k}+C_i)\hat{y}_2']}{\exp[-(\hat{k}+C_i)e] - \exp[-(\hat{k}+C_i)f]} \quad \text{(J-21)}$$

and

$$\hat{y}_2' = -\ln\left[1 - w\{\exp[-(\hat{k}+C_i)e] - \exp[-(\hat{k}+C_i)f]\}\right]/(\hat{k}+C_i)$$

(J-22)

APPENDIX K

COMPUTER PROGRAM LISTING

```
C * * * * * * * * * * * * * * * * * * * * * * * * * * * * * * * * * * * * MCAR0010
C  MONTE CARLO INTEGRATION OF THE WAVE NUUBER SPECTRUM EQUATION FOR THE MCAR0020
C  SURFACE-PRESSURE FLUCTUATIONS UNDER A TURBULENT BOUNDARY LAYER.      MCAR0030
C * * * * * * * * * * * * * * * * * * * * * * * * * * * * * * * * * * * * MCAR0040
C  PROGRAM INPUTS:                                                       MCAR0050
C  ENTER THE BOUNDARY LAYER PARAMETERS IN BLOCK DATA.  THOSE NEEDED ARE MCAR0060
C  DEL - B.L. THICKNESS (FT.); DELST - B.L. DISPLACEMENT THICKNESS (FT.)MCAR0070
C  UTAU - FRICTION VELOCITY (FPS); (THE PRECEEDING MUST BE COMPUTED FROMMCAR0080
C  THE LAW OF THE WALL AND WAKE); UINFN - FREE STREAM VELOCITY (FPS);   MCAR0090
C  ANU - THE KINEMATIC VISCOSITY (FT.SQ/SEC).  ENTER N, THE NUMBER OF   MCAR0100
C  NON-ZERO ITERATIONS IN CARD MCAR0340.  ENTER ALPHA, THE SCALE ANISO- MCAR0110
C  TROPY FACTOR IN CARD MCAR0350.  ENTER BRK1, THE STREAMWISE WAVE      MCAR0120
C  NUMBER IN CARD NUMBER MCAR0370..  AFTER N ITERATIONS THE INTEGRAL    MCAR0130
C  VALUE, ERROR VALUES, AND REGIONAL CONTRIBUTIONS ARE PRINTED OUT.     MCAR0140
C * * * * * * * * * * * * * * * * * * * * * * * * * * * * * * * * * * * * MCAR0150
C                                                                       MCAR0160
C                                                                       MCAR0170
      COMMON/BLPAR/ANU,DEL,DELST,UTAU,UINFN,VKC,TURPI,ALFAC,EM,A,B      MCAR0180
      COMMON/BLCMP/ TRENO, SLOLM, SVK1, SVK3, SVK4, SVK5, SVK6, SVK7,   MCAR0190
     *SVK8,BI,DELRA,ALIM,AK,BK                                          MCAR0200
      COMMON BRK1,BARK,ALPHA                                            MCAR0210
      DIMENSION TERM(200)                                               MCAR0220
      DOUBLE PRECISION SAV15,SAV16,SAV25,SAV26,SAV35,SAV36,SAV45,SAV46,SMCAR0230
     $AV55,SAV56,SAV65,SAV66,SAV75,SAV76,SAV85,SAV86,SAV95,SAV96        MCAR0240
      WRITE(6,501)                                                      MCAR0250
  501 FORMAT(1H1,50X,'M O N T E   C A R L O ',/,51X,'__________________MCAR0260
     $__'   ,/,43X,'M U L T I P L E   I N T E G R A T I O N ',/,43X,    MCAR0270
     $'______________________________________'   ,/,53X,'T E C H N I Q MCAR0280
      U E',/,53X,'_________________')                                   MCAR0290
C                                  * PROGRAM MULTIPLIERS AND CONSTANTS *MCAR0300
      PI = 3.1417                                                       MCAR0310
      PI2=PI/2.                                                         MCAR0320
      K=100                                                             MCAR0330
      N=5000                                                            MCAR0340
      ALPHA=1.                                                          MCAR0350
C                                      * K1 *                           MCAR0360
      BRK1=1.                                                           MCAR0370
      BK1SQ=BRK1**2                                                     MCAR0380
C                                      * C1 FOR VARIANCE REDUCTION *    MCAR0390
      C1IN=1.+.111/(.7478E-7+.025)**.9367                               MCAR0400
      C1MD=1.+.111/(.7478E-7+.20)**.9367                                MCAR0410
      C1OT=1.+.111/(.7478E-7+1.)**.9367                                 MCAR0420
C                                      * BOUNDARY LAYER PARAMETERS *    MCAR0430
      VRAT = UTAU/UINFN                                                 MCAR0440
      DELRA=DELST/DEL                                                   MCAR0450
      TRENO = UTAU*DEL/ANU                                              MCAR0460
      SLOLM = 33.2/TRENO                                                MCAR0470
      SVK1 = 1.0/VKC                                                    MCAR0480
      SVK2 = ALFAC*VKC                                                  MCAR0490
      SVK3 = PI*TURPI/SVK2                                              MCAR0500
      SVK4 = PI/ALFAC                                                   MCAR0510
      SVK5 = 1.0/SVK2                                                   MCAR0520
      SVK6 = 1.0 - ALFAC                                                MCAR0530
      SVK7 = EM - 1.0                                                   MCAR0540
```

```
      SVK8 =TRENO/A                                                     MCAR0550
      BI = 1.0/B                                                        MCAR0560
C                                       * SUBLAYER PARAMETERS *         MCAR0570
      YSTR=8.                                                           MCAR0580
      ALIM=YSTR/TRENO                                                   MCAR0590
      AK=.75/ALIM**1.5-16.3                                             MCAR0600
      BK=-.45/ALIM**2.5                                                 MCAR0610
C                                                                       MCAR0620
C                                       * K3 UPPER LIMIT *              MCAR0630
      ULIMK=50.                                                         MCAR0640
      ARGX1=ATAN(ULIMK/BRK1)                                            MCAR0650
C                                       * INTEGRAL MULTIPLIER *         MCAR0660
      CFSQ=4.*VRAT**4                                                   MCAR0670
      FACT1=8.*ALPHA*CFSQ/PI**2                                         MCAR0680
      VOLX1=PI2*BRK1                                                    MCAR0690
      VOLX4=2.*PI                                                       MCAR0700
      FACT=VOLX1*VOLX4*FACT1                                            MCAR0710
C                                       * INITIALIZE *                  MCAR0720
      SUM=0.                                                            MCAR0730
      SUMSQ=0.                                                          MCAR0740
      SUMT=0.                                                           MCAR0750
      SUMIN=0.                                                          MCAR0760
      SUMMD=0.                                                          MCAR0770
      SUMOT=0.                                                          MCAR0780
      I=0                                                               MCAR0790
      KOUNT=0                                                           MCAR0800
      J=0                                                               MCAR0810
C                                       * K1 LOOP *                     MCAR0820
   40 SUM15=0.                                                          MCAR0830
      SUM16=0.                                                          MCAR0840
      SUM25=0.                                                          MCAR0850
      SUM26=0.                                                          MCAR0860
      SUM35=0.                                                          MCAR0870
      SUM36=0.                                                          MCAR0880
      SUM45=0.                                                          MCAR0890
      SUM46=0.                                                          MCAR0900
      SUM55=0.                                                          MCAR0900
      SUM55=0.                                                          MCAR0910
      SUM56=0.                                                          MCAR0920
      SUM65=0.                                                          MCAR0930
      SUM66=0.                                                          MCAR0940
      SUM75=0.                                                          MCAR0950
      SUM76=0.                                                          MCAR0960
      SUM85=0.                                                          MCAR0970
      SUM86=0.                                                          MCAR0980
      SUM95=0.                                                          MCAR0990
      SUM96=0.                                                          MCAR1000
C                                       * ITERATION STARTING POINT *    MCAR1010
   50 I=I+1                                                             MCAR1020
      M=0                                                               MCAR1030
C                                       * VARIABLE FOR KTIL3 *          MCAR1040
      U1=CORPUT(1,M)                                                    MCAR1050
      X1A=TAN(ARGX1*U1)                                                 MCAR1050
      X1=BRK1*X1A                                                       MCAR1060
```

```
      BRKSQ=BK1SQ+X1**2                                              MCAR1070
      BARK=SQRT(BRKSQ)                                               MCAR1080
C                                   * VARIABLE FOR YTIL2 *           MCAR1090
      U2=CORPUT(2,M)                                                 MCAR1100
C                                   * INNER REGION *                 MCAR1110
      CIN=14.+BARK                                                   MCAR1120
      EXPIN=1.-EXP(-.025*CIN/DELRA)                                  MCAR1130
      VOLIN=EXPIN/CIN                                                MCAR1140
      X2AI=1.-U2*EXPIN                                               MCAR1150
      X2I=-ALOG(X2AI)/CIN                                            MCAR1160
      XF2I=VOLIN/X2AI                                                MCAR1170
      ARG2I=DELRA*X2I                                                MCAR1180
C                                   * MIDDLE REGION *                MCAR1190
      CMD=1.6+BARK                                                   MCAR1200
      XPMD=EXP(-.025*CMD/DELRA)                                      MCAR1210
      EXPMD=XPMD-EXP(-.2*CMD/DELRA)                                  MCAR1220
      VOLMD=EXPMD/CMD                                                MCAR1230
      X2AM=XPMD-U2*EXPMD                                             MCAR1240
      X2M=-ALOG(X2AM)/CMD                                            MCAR1250
      XF2M=VOLMD/X2AM                                                MCAR1260
      ARG2M=DELRA*X2M                                                MCAR1270
C                                   * OUTER REGION *                 MCAR1280
      COT=.3+BARK                                                    MCAR1290
      XPOT=EXP(-.2*COT/DELRA)                                        MCAR1300
      IF(XPOT)50,50,200                                              MCAR1310
  200 EXPOT=XPOT-EXP(-COT/DELRA)                                     MCAR1320
      VOLOT=EXPOT/COT                                                MCAR1330
      X2AT=XPOT-U2*EXPOT                                             MCAR1340
      X2T=-ALOG(X2AT)/COT                                            MCAR1350
      XF2T=VOLOT/X2AT                                                MCAR1360
      ARG2T=DELRA*X2T                                                MCAR1370
C                                   * VARIABLE FOR YTIL2' *          MCAR1380
      U3=CORPUT(3,M)                                                 MCAR1390
C                                   * INNER REGION *                 MCAR1400
      X3AI=1.-U3*EXPIN                                               MCAR1410
      X3I=-ALOG(X3AI)/CIN                                            MCAR1420
      XF3I=VOLIN/X3AI                                                MCAR1430
      ARG3I=DELRA*X3I                                                MCAR1440
C                                   * MIDDLE REGION *                MCAR1450
      X3AM=XPMD-U3*EXPMD                                             MCAR1460
      X3M=-ALOG(X3AM)/CMD                                            MCAR1470
      XF3M=VOLMD/X3AM                                                MCAR1480
      ARG3M=DELRA*X3M                                                MCAR1490
C                                   * OUTER REGION *                 MCAR1500
      X3AT=XPOT-U3*EXPOT                                             MCAR1510
      X3T=-ALOG(X3AT)/COT                                            MCAR1520
      XF3T=VOLOT/X3AT                                                MCAR1530
      ARG3T=DELRA*X3T                                                MCAR1540
C                                   * VARIABLE FOR THETA *           MCAR1550
      U4=CORPUT(4,M)                                                 MCAR1560
      X4=2.*PI*U4                                                    MCAR1570
C                                   * C1 FOR FUNCTION COMPUTATION *  MCAR1580
      C1I=1.+.111/(.7478E-7+DELRA*X2I)**.9367                        MCAR1590
      C1M=1.+.111/(.7478E-7+DELRA*X2M)**.9367                        MCAR1600
```

```
      C1T=1.+.111/(.7478E-7+DELRA*X2T)**.9367                           MCAR1610
C                                          * VARIABLE FOR RTIL TERMS *  MCAR1620
      U5=CORPUT(5,M)                                                    MCAR1620
C                                          * VARIABLE FOR RTIL *        MCAR1630
      CALL XMEAX(1,-C1IN,U5,X5,XF5)                                     MCAR0640
      X5I=X5                                                            MCAR0650
      XF5I=XF5                                                          MCAR1660
      CALL XMEAX(1,-C1MD,U5,X5,XF5)                                     MCAR1670
      X5M=X5                                                            MCAR1680
      XF5M=XF5                                                          MCAR1690
      CALL XMEAX(1,-C1OT,U5,X5,XF5)                                     MCAR1700
      X5T=X5                                                            MCAR1710
      XF5T=XF5                                                          MCAR1720
C                                          * VARIABLE FOR RTILSQ *      MCAR1730
      CALL XMEAX(2,-C1IN,U5,X6,XF6)                                     MCAR1740
      X6I=X6                                                            MCAR1750
      XF6I=XF6                                                          MCAR1760
      CALL XMEAX(2,-C1MD,U5,X6,XF6)                                     MCAR1770
      X6M=X6                                                            MCAR1780
      XF6M=XF6                                                          MCAR1790
      CALL XMEAX(2,-C1OT,U5,X6,XF6)                                     MCAR1800
      X6T=X6                                                            MCAR1810
      XF6T=XF6                                                          MCAR1820
C                                                                       MCAR1830
C                                          * TERMS OF TOTAL INTEGRAL *  MCAR1840
C                                                                       MCAR1850
C                                          * X2 TERMS *                 MCAR1860
      CALL SUBX2(FX2,X2I,ARG2I,XF2I)                                    MCAR1870
      IF(FX2)50,50,210                                                  MCAR1880
  210 FX2I=FX2                                                          MCAR1890
      CALL SUBX2(FX2,X2M,ARG2M,XF2M)                                    MCAR1900
      IF(FX2)50,50,220                                                  MCAR1910
  220 FX2M=FX2                                                          MCAR1920
      CALL SUBX2(FX2,X2T,ARG2T,XF2T)                                    MCAR1930
      IF(FX2)50,50,230                                                  MCAR1940
  230 FX2T=FX2                                                          MCAR1950
C                                          * X3 TERMS *                 MCAR1960
      CALL SUBX3(FX3,X3I,ARG3I,XF3I)                                    MCAR1970
      IF(FX3)50,50,240                                                  MCAR1980
  240 FX3I=FX3                                                          MCAR1990
      CALL SUBX3(FX3,X3M,ARG3M,XF3M)                                    MCAR2000
      IF(FX3)50,50,250                                                  MCAR2010
  250 FX3M=FX3                                                          MCAR2020
      CALL SUBX3(FX3,X3T,ARG3T,XF3T)                                    MCAR2030
      IF(FX3)50,50,260                                                  MCAR2040
  260 FX3T=FX3                                                          MCAR2050
C                                          * X4,X5,&X6 TERMS *          MCAR2060
C                                                                       MCAR2070
      CALL SUBU5(X1,X2I,X3I,X4,X5I,X6I,C1I,XF5I,XF6I,FX5,FX6)           MCAR2080
      F1X5=FX5                                                          MCAR2090
      F1X6=FX6                                                          MCAR2100
      IF(FX5.EQ.0.) GO TO 50                                            MCAR2110
      IF(FX6.EQ.0.) GO TO 50                                            MCAR2120
      CALL SUBU5(X1,X2I,X3M,X4,X5I,X6I,C1I,XF5I,XF6I,FX5,FX6)           MCAR2130
```

```
      F2X5=FX5                                                          MCAR2140
      F2X6=FX6                                                          MCAR2150
      IF(FX5.EQ.0.) GO TO 50                                            MCAR2160
      IF(FX6.EQ.0.) GO TO 50                                            MCAR2170
      CALL SUBU5(X1,X2I,X3T,X4,X5I,X6I,C1I,XF5I,XF6I,FX5,FX6)           MCAR2180
      F3X5=FX5                                                          MCAR2190
      F3X6=FX6                                                          MCAR2200
      IF(FX5.EQ.0.) GO TO 50                                            MCAR2210
      IF(FX6.EQ.0.) GO TO 50                                            MCAR2220
      CALL SUBU5(X1,X2M,X3I,X4,X5M,X6M,C1M,XF5M,XF6M,FX5,FX6)           MCAR2230
      F4X5=FX5                                                          MCAR2240
      F4X6=FX6                                                          MCAR2250
      IF(FX5.EQ.0.) GO TO 50                                            MCAR2260
      IF(FX6.EQ.0.) GO TO 50                                            MCAR2270
      CALL SUBU5(X1,X2M,X3M,X4,X5M,X6M,C1M,XF5M,XF6M,FX5,FX6)           MCAR2280
      F5X5=FX5                                                          MCAR2290
      F5X6=FX6                                                          MCAR2300
      IF(FX5.EQ.0.) GO TO 50                                            MCAR2310
      IF(FX6.EQ.0.) GO TO 50                                            MCAR2320
      CALL SUBU5(X1,X2M,X3T,X4,X5M,X6M,C1M,XF5M,XF6M,FX5,FX6)           MCAR2330
      F6X5=FX5                                                          MCAR2340
      F6X6=FX6                                                          MCAR2350
      IF(FX5.EQ.0.) GO TO 50                                            MCAR2360
      IF(FX6.EQ.0.) GO TO 50                                            MCAR2370
      CALL SUBU5(X1,X2T,X3I,X4,X5T,X6T,C1T,XF5T,XF6T,FX5,FX6)           MCAR2380
      F7X5=FX5                                                          MCAR2390
      F7X6=FX6                                                          MCAR2400
      IF(FX5.EQ.0.) GO TO 50                                            MCAR2410
      IF(FX6.EQ.0.) GO TO 50                                            MCAR2420
      CALL SUBU5(X1,X2T,X3M,X4,X5T,X6T,C1T,XF5T,XF6T,FX5,FX6)           MCAR2430
      F8X5=FX5                                                          MCAR2440
      F8X6=FX6                                                          MCAR2450
      IF(FX5.EQ.0.) GO TO 50                                            MCAR2460
      IF(FX6.EQ.0.) GO TO 50                                            MCAR2470
      CALL SUBU5(X1,X2T,X3T,X4,X5T,X6T,C1T,XF5T,XF6T,FX5,FX6)           MCAR2480
      F9X5=FX5                                                          MCAR2490
      F9X6=FX6                                                          MCAR2500
      IF(FX5.EQ.0.) GO TO 50                                            MCAR2510
      IF(FX6.EQ.0.) GO TO 50                                            MCAR2520
      KOUNT=KOUNT+1                                                     MCAR2530
C                                         * COMPUTE INTEGRAND *         MCAR2540
      F15=FX2I*FX3I*F1X5                                                MCAR2550
      F16=FX2I*FX3I*F1X6                                                MCAR2560
      F25=FX2I*FX3M*F2X5                                                MCAR2570
      F26=FX2I*FX3M*F2X6                                                MCAR2580
      F35=FX2I*FX3T*F3X5                                                MCAR2590
      F36=FX2I*FX3T*F3X6                                                MCAR2600
      F45=FX2M*FX3I*F4X5                                                MCAR2610
      F46=FX2M*FX3I*F4X6                                                MCAR2620
      F55=FX2M*FX3M*F5X5                                                MCAR2630
      F56=FX2M*FX3M*F5X6                                                MCAR2640
      F65=FX2M*FX3T*F6X5                                                MCAR2650
      F66=FX2M*FX3T*F6X6                                                MCAR2660
      F75=FX2T*FX3I*F7X5                                                MCAR2670
```

```
      F76=FX2T*FX3I*F7X6                                                  MCAR2680
      F85=FX2T*FX3M*F8X5                                                  MCAR2690
      F86=FX2T*FX3M*F8X6                                                  MCAR2700
      F95=FX2T*FX3T*F9X5                                                  MCAR2710
      F96=FX2T*FX3T*F9X6                                                  MCAR2720
C                                * SUM INTEGRAND *                        MCAR2730
      SUM15=SUM15+F15                                                     MCAR2740
      SUM16=SUM16+F16                                                     MCAR2750
      SUM25=SUM25+F25                                                     MCAR2760
      SUM26=SUM26+F26                                                     MCAR2770
      SUM35=SUM35+F35                                                     MCAR2780
      SUM36=SUM36+F36                                                     MCAR2790
      SUM45=SUM45+F45                                                     MCAR2800
      SUM46=SUM46+F46                                                     MCAR2810
      SUM55=SUM55+F55                                                     MCAR2820
      SUM56=SUM56+F56                                                     MCAR2830
      SUM65=SUM65+F65                                                     MCAR2840
      SUM66=SUM66+F66                                                     MCAR2850
      SUM75=SUM75+F75                                                     MCAR2860
      SUM76=SUM76+F76                                                     MCAR2870
      SUM85=SUM85+F85                                                     MCAR2880
      SUM86=SUM86+F86                                                     MCAR2890
      SUM95=SUM95+F95                                                     MCAR2900
      SUM96=SUM96+F96                                                     MCAR2910
      IF(KOUNT.LT.K)GO TO 50                                              MCAR2920
C                                * COMPUTE OUTPUT *                       MCAR2930
      AI=100                                                              MCAR2940
      SAV15=SUM15/AI                                                      MCAR2950
      SAV16=SUM16/AI                                                      MCAR2960
      SAV25=SUM25/AI                                                      MCAR2970
      SAV26=SUM26/AI                                                      MCAR2980
      SAV35=SUM35/AI                                                      MCAR2990
      SAV36=SUM36/AI                                                      MCAR3000
      SAV45=SUM45/AI                                                      MCAR3010
      SAV46=SUM46/AI                                                      MCAR3020
      SAV55=SUM55/AI                                                      MCAR3030
      SAV56=SUM56/AI                                                      MCAR3040
      SAV65=SUM65/AI                                                      MCAR3050
      SAV66=SUM66/AI                                                      MCAR3060
      SAV75=SUM75/AI                                                      MCAR3070
      SAV76=SUM76/AI                                                      MCAR3080
      SAV85=SUM85/AI                                                      MCAR3090
      SAV86=SUM86/AI                                                      MCAR3100
      SAV95=SUM95/AI                                                      MCAR3110
      SAV96=SUM96/AI                                                      MCAR3120
      SAV5=SAV15+SAV25+SAV35+SAV45+SAV55+SAV65+SAV75+SAV85+SAV95          MCAR3130
      SAV6=SAV16+SAV26+SAV36+SAV46+SAV56+SAV66+SAV76+SAV86+SAV96          MCAR3140
      VAL1=FACT*(SAV5-SAV6)                                               MCAR3150
      SUMIN=(SAV15-SAV16)+SUMIN                                           MCAR3160
      SUMMD=(SAV55-SAV56)+SUMMD                                           MCAR3170
      SUMOT=(SAV95-SAV96)+SUMOT                                           MCAR3180
      K=K+100                                                             MCAR3190
      J=J+1                                                               MCAR3200
      SUMT=SUMT+VAL1                                                      MCAR3210
```

```
      TERM(J)=VAL1                                                      MCAR3220
      AJ=J                                                              MCAR3230
      VAL2=SUMT/AJ                                                      MCAR3240
      VAL3=VAL2/CFSQ                                                    MCAR3250
      AVIN=SUMIN/AJ                                                     MCAR3260
      AVMD=SUMMD/AJ                                                     MCAR3270
      AVOT=SUMOT/AJ                                                     MCAR3280
      SUM=AVIN+AVMD+AVOT                                                MCAR3290
      RATIN=AVIN/SUM                                                    MCAR3300
      RATMD=AVMD/SUM                                                    MCAR3310
      RATOT=AVOT/SUM                                                    MCAR3320
C                                         * PRINT OUT OF VALUES *       MCAR3330
      WRITE(6,10)                                                       MCAR3340
   10 FORMAT(///)                                                       MCAR3350
      WRITE(6,601)VAL2,SAV5,SAV6,SAV15,SAV16,SAV25,SAV26,SAV35,SAV36,SAVMCAR3360
     $45,SAV46,SAV55,SAV56,SAV65,SAV66,SAV75,SAV76,SAV85,SAV86,SAV95,SAVMCAR3370
     $96,KOUNT,I,J                                                      MCAR3380
  601 FORMAT(2X,3E15.8,5D15.8/2X,8D15.8/2X,5D15.8,3I6)                  MCAR3390
      IF(KOUNT-N)40,60,60                                               MCAR3400
C                                         * ERROR COMPUTATION LOOP *    MCAR3410
   60 DO 70 L=1,J                                                       MCAR3420
   70 SUMSQ=(TERM(L)-VAL2)**2+SUMSQ                                     MCAR3430
      VAR=SUMSQ/AJ                                                      MCAR3440
      SIG=SQRT(VAR/AJ)                                                  MCAR3450
      SIG1=SQRT(VAR)/AJ                                                 MCAR3460
      WRITE(6,502)                                                      MCAR3470
  502 FORMAT(//7X,'K1',8X,'ALPHA')                                      MCAR3480
      WRITE(6,500)BRK1,ALPHA                                            MCAR3490
  500 FORMAT(/2(5X,F6.3))                                               MCAR3500
      WRITE(6,20)                                                       MCAR3510
   20 FORMAT(//3X,'INTEGRAL VALUE',6X,'ERROR 1',10X,'ERROR 2',7X,'SPECTRMCAR3520
     $UM VALUE'/)                                                       MCAR3530
      WRITE(6,30)VAL3,SIG,SIG1,VAL2                                     MCAR3540
   30 FORMAT(4(2X,E15.8))                                               MCAR3550
      WRITE(6,25)                                                       MCAR3560
   25 FORMAT(//6X,'INSIDE',11X,'MIDDLE',10X,'OUTSIDE')                  MCAR3570
      WRITE(6,34)AVIN,AVMD,AVOT                                         MCAR3580
   34 FORMAT(/3(2X,E15.8),3X,'MAGNITUDE')                               MCAR3590
      WRITE(6,35)RATIN,RATMD,RATOT                                      MCAR3600
   35 FORMAT(/3(2X,E15.8),3X,'RELATIVE CONTRIBUTION')                   MCAR3610
      STOP                                                              MCAR3620
      END                                                               MCAR3630
      BLOCK DATA                                                        MCAR3640
      COMMON/BLPAR/ANU,DEL,DELST,UTAU,UINFN,VKC,TURPI,ALFAC,EM,A,B      MCAR3650
      DATA ANU,DEL,DELST,UTAU,UINFN,VKC,TURPI,ALFAC,EM,A,B/1.69E-04,0.23MCAR3660
     ,.03333,1.85,050.0,0.41,0.60,0.837,1.67,4.0,1300.0/                MCAR3670
      END                                                               MCAR3680
C
C
      SUBROUTINE XMEAX (MM,AA,UU,XX,PDF)
C
C  GENERATES A RANDOM NUMBER FROM THE PROBABILITY DENSITY FUNCTION
C  PROPORTIONAL TO X**M*EXP(A*X), WHERE M IS EQUAL TO 1 OR 2 AND
C  A IS .LT. ZERO.
```

```
C  BEFORE CALLING XMEAX, SET UU EQUAL TO A PSEUDO-RANDOM OR
C  QUASI-RANDOM NUMBER UNIFORMLY DISTRIBUTED ON (0,1).
C  XX RETURNS THE RANDOM NUMBER AND PDF RETURNS THE PROPERLY NORMALIZED
C  VALUE OF THE PROBABILITY DENSITY FUNCTION.
C
C  J. P. CHANDLER, COMPUTER SCIENCE DEPT., OKLAHOMA STATE UNIVERSITY
C
      FA(X,EX)=EX*(A*X-1.)+U
      FB(X,EX)=-EX*(ASQ*X*X/2.-A*X+1.)+U
C
      KW=1
      KW=6
      RAT=2.
      RELEP=.0001
      ACK=1.5
      NPR=1
      NPR=0
      BIG=90.
      M=MM
      A=AA
      U=UU
      ASQ=A*A
      FAC=ACK
      X=-1.
      NIT=0
      IF(A)4,5,5
    4 IF(U)1,1,2
    1 X=-BIG/A
      GO TO 5
    2 IF(U-1.)6,7,7
    7 X=0.
      GO TO 5
    6 IF(U-.5)80,80,81
   80 X=ALOG(U)/A
      EX=U
      GO TO 82
   81 X=-SQRT(1.-U)/A
      EX=EXP(A*X)
   82 IF(EX)1,1,10
   10 IF(M-1)11,11,12
   11 F=FA(X,EX)
      GO TO 35
   12 F=FB(X,EX)
   35 IF(NPR)71,71,72
   72 WRITE(KW,21)XA,FAA,XB,FBB,X,F
   21 FORMAT(6E12.4)
   71 IF(F)30,5,31
C                                 BRACKET X FROM ABOVE.
   30 XA=X
      FAA=F
      X=XA*FAC
      FAC=FAC*ACK
      EX=EXP(A*X)
      IF(EX)36,36,37
```

```
   37 IF(M-1)32,32,33
   32 F=FA(X,EX)
      GO TO 34
   33 F=FB(X,EX)
   34 IF(F)35,5,36
   36 XB=X
      FBB=F
      GO TO 38
C                                  BRACKET X FROM BELOW.
   31 XB=X
      FBB=F
      X=XB/FAC
      FAC=FAC*ACK
      EX=EXP(A*X)
      IF(M-1)40,40,41
   40 F=FA(X,EX)
      GO TO 42
   41 F=FB(X,EX)
   42 IF(F)43,5,35
   43 XA=X
      FAA=F
C                                  USE A VARIATION ON HAMMING-S VERSION OF
C                                       REGULA FALSI.
   38 DENOM=FBB-FAA
      IF(DENOM)5,5,47
   47 X=XA-FAA*(XB-XA)/DENOM
      EX=EXP(A*X)
      IF(X-XA)5,5,48
   48 IF(X-XB)49,5,5
   49 IF(M-1)50,50,51
   50 F=FA(X,EX)
      GO TO 52
   51 F=FB(X,EX)
   52 NIT=NIT+1
      IF(NPR)73,73,74
   74 WRITE (KW,55)NIT,XA,FAA,XB,FBB,X,EX,F
   55 FORMAT(1XI3,7E12.4)
   73 IF(F)53,5,54
   53 XA=X
      FAA=F
      IF(FBB-RAT*(-FAA))57,57,61
   61 FBB=.5*FBB
      GO TO 57
   54 XB=X
      FBB=F
      IF(-FAA-RAT*FBB)57,57,62
   62 FAA=.5*FAA
   57 IF((XB-XA)-RELEP*XB)5,5,38
C
    5 XX=X
      IF(M-1)44,44,45
   44 DFDX=ASQ*X*EX
      GO TO 46
   45 DFDX=-ASQ*A*X*X*EX/2.
```

```
 46 PDF=DFDX
    IF(NPR)75,75,76
 76 WRITE(KW,56)NIT,XA,FAA,XB,FBB,X,EX,F,DFDX
 56 FORMAT(1XI3,8E12.4)
 75 RETURN
    END
C
C
    SUBROUTINE SUBX2(FX2,X2,ARG2,XF2)
    COMMON BRK1,BARK,ALPHA
    FX2=EXP(-(BARK*X2))*SG(ARG2)*VI(ARG2)*XF2
    RETURN
    END
C
C
    SUBROUTINE SUBX3(FX3,X3,ARG3,XF3)
    COMMON BRK1,BARK,ALPHA
    FX3=EXP(-(BARK*X3))*SG(ARG3)*VI(ARG3)*XF3
    RETURN
    END
C
C
    SUBROUTINE SUBU5(X1,X2,X3,X4,X5,X6,C1,XF5,XF6,FX5,FX6)
    COMMON BRK1,BARK,ALPHA
    YZ=(X3-X2)**2
    XP5=SQRT(X5**2+YZ)
    XP6=SQRT(X6**2+YZ)
    F1X5=X5*EXP(-C1*XP5)
    F1X6=(C1/2.)*(X6**3/XP6)*EXP(-C1*XP6)
    A=BRK1*ALPHA*COS(X4)
    B=X1*SIN(X4)
    F2X5=COS(A*X5)
    F2X6=COS(A*X6)
    F3X5=COS(B*X5)
    F3X6=COS(B*X6)
    FX5=F1X5*F2X5*F3X5/XF5
    FX6=F1X6*F2X6*F3X6/XF6
    RETURN
    END
C
C
    FUNCTION VI(YBAR2)
    COMMON/BLCMP/ TRENO, SLOLM, SVK1, SVK3, SVK4, SVK5, SVK6, SVK7,
   *SVK8,BI,DELRA,ALIM,AK,BK
    RATIO=27.
    YBAR2=3.*YBAR2/2.76
    IF(YBAR2.GT.1.)GO TO 5
    IF(YBAR2.GT..9)GO TO 10
    IF(YBAR2.GT..575)GO TO 20
    IF(YBAR2.GT..1)GO TO 30
    IF(YBAR2.GT..017)GO TO 40
    IF(YBAR2.GT.ALIM)GO TO 50
    VI=RATIO*(AK*YBAR2**2+BK*YBAR2**3)
    RETURN
```

```
    5 VI=RATIO*.0068
      RETURN
   10 VI=RATIO*(.0068+(YBAR2-1.)**2/1.25)
      RETURN
   20 VI=RATIO*(.0638-.057*YBAR2)
      RETURN
   30 VI=RATIO*(.0394-(YBAR2-.14)**2/21.5)
      RETURN
   40 VI=RATIO*(.0395-(YBAR2-.1)**2/1.24)
      RETURN
   50 VI=RATIO*(SQRT(.09*YBAR2)-16.3*YBAR2**2)
      RETURN
      END
C
C
      FUNCTION SG(YBAR2)
      COMMON/BLPAR/ ANU, DEL, DELST, UTAU, UINFN, VKC, TRUPI, ALFAC, EM,
     $A, B
      COMMON/BLCMP/ TRENO, SLOLM, SVK1, SVK3, SVK4, SVK5, SVK6, SVK7,
     *SVK8,BI,DELRA,ALIM,AK,BK
      IF(YBAR2.GE.1.0) GO TO 30
      IF(YBAR2.GE.ALFAC) GO TO 10
      IF(YBAR2.GT.SLOLM) GO TO 20
      YSTR = SVK8*YBAR2
      SG = DELRA*TRENO*(1.0 + YSTR+0.5*YSTR**2 + BI*YSTR**6)*EXP(-YSTR)
      RETURN
   10 SG = DELRA*SVK5*((1.0 - YBAR2)/SVK6)**SVK7
      RETURN
   20 SG = DELRA*(SVK1/YBAR2 + SVK3*SIN(SVK4*YBAR2))
      RETURN
   30 SG = 0.0
      RETURN
      END
C
C
      FUNCTION CORPUT(NR,NRESET)                                        CORPUT 1
C                                                                       CORPUT 2
C  QUASI-RANDOM NUMBERS BY VAN DER CORPUT-S METHOD                      CORPUT 3
C  QUA                                                                  CORPUT 4
C  J. P. CHANDLER, F.S.U. PHYSICS DEPT., TALLAHASSEE, FLORIDA           CORPUT 5
C                                                                       CORPUT 6
C  CORPUT RETURNS THE NEXT (I-TH) NUMBER IN THE R-TH VAN DER CORPUT     CORPUT 7
C  SEQUENCE, PSUBR(I), WHERE R IS THE NR-TH PRIME.                      CORPUT 8
C  NR MUST BE GREATER THAN ZERO AND LESS THAN OR EQUAL TO NMAX.         CORPUT 9
C                                                                       CORPUT10
C  REFERENCES....                                                       CORPUT11
C        YU. SHREIDER, ED., THE MONTE CARLO METHOD (PERGAMON)           CORPUT12
C        P. J. DAVIS AND P. RABINOWITZ, NUMERICAL INTEGRATION (BLAISDELL)CORPUT13
C        J. M. HAMMERSLEY AND D. C. HANDSCOMB, MONTE CARLO METHODS      CORPUT14
C             (METHUEN)                                                 CORPUT15
C                                                                       CORPUT16
C  IF NRESET IS NONZERO, THE NR-TH SEQUENCE (ONLY) IS RESTARTED AND     CORPUT17
C  THE FIRST VALUE IS RETURNED.                                         CORPUT18
C                                                                       CORPUT19
```

```
C  THE NUMBER OF CALLS TO CORPUT WITH ANY PARTICULAR VALUE OF NR,         CORPUT20
C  WITHOUT RESTARTING, MUST NOT EXCEED THE LARGEST FORTRAN INTEGER.       CORPUT21
C  (THIS SHOULD NOT BE A PROBLEM AT PRESENT DAY SPEEDS IF THE INTEGER     CORPUT22
C  LENGTH IS MORE THAN ABOUT 26 OR 27 BITS.)                              CORPUT23
C  A CHECK FOR INTEGER OVERFLOW IS PERFORMED WHICH SHOULD WCRK ON MOST    CORPUT24
C  COMPUTERS....                                                          CORPUT25
C                                                                         CORPUT26
C  PROVISION IS MADE FOR THE USE OF A FASTER ROUTINE FOR NR=1,            CORPUT27
C  IF ONE IS AVAILABLE.  (ON A BINARY MACHINE THE INTEGER CAN BE          CORPUT28
C  STORED IN BIT-REVERSED FORM, AND INCREMENTED BY DOING THE CARRIES      CORPUT29
C  -BY HAND-.)  SUCH A ROUTINE EXISTS FOR THE CDC 6400.  IT IS ABOUT      CORPUT30
C  FIVE TIMES AS FAST AS CORPUT FOR SMALL I, AND HAS A GREATER            CORPUT31
C  ADVANTAGE FOR LARGE I.                                                 CORPUT32
C                                                                         CORPUT33
C * * * * * * * * * * * * * * * * * * * * * * * * * * * * * * * * * * *  CORPUT34
C                                                                         CORPUT35
      DIMENSION NPRIME(25),JP(25)                                         CORPUT36
C                                                                         CORPUT37
      DATA NFIRST/7/                                                      CORPUT38
C                               NMAX IS THE DIMENSION OF NPRIME AND JP.   CORPUT39
      DATA NMAX/25/                                                       CORPUT40
      DATA NPRIME/2,3,5,7,11,13,17,19,23,29,31,37,41,43,47,53,59,61,67,7CORPUT41
     1,73,79,83,89,97/                                                    CORPUT42
C * * * * * * * * * * * * * * * * * * * * * * * * * * * * * * * * * * *  CORPUT54
C                                                                         CORPUT55
C                               MOVE THE ARGUMENTS.                       CORPUT56
      MR=NR                                                               CORPUT57
      MRESET=NRESET                                                       CORPUT58
C                               CHECK FOR ILLEGAL VALUES OF NR.           CORPUT59
      IF(MR-1)20,40,10                                                    CORPUT60
   10 IF(MR-NMAX)50,50,20                                                 CORPUT61
   20 PRINT 30,MR,NMAX                                                    CORPUT62
   30 FORMAT(/53H ILLEGAL VALUE OF NR IN FUNCTION CORPUT.  NR, NMAX =     CORPUT63
     *   2I8 //)                                                          CORPUT64
      STOP                                                                CORPUT65
   40 CONTINUE                                                            CORPUT66
C                               CALL A FASTER ROUTINE FOR BASE 2, IF ONE  CORPUT67
C                                    IS AVAILABLE.                        CORPUT68
C     CORP=CORPUS(MRESET)                                                 CORPUT69
C     GO TO 180                                                           CORPUT70
C                               INITIALIZE ALL SEQUENCES ON THE FIRST CALL.CORPUT71
   50 IF(NFIRST)60,80,60                                                  CORPUT72
   60 NFIRST=0                                                            CORPUT73
C                               GET THE PRIMES FROM SUBROUTINE PRIMES,    CORPUT74
C                                    IF DESIRED.                          CORPUT75
C     CALL PRIMES(NPRIME,NMAX)                                            CORPUT76
C                                                                         CORPUT77
      DO 70 J=1,NMAX                                                      CORPUT78
   70 JP(J)=0                                                             CORPUT79
      GO TO 140                                                           CORPUT80
C                               RESTART THE NR-TH SEQUENCE IF REQUESTED.  CORPUT81
   80 IF(MRESET)140,90,85                                                 CORPUT82
   85 JP(MR) = MRESET                                                     CORPU82A
      GO TO 150                                                           CORPU82B
```

```
C                                   INCREMENT THE INTEGER FOR THIS SEQUENCE,   CORPUT83
C                                        AND TEST FOR OVERFLOW.                 CORPUT84
   90 JOLD=JP(MR)                                                              CORPUT85
      JP(MR)=JP(MR)+1                                                          CORPUT86
      IF(JP(MR))120,120,100                                                    CORPUT87
  100 IF(JP(MR)-JOLD)120,120,110                                               CORPUT88
  110 JCOMP=JP(MR)-1                                                           CORPUT89
      IF(JCOMP-JOLD)120,150,120                                                CORPUT90
  120 PRINT 130,MR                                                             CORPUT91
  130 FORMAT(/38H OVERFLOW IN FUNCTION CORPUT FOR NR = I5,                     CORPUT92
     *   23H .  SEQUENCE RESTARTED.)                                           CORPUT93
  140 JP(MR)=1                                                                 CORPUT94
C                                   SET UP FOR THE LOOP.                       CORPUT95
  150 JINT=JP(MR)                                                              CORPUT96
      NPR=NPRIME(MR)                                                           CORPUT97
      PR=NPR                                                                   CORPUT98
      POW=PR                                                                   CORPUT99
      CORP=0.                                                                  CORPU100
      GO TO 170                                                                CORPU101
C                                   FORM THE QUASI-RANDOM NUMBER BY REVERSING  CORPU102
C                                        THE DIGITS (BASE NPR) OF JINT.        CORPU103
  160 POW=POW*PR                                                               CORPU104
      JINT=K                                                                   CORPU105
  170 K=JINT/NPR                                                               CORPU106
      A=JINT-K*NPR                                                             CORPU107
      CORP=CORP+A/POW                                                          CORPU108
      IF(K)180,180,160                                                         CORPU109
C                                                                              CORPU110
  180 CORPUT=CORP                                                              CORPU111
      RETURN                                                                   CORPU112
      END                                                                      CORPU113
```

APPENDIX L

THE INTEGRATION PROGRAM CHRONOLOGY

This Appendix contains a discussion of the logic sequence of the integration program, the interface between the analytical development and the numerical computation, and a listing of the computer pseudonyms and their definitions. The discussion follows the sequence of the program listing found in Appendix K. On the right hand side of the program listing, headings are found which describe what the ensuing program block is accomplishing. These same headings are used in this Appendix in order to correlate the discussion with the program listing.

* PROGRAM MULTIPLIERS AND CONSTANTS *

Pseudonym	Definition
K	Number of iterations between computations of the answer.
N	Total number of iterations
ALPHA	Scale anisotropy parameter
	* K1 *
BRK1	The wave number, $\hat{k}_1$
BK1SQ	$\hat{k}_1^2$

* C1 FOR VARIANCE REDUCTION *

Pseudonym	Definition
C1IN	The value of the exponent, C, for the inner region used in the variance reduction of the $\hat{r}$ dependent terms. It is computed from the equation for C_1 $(\hat{y}_2)$ at $\hat{y}_2 = .025\delta/\delta*$.
C1MD	The same as C1IN except it is for the middle region. It is computed at $\hat{y}_2 = .2\delta/\delta*$.
C1OT	The same as C1IN except it is for the outer region. It is computed at $\hat{y}_2 = \delta/\delta*$.

C1IN, C1MD, and C1OT are the three values for C used in equation (J-19). The value of C is the lowest value of C_1 for that region. This insures that the transformed function has the proper behavior as $\hat{r}$ gets large.

* BOUNDARY LAYER PARAMETERS *

Pseudonym	Definition
VRAT	Velocity ratio.
UTAU	U_τ, friction velocity, from BLOCK DATA.
UINFN	U_∞, free stream velocity, from BLOCK DATA.
DELRA	$\delta*/\delta$, boundary layer thickness ratio from BLOCK DATA.
DEL	δ, boundary layer thickness, from BLOCK DATA.
DELST	$\delta*$, displacement thickness, from BLOCK DATA.
TRENO	A turbulence Reynolds number, $U_\tau\delta/\nu$.
SLOLM	The y_2/δ lower limit on the mean-shear.
SVK1	Shear velocity constant #1, the reciprocal of the Von Karman Constant.

Pseudonym	Definition
VKC	Von Karman Constant.
SVK2	Shear velocity constant #2, the denominator of the multiplier of equation (4-6).
SVK3	Shear velocity constant #3, the multiplier of the sine term in equation (4-6).
TURPI	Turbulence pi, π, from BLOCK DATA.
SVK4	Shear velocity constant #4, part of the argument sine term in equation (4-6).
SVK5	Shear velocity constant #5, the reciprocal of SVK2.
SVK6	Shear velocity constant #6, used in equation (4-7).
ALFAC	α_c in equation (4-7).
SVK7	Shear velocity constant #7, the exponent in equation (4-7).
EM	The parameter, m, in the exponent of equation (4-7).
SVK8	Shear velocity constant #8, the term $\tilde{y}_2/a$ in equation (4-5).
A	The parameter, a, in equation (4-5) from BLOCK DATA.
BI	The reciprocal of the parameter, b, in equation (4-5) from BLOCK DATA.

The equations for computing the shear gradient are found in the subroutine SG(YBAR2). The argument, YBAR2, is $\dot{y}_2/\delta$.

* SUB LAYER PARAMETERS *

Pseudonym	Definition
YSTR	Y-STAR, the value of $y_2{}^*$ at the outer boundary of the viscous sublayer.
ALIM	The value of $\hat{y}_2$ at the outer boundary of the viscous sublayer.
AK, BK	Constants in viscous sublayer intensity equation.

These values are used in the subroutine VI(YBAR2) which computes the velocity intensity.

* K3 UPPER LIMIT *

Pseudonym	Definition
ULIMK	Upper limit of the wave number, $\hat{k}_3$. It is the value, d, in equation (5-23).
ARGX1	Argument for the transformed value of $\hat{k}_3$ designated as X1. It is in the denominator of equation (J-8).

* INTEGRAL MULTIPLIER *

Pseudonym	Definition
CFSQ	C_f^2, C_f is the friction factor.
FACT1	Factor #1, the integral multiplier in equation (4-19).
VOLX1	Volume X1, this is the value of $\hat{k}_1^2/\hat{k}^2$ in the integrand of equation (4-19). Since the importance sampling of this factor is exact, the contribution of this term is known after one sample or iteration.
VOLX4	Volume X4, which is the multiplier contributed by the variable θ. Part of 8π factor in equation (4-19).

* INITIALIZE *

This block initializes the program counters for each run. SUM, SUMT, SUMIN, SUMMD, and SUMOT will be defined under the heading, COMPUTE OUTPUT.

Pseudonym	Definition
I	The total number of iterations.
KOUNT	The total number of non-zero iterations.
J	Increments one every time KOUNT sequences K iterations.

* K1 LOOP *

The program sequences to this point every time J increments. The SUM15, SUM16, etc. terms will be defined under the heading, SUM INTEGRAND. They are initialized when J increments.

* ITERATION STARTING POINT *

Pseudonym	Definition
M	Parameter in the argument of the subroutine CORPUT. It specifies the starting point in the sequence of quasirandom numbers.

This is the point at which all iterations start or loop to whether they contribute or not to the integrand. Should a number other than zero be desired for M, substitute for the statement M = 0 the statement M = I + NUMBER where NUMBER is desired starting integer number.

* VARIABLE FOR KTIL3 *

Pseudonym	Definition
U1	The quasirandom value of the transformed variable, u, for $\hat{k}_3$. (Equation J-11).

Pseudonym	Definition
X1A	Program variable.
X1	The transformed variable for $\hat{k}_3$. (Equation J-12).
BRKSQ	The term, $\hat{k}^2$, where $\hat{k}^2 = \hat{k}_1^2 + \hat{k}_3^2$.
BARK	$\hat{k}$.

This block computes the transformed variable for $\hat{k}_3$ and some of the terms in which it appears.

* VARIABLE FOR YTIL2 *

Pseudonym	Definition
U2	The quasirandom value of the transformed variable, v for $\hat{y}_2$. (Equation J-17).

* INNER REGION *

Pseudonym	Definition
CIN	The term $C_i + \hat{k}$ where $C_i = C_I$.
EXPIN	The term $\exp[-(\hat{k} + C_i)a] - \exp[-(\hat{k} + C_i)b]$ where $C_i = C_I$, $a = 0$, and $b = .025\delta/\delta*$, see equation (J-19).
VOLIN	EXPIN/CIN
X2AI	The argument of 'ln' in equation (J-18) for the inner region.
X2I	$\hat{y}_2$ for the inner region as in equation (J-18).
XF2I	The $\hat{y}_2$ contribution to the probability density function, equation (J-19), for the inner region. (Includes part of k_3 term through BARK).
ARG2I	The term $\hat{y}_2\delta*/\delta$ for the inner region. This term is used to evaluate the shear gradient and the velocity intensity.

* MIDDLE REGION *

Pseudonym	Definition
CMD	$C_i + \hat{k}$ where $C_i = C_{MD}$.
EXPMD	Analogous to EXPIN except $a = .025\delta/\delta*$ and $b = .2\delta/\delta*$.
VOLIN	EXPMD/CMD.
X2AM	Middle region analog of X2AI.
XF2M	Middle region analog of XF2I.
ARG2M	Middle region analog of ARG2I.

* OUTER REGION *

This region is analogous to the other two regions.

* VARIABLE FOR YTIL2$'$ *

This block is analogous to the previous, VARIABLE FOR YTIL2, block because of the symmetry in $\hat{y}_2$ and $\hat{y}'_2$.

* VARIABLE FOR THETA *

Pseudonym	Definition
U4	The quasirandom value used to select theta for each iteration.
X4	Theta.

* C1 FOR FUNCTION COMPUTATION *

C1I	C_1 for the inner region.
C1M	C_1 for the middle region.
C1T	C_1 for the outer region.

* VARIABLE FOR R TERMS *

Pseudonym	Definition
U5	The quasirandom value of the transformed value for the '$\hat{r}$' terms.

* VARIABLE FOR R *

Pseudonym	Definition
XMEAX	$X^M \exp(AX)$, the subroutine to compute the p.d.f. and the value of $\hat{r}$.
X5	The value of $\hat{r}$, equation (5-19).
XF5	The value of the p.d.f., equation (5-17).

The remainder of this block computed the values of the above for the inner, middle and outer regions.

* VARIABLE FOR RSQ *

This block is analogous to the one above except that the apropos equations are (5-20) and (5-21).

* TERMS OF THE TOTAL INTEGRAL *

Having computed the p.d.f. values and the transformed variables or, as in the case of θ, the value of the variable itself, the following block is used to compute the contribution of an iteration to the integrand.

* X2 TERMS *

Pseudonym	Definition
SUBX2	The subroutine used to compute the contribution to the integrand of the term $\exp(-\hat{k}\hat{y}_2)\frac{dU^*}{d\hat{y}_2}(\hat{y}_2)\hat{u}_2(\hat{y}_2)$.
FX2I, FX2M, FX2T	The value computed in SUBX2 for the inner, middle, and outer regions.

* X3 TERMS *

Pseudonym	Definition
SUBX3	Analogous to SUBX2 for $\hat{y}_2'$.
FX3I, FX2M, FX3T	The value computed in SUBX3 for the inner, middle, and outer regions. Note that each term is checked in this block to see if it is zero.

* X4, X5, and X6 TERMS *

Pseudonym	Definition
SUBU5	The subroutine that computes the contribution to the integrand of the term, $\left\{\hat{r} - \frac{C_1 \hat{r}^3}{2[\hat{r}^2+(\hat{y}_2'-\hat{y}_2)^2]^{1/2}}\right\} \exp\{C_1[\hat{r}^2+(\hat{y}_2'-\hat{y}_2)^2]^{1/2}\}\ldots$ $\ldots\cos(\alpha\hat{k}_1\hat{r}\cos\theta)\cos(\hat{k}_3\hat{r}\sin\theta)$.
FX5	The contribution to the integrand of the term, $\hat{r}\exp\{-C_1[\hat{r}^2+(\hat{y}_2'-\hat{y}_2)^2]^{1/2}\}\ldots$ $\ldots\cos(\alpha\hat{k}_1\hat{r}\cos\theta)\cos(\hat{k}_3\hat{r}\sin\theta)$.
FX6	The contribution to the integrand of the term, $\left\{\frac{C_1 \hat{r}^3}{2[\hat{r}^2+(\hat{y}_2'-\hat{y}_2)^2]^{1/2}}\right\} \exp\{-C_1[\hat{r}^2+(\hat{y}_2'-\hat{y}_2)^2]^{1/2}\}\ldots$ $\ldots\cos(\alpha\hat{k}_1\hat{r}\cos\theta)\cos(\hat{k}_3\hat{r}\sin\theta)$.

The integrand is separated into I_1 and I_2 as per equation (5-12). The number, 5, in a term is associated with the integral, I_1 , and the number, 6, is associated with the integral, I_2 . Each of these integrals is separated into the sum of nine integrals, equation (5-23). The contribution to each of these eighteen integrals of either FX5 or FX6 is computed in this block. Thus, F1X5, F2X5, F3X5, etc. contribute to I_1 . F1X6, F2X6, F3X6, etc. to I_2 . Each of the terms is checked for the value zero before continuing the iteration. KOUNT is incremented if none of the preceeding terms is zero.

* COMPUTE INTEGRAND *

This block is best explained by two equations.

$$I_1 = F15 + F25 + F35 + F45 + F55 + F65 + F75 + F85 + F95. \tag{L-1}$$

$$I_2 = F16 + F26 + F36 + F46 + F56 + F66 + F76 + F86 + F96. \tag{L-2}$$

* SUM INTEGRAND *

The SUM terms correspond to the terms in equations (L-1) and (L-2).

* COMPUTE OUTPUT *

The SAV15, etc. terms are the average values of the eighteen integrands for K iterations.

Pseudonym	Definition
SAV5	I_1
SAV6	I_2
VAL1	$\hat{\pi}(\hat{k}_1)$, equation (4-19), for K iterations.
SUMIN	A measure of the contribution to $\hat{\pi}(\hat{k}_1)$ by the inner region.
SUMMD	Analogous to SUMIN for the middle region.
SUMOT	Analogous to SUMMD for the outer region.

Pseudonym	Definition
SUMT	The sum of the values computed for VAL1 every K iteration.
TERM(J)	This term stores VAL1 for error computation purposes.
VAL2	The value of $\hat{\pi}(\hat{k}_1)$ every K*J iterations.
VAL3	$\hat{\pi}(\hat{k}_1)/C_f^2$.
AVIN, AVMD, AVOT	The average values of the inside, middle, and outer region contributions. Each of these is the sum of two of the eighteen integrals in $\hat{\pi}(\hat{k}_1)$.
SUM	The SUM of the inside, middle, and outer region contributions.
RATIN, RATMD, RATOT	Contribution ratios.

* PRINT OUT OF VALUES *

The values are printed out every K iterations and after K*J iterations.

* ERROR CONTRIBUTION *

Pseudonym	Definition
SUMSQ	A term in the statistical variation equation (5-37).
VAR	The variation, equation (5-37).
SIG	A first estimate of the standard deviation, equation (5-36).
SIG1	A second estimate of the standard deviation, equation (5-35).

This is the end of the main program.

SUBROUTINES

BLOCK DATA

The boundary layer data is entered here as defined in the main program.

SUBROUTINE XMEAX

The use of this subroutine has been explained in the main program. In addition it contains its own comment cards.

SUBX2, SUBX3, AND SUBU5

These subroutines have been explained in the main program.

FUNCTION SG(YBAR2)

This is the subroutine which computes the shear gradient as per equations (4-5) through (4-7).

FUNCTION VI(YBAR2)

In this subroutine the velocity intensity as per equations (4-9) through (4-18) and the viscous sublayer model $a\hat{y}_2^2 + b\hat{y}_2^3$. RATIO is U_∞/U_τ from Klebanoff's data.

SUBROUTINE CORPUT

This subroutine contains its own comment cards.

PROGRAM OUTPUT

After K iterations the value of $\hat{\pi}(\hat{k}_1)$ for the total number of iterations to that point and the contribution of each of the eighteen integrals for those K iterations is pointed out. Upon completion of N non-zero iterations the values of $\hat{k}_1$ and α head the output followed by:

Title	Definition
INTEGRAL VALUE	$\hat{\pi}(\hat{k}_1)/C_f^2$.
ERROR 1	First estimate of σ.
ERROR 2	Second estimate of σ.
SPECTRUM VALUE	$\hat{\pi}(\hat{k}_1)$.
INSIDE MAGNITUDE	Equation (5-41)
MIDDLE MAGNITUDE	Equation (5-42)
OUTER MAGNITUDE	Equation (5-43)
INSIDE RELATIVE CONTRIBUTION	
MIDDLE RELATIVE CONTRIBUTION	
OUTSIDE RELATIVE CONTRIBUTION	

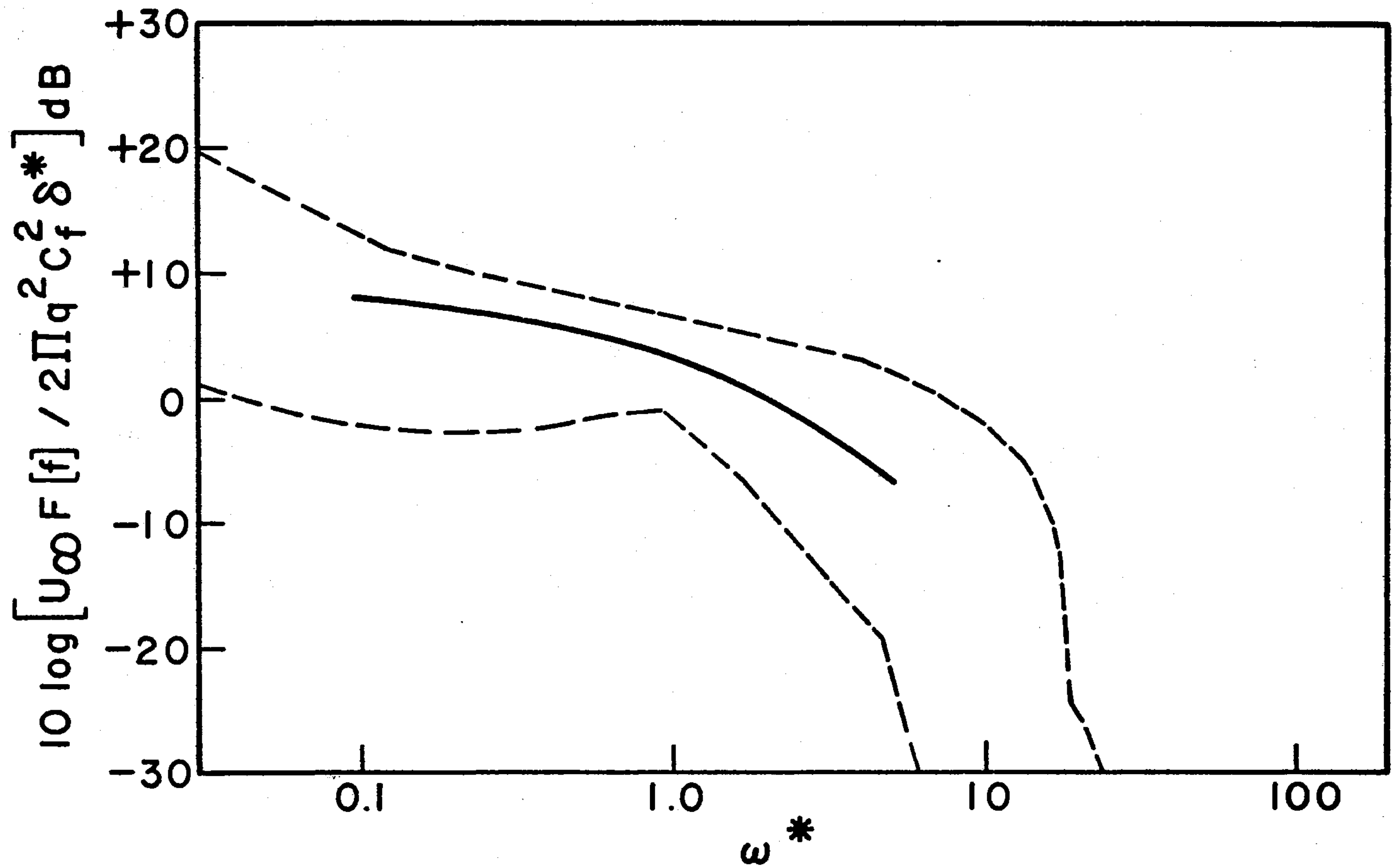

Figure 1. Wind Tunnel Measurement of Boundary Layer Pressure Fluctuations, Bies (1966). ——— Line of Greatest Data Cluster. — — — — Defines Area Which Contains Experimental Data.

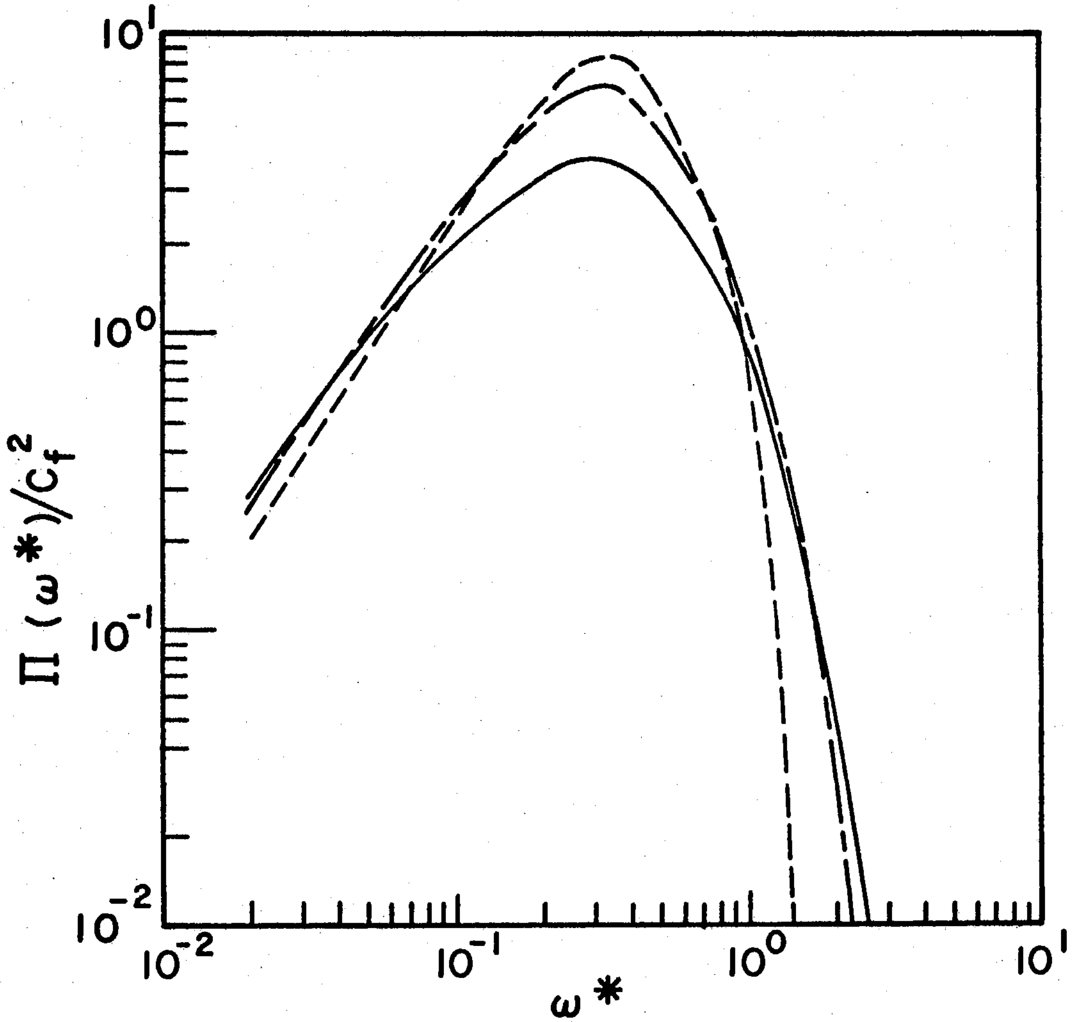

Figure 2. Frequency Spectra. ——— Hodgson's (1962) Measured Spectrum on a Glider Wing. — — — — Predicted Green's Function Spectrum, Hodgson's (1962) Simplified Solution. — ——— — Predicted Fourier Transform Spectrum With 'Mirrow-Flow' Model, Hodgson (1962). $\Pi = \overline{p}^2(\omega)U_\infty/\delta^* q^2$.

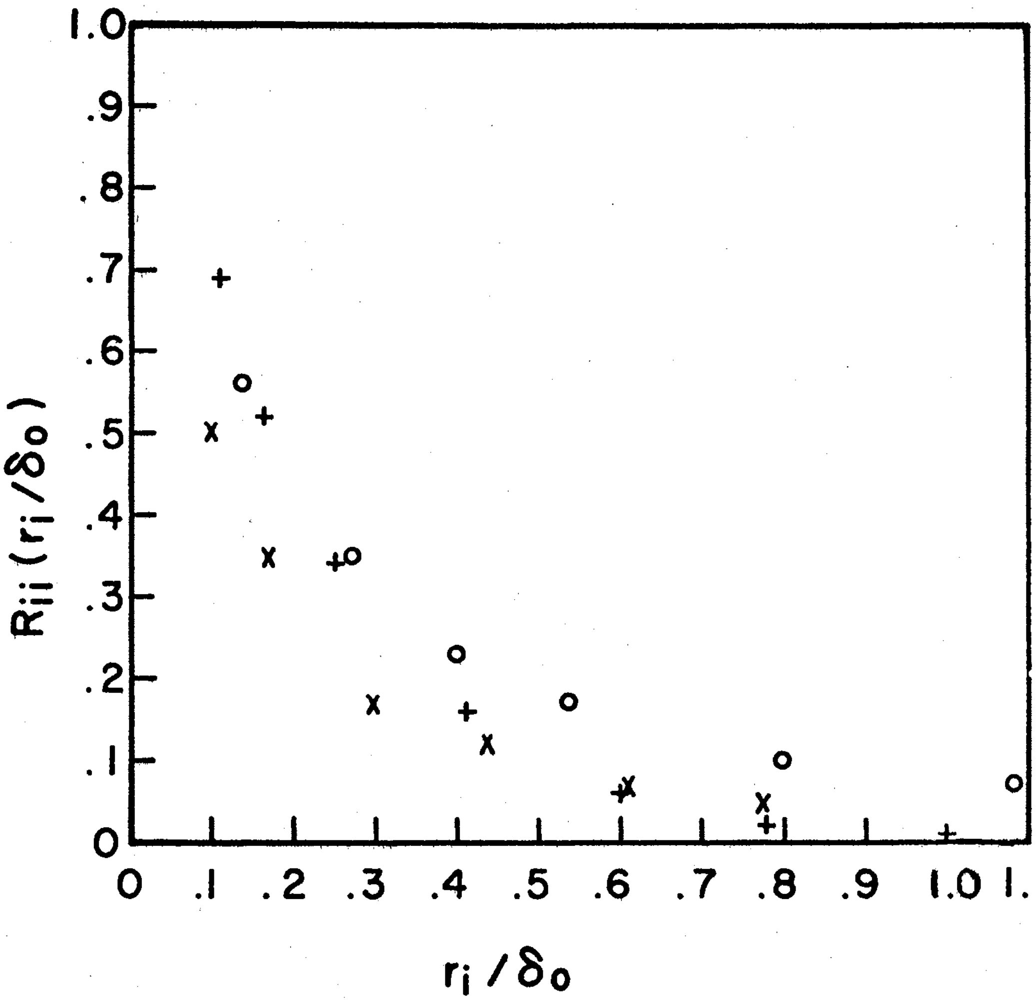

Figure 3. Measured Velocity Correlation Components R_{11}, R_{22}, R_{33}, Grant (1958). o R_{11} $(r_1/\delta_o, 0, 0)$; x R_{22} $(0, r_{22}/\delta_o, 0)$; + R_{33} $(0, 0, r_3/\delta_o)$. δ_o is value of y_2 where $U_1 = U_\infty - U_\tau$. $\delta_o/\delta = .69$.

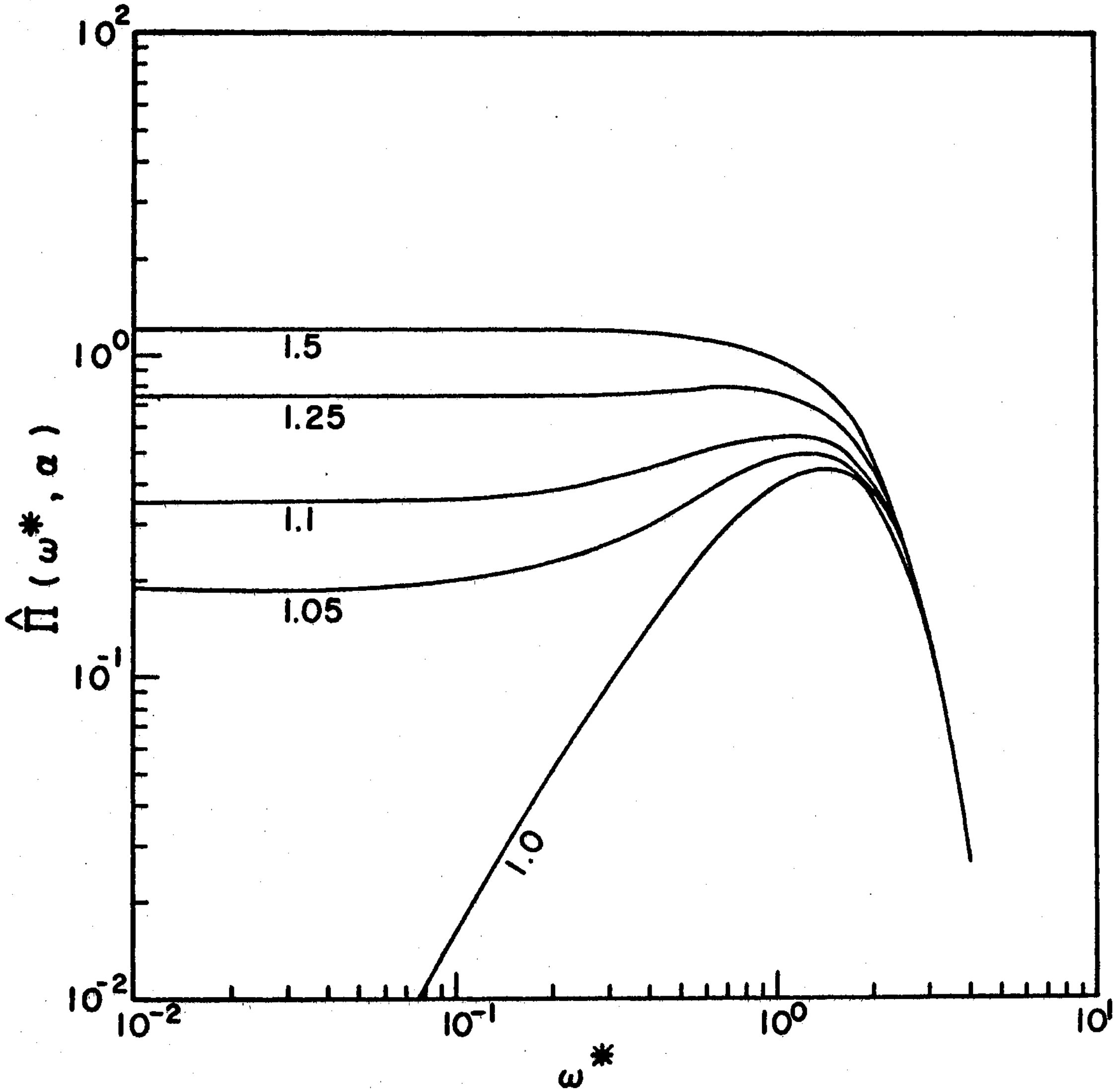

Figure 4. The Effect of Scale Anisotropy on Hodgson's Predicted Green's Function Frequency Spectrum. α = 1.0, 1.05, 1.1, 1.25, 1.5.

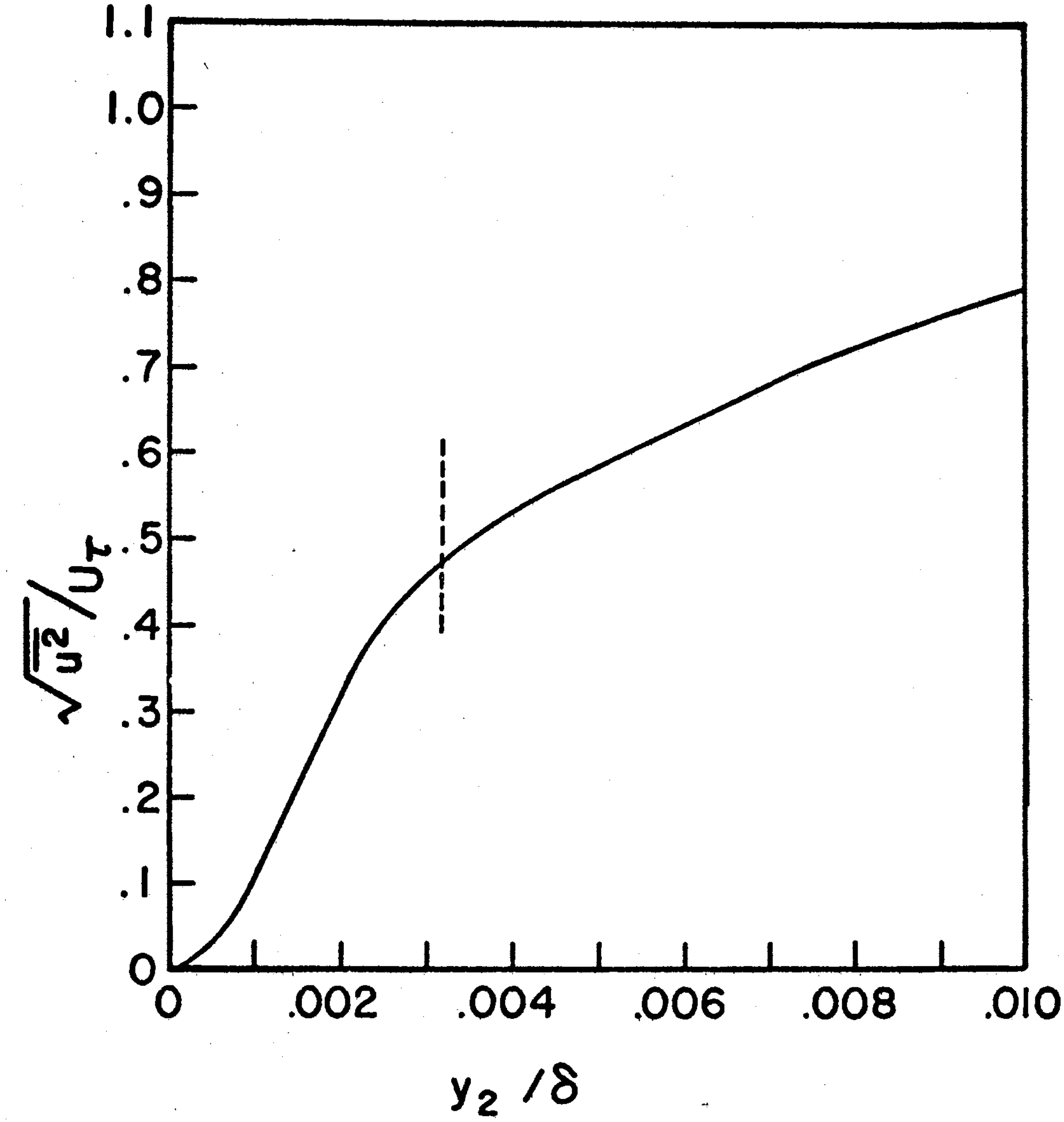

Figure 5. Velocity Intensity, $\sqrt{\overline{u_2}^2}/U_\tau$. $0 \leq y_2/\delta \leq .01$. Model of Klebanoff's (1954) Data Scaled With δ Determined From 'Law of Wall and Wake'. The Viscous Sublayer Model From $y^* = 8$ to the Wall is $a(y_2/\delta)^2 + b(y_2/\delta)^3$, $Re_\delta{}^* = 9.9 \cdot 10^3$. ------ $y^* = 8$.

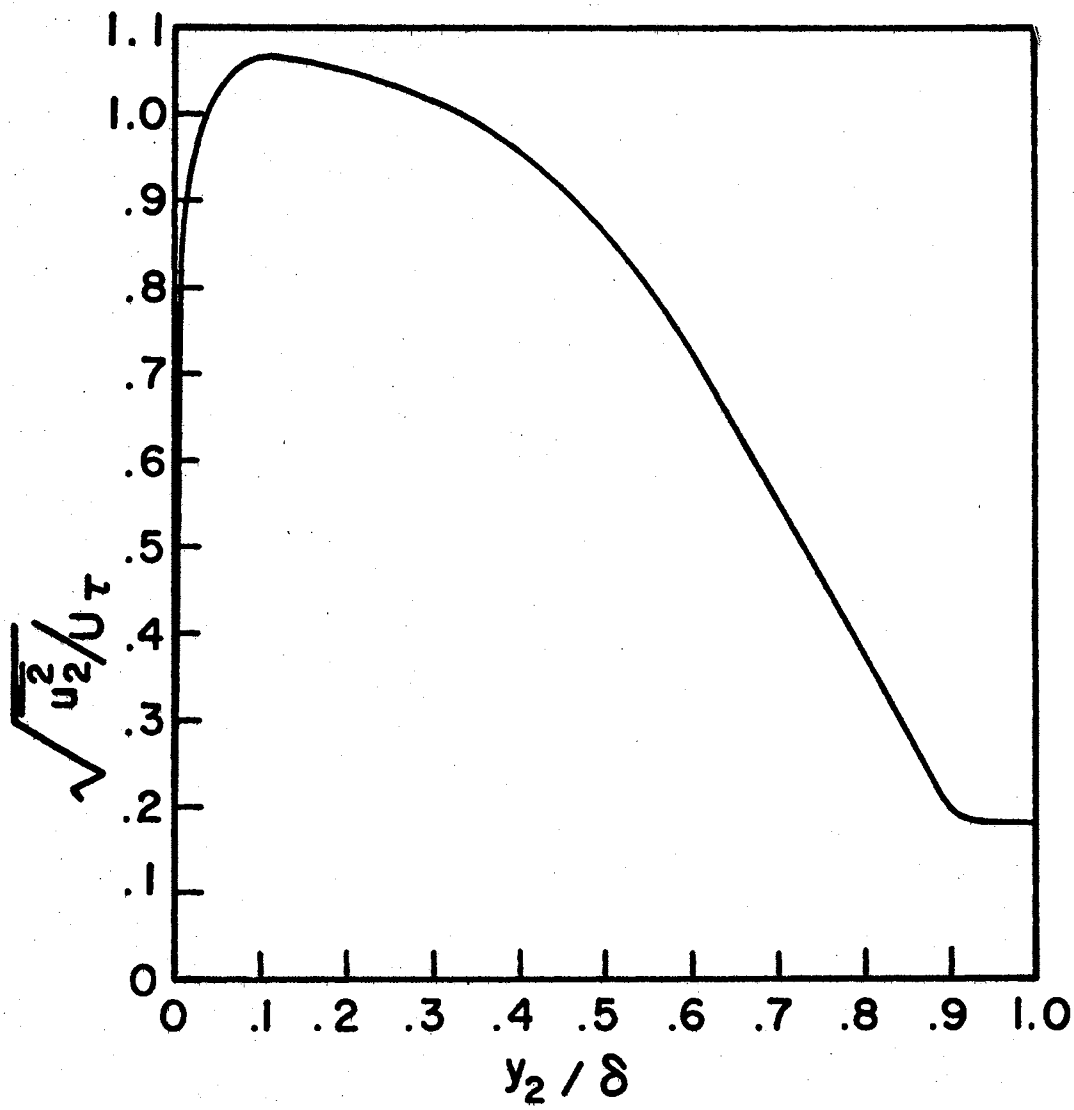

Figure 6. Velocity Intensity, $\sqrt{\overline{u_2}^2}/U_\tau$. $0 \leq y_2/\delta \leq 1.0$. Model of Klebanoff's (1954) Data Scaled With δ Determined From 'Law of Wall and Wake'.

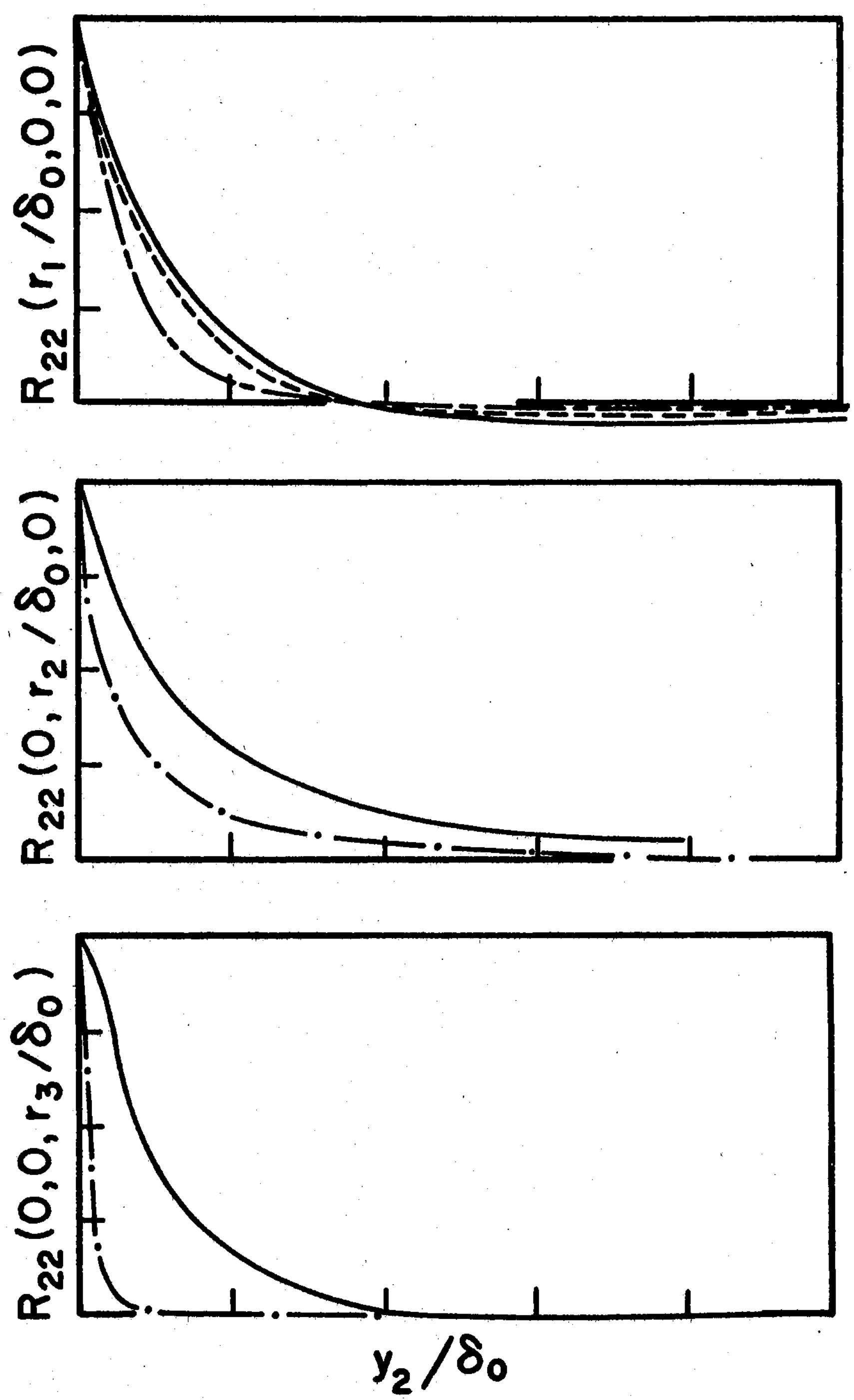

Figure 7. Measured Velocity Correlation Components, Grant (1958). ——— $y_2/\delta_0 = .66$, – – – – $y_2/\delta_0 = .25$, — —— $y_2/\delta_0 = .13$, ·——· $y_2/\delta_0 = .056$. $\delta_0/\delta = .69$.

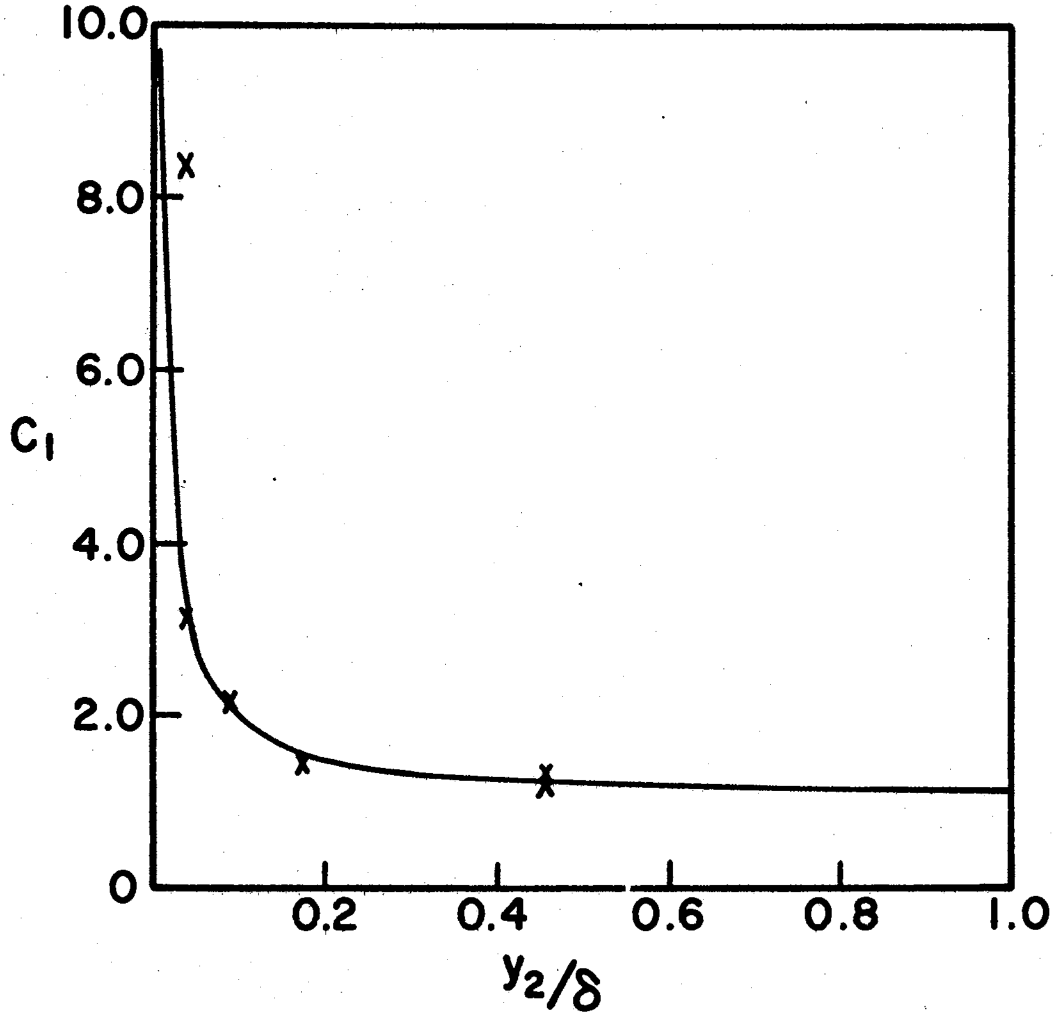

Figure 8. The Variation of the Inverse of the Integral Scale $C_1 (y_2/\delta)$ Across the Boundary Layer. × Values of C_1 Determined by Curve Fit to Grant's (1958) Data. ——— Curve Fit to Values of C_1, $C_1 = 1 + .111/(.748 \cdot 10^{-7} + y_2/\delta)^{.937}$.

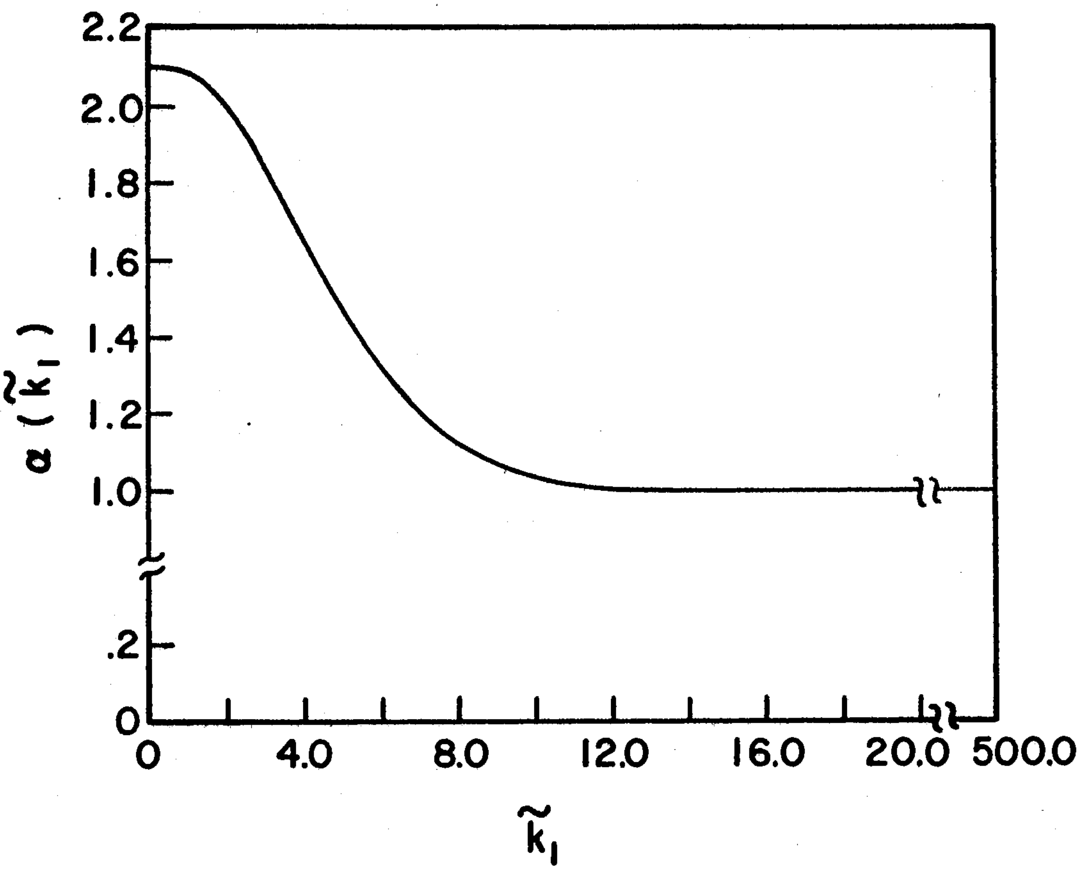

Figure 9. The Variation of the Scale Anisotropy Factor With Streamwise Wave Number, $\alpha(\tilde{k}_1)$. $\hat{k}_1 = \tilde{k}_1 \delta^*/\delta$ Where $\delta^*/\delta = .145$.

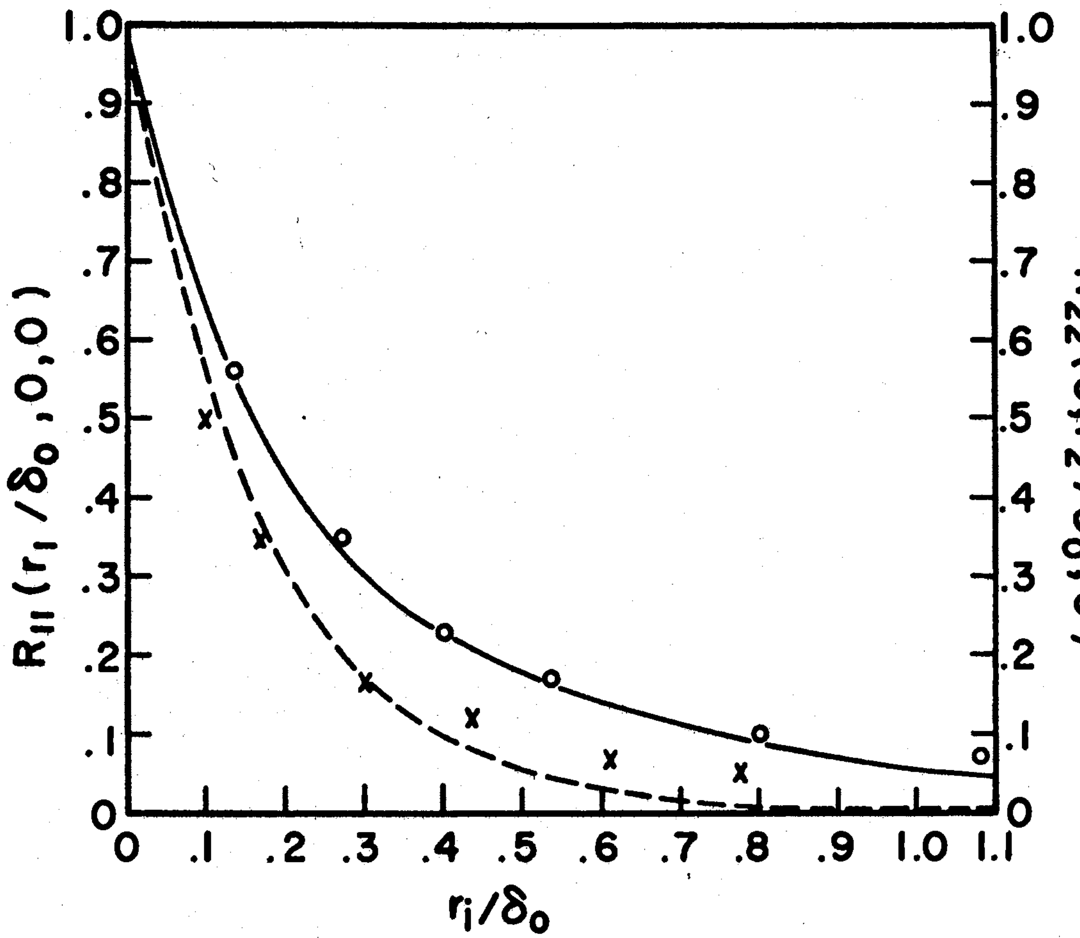

Figure 10. Comparison of Measured and Theoretical Values of Velocity Correlation of R_{11} and R_{22}. ○ $R_{11}(r_1/\delta_0, 0, 0)$ and × $R_{22}(0, r_2/\delta_0, 0)$, Grant (1958). ——— $\widetilde{R}_{11}(r_1/\delta_0, 0, 0)$; – – – – $\hat{R}_{22}(0, r_2/\delta_0, 0)$. $y_2/\delta = .45$ for Computed and Measured Data.

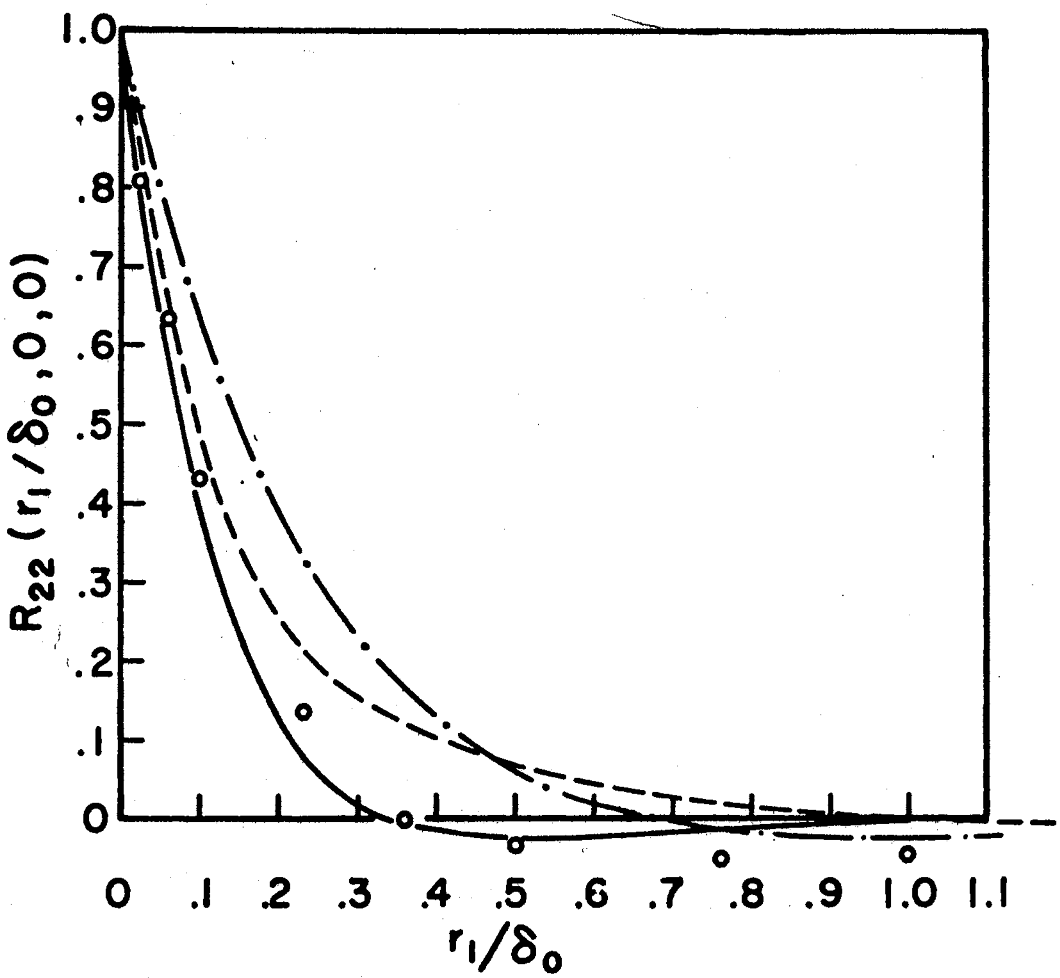

Figure 11. Comparison of Measured and Theoretical Values of Velocity Correlation Components of R_{22}.
o $R_{22}(r_1/\delta_0,0,0)$, Grant (1958).
——— $\hat{R}_{22}(r_1/\delta_0,0,0;\alpha)$, $\alpha = 1.0$.
·——· $\hat{R}_{22}(r_1/\delta_0,0,0;\alpha)$, $\alpha = 2.0$.
— — — $R_{22}(r_1/\delta_0,0,0)$, Variable α.
$y_2/\delta = .45$ for Computed and Measured Data.

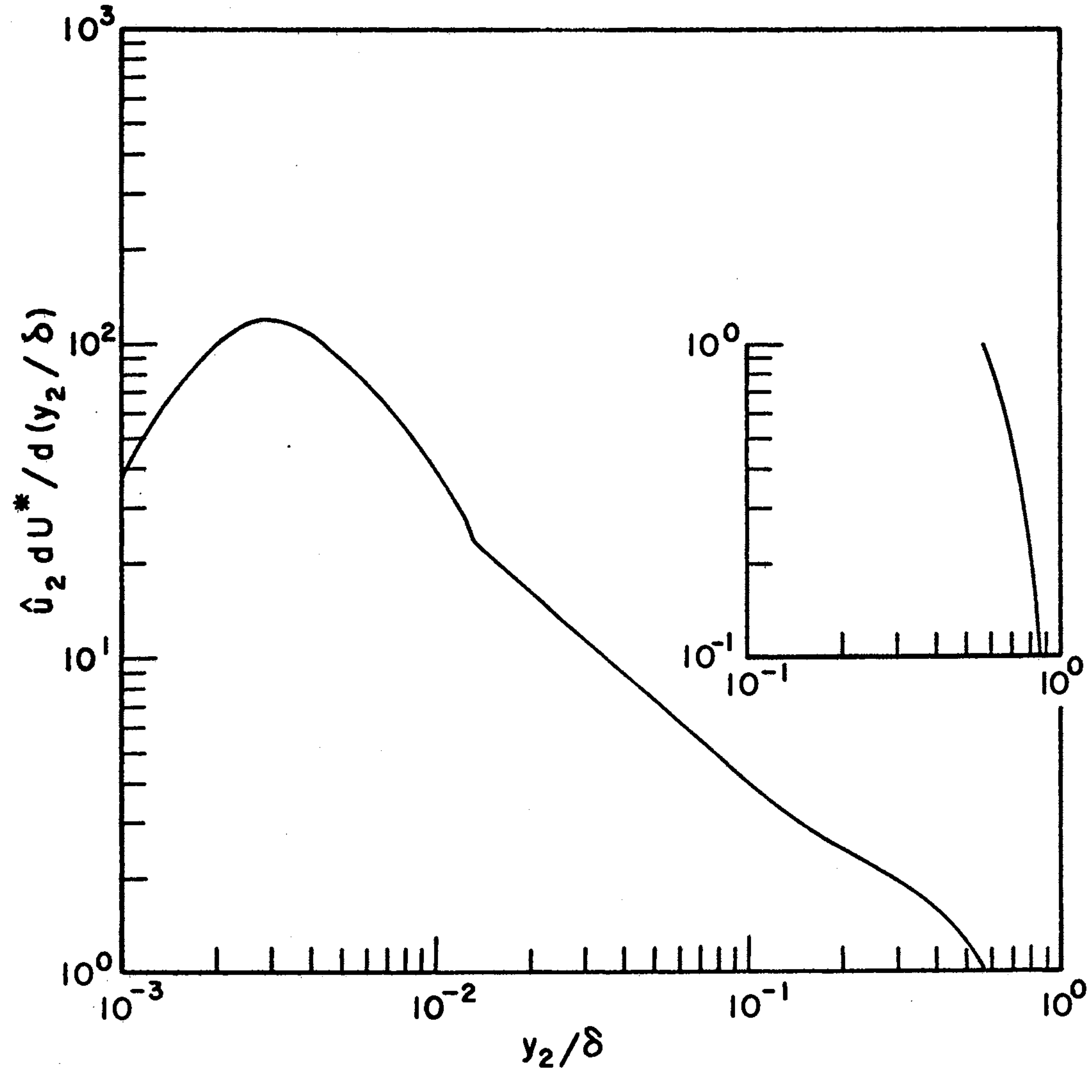

Figure 12. Shear Gradient, Velocity Intensity Variation Across the Boundary Layer. $\tilde{y}_2 = y_2/\delta = \hat{y}_2 \delta^*/\delta$ Where $\delta^*/\delta = .145$.

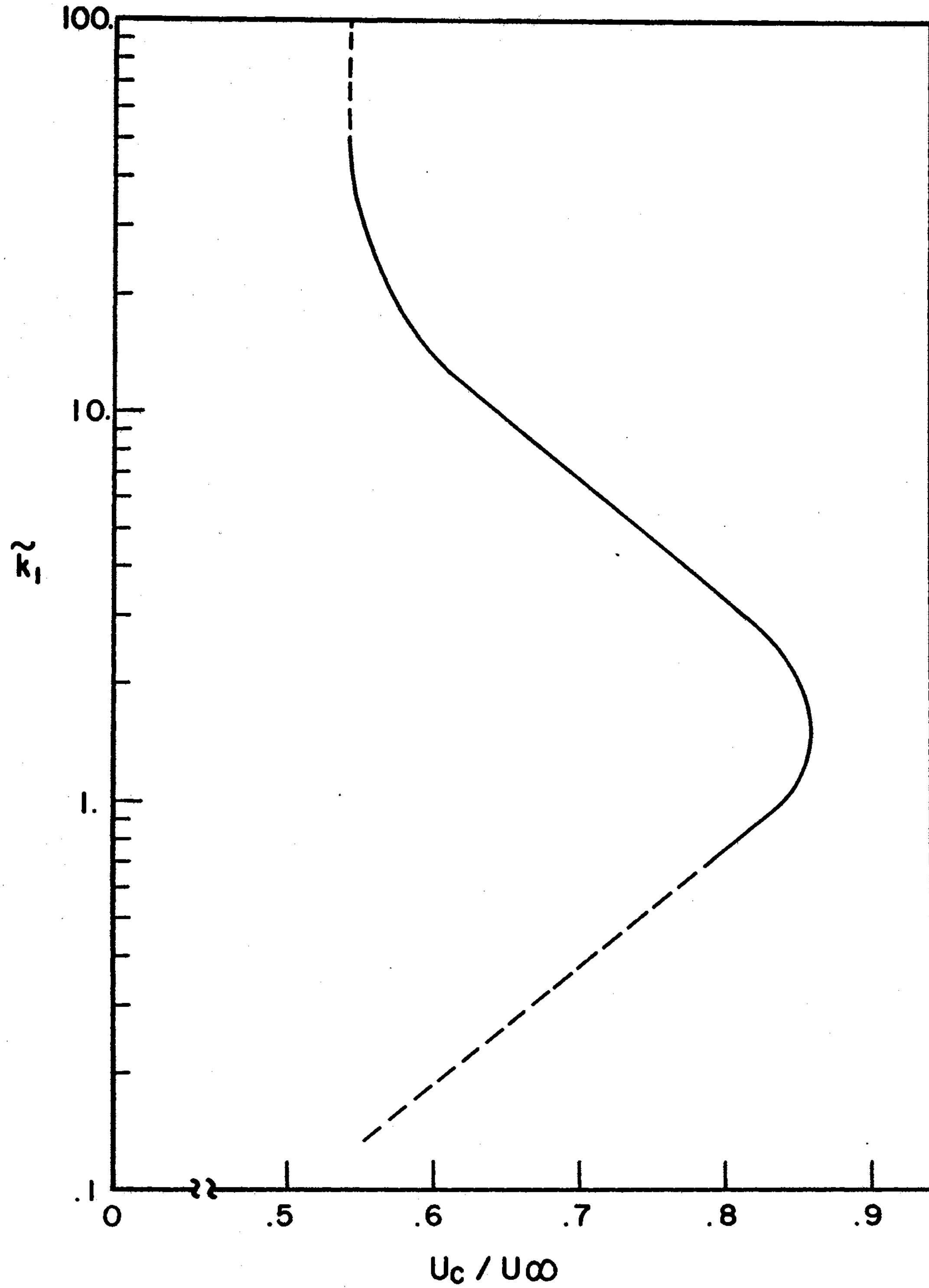

Figure 13. Convective Velocity, $U_c(\tilde{k}_1)/U_\infty$. ———— Wills' (1970) Data. — — — — Extrapolation of Wills' Data. $Re_{\delta^*} = 13.5 \cdot 10^3$.

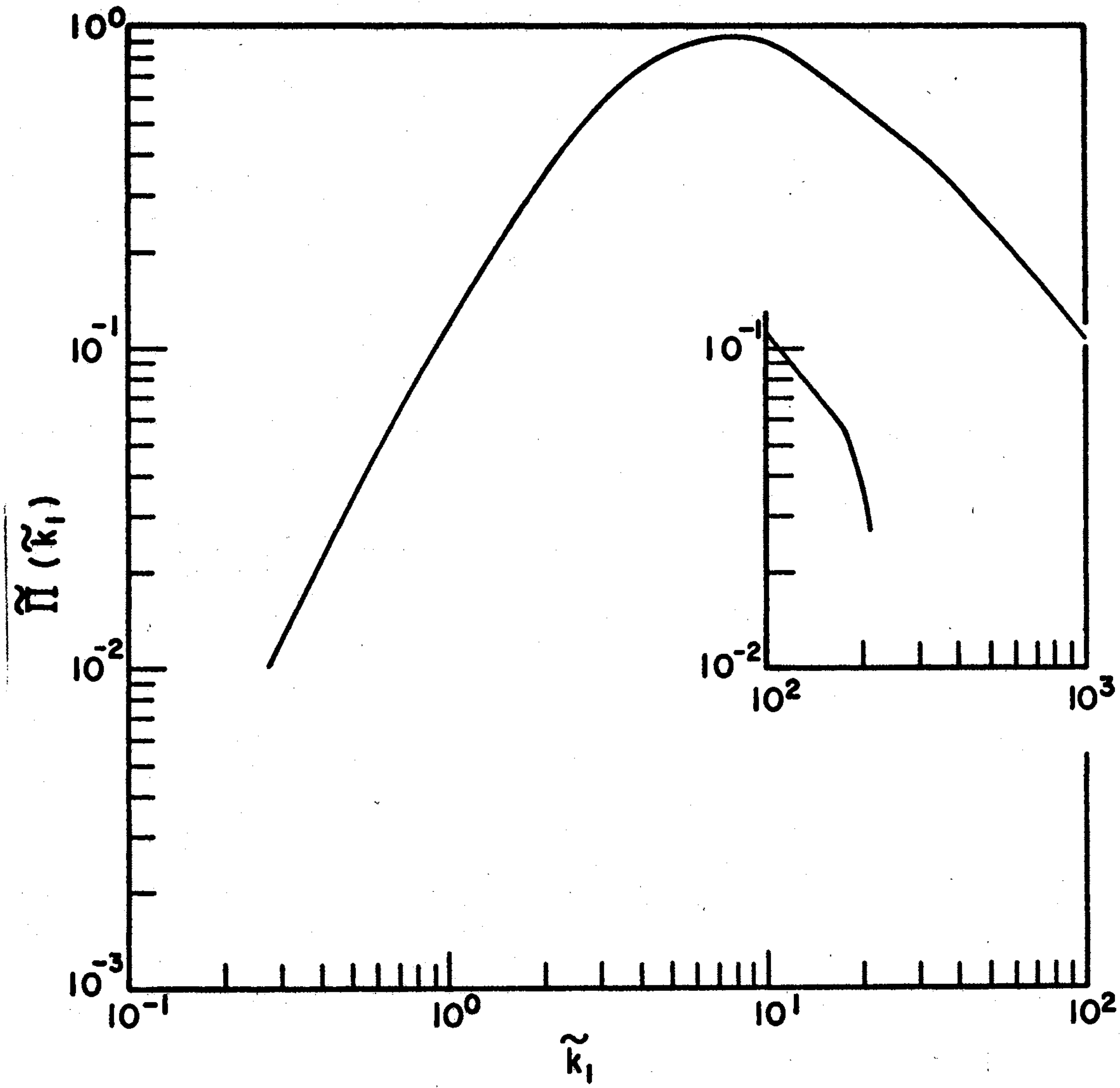

Figure 14. Computed Wave Number Spectrum. α = 1.0.

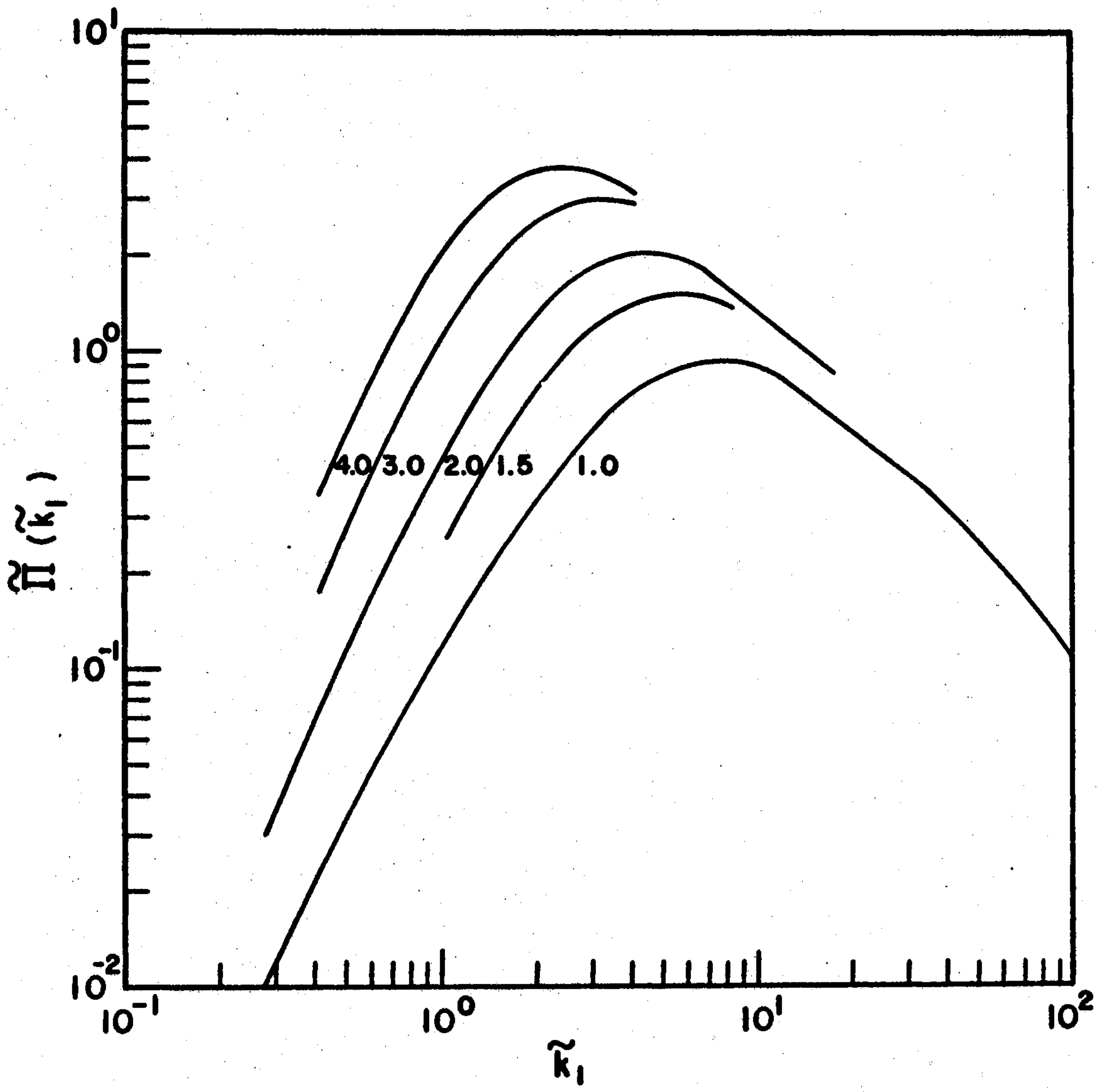

Figure 15. Computed Wave Number Spectra. α = 1.0, 1.5, 2.0, 3.0, 4.0.

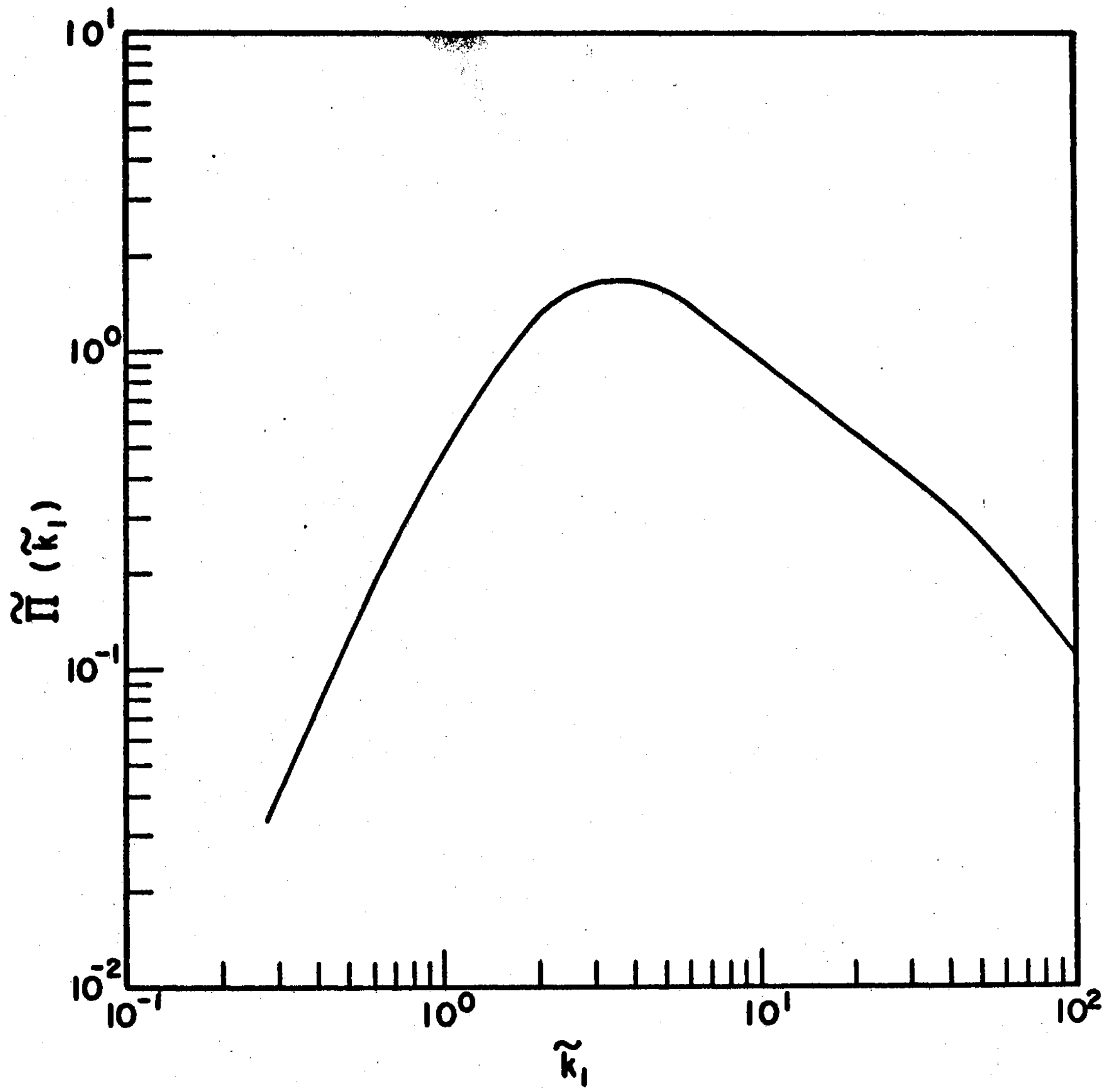

Figure 16. Computed Wave Number Spectrum. $\alpha = \alpha(\tilde{k}_1)$.

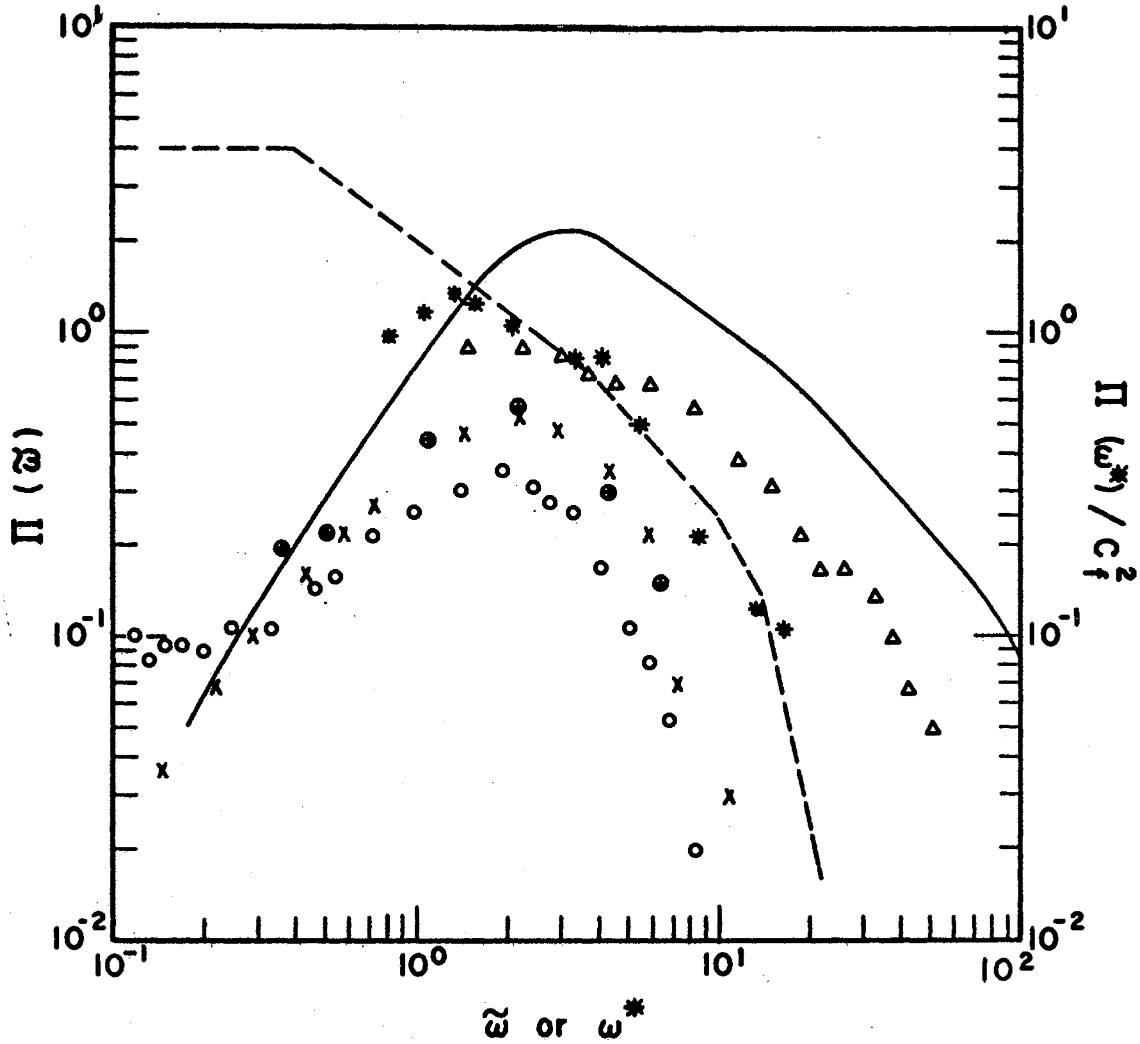

Figure 17. Comparison of Computed and Measured Frequency Spectra. On the $\Pi(\tilde{\omega})$ vs. $\tilde{\omega}$ Scale: —— Theory $Re_\delta = 9.9 \cdot 10^3$; ○ $Re_{\delta^*} = 4.2 \cdot 10^3$, $d/\delta^* = 3.18$, ⊕ $Re_{\delta^*} = 6.6 \cdot 10^3$, $d/\delta^* = 2.06$, Panton, et al. (1971); × $Re_{\delta^*} = 8 \cdot 10^3$, $d/\delta^* = 2.93$, Hodgson (1962); * $Re_{\delta^*} = 13.5 \cdot 10^3$, $d/\delta^* = 1.33$, Δ $Re_{\delta^*} = 81.5 \cdot 10^3$, $d/\delta^* = .22$, Serafini (1963). On the $\Pi(\hat{\omega})/C_f^2$ vs. $\hat{\omega}$ Scale: — — — $Re_{\delta^*} = 1.8 \cdot 10^3$, $d/\delta^* = .147$, Outline of Hodgson's Wind Tunnel Data (Private Communication). Note: $\Pi(\tilde{\omega})$ Scale, $\Pi = [U_\infty/U_c(\tilde{k}_1)]\,\tilde{\Pi}(U_\infty\tilde{\omega}/U_c(\tilde{k}_1))$; $\Pi(\omega^*)/C_f^2$ Scale, $\Pi = \overline{p^2}(\omega)U_\infty/\delta^* q^2$.

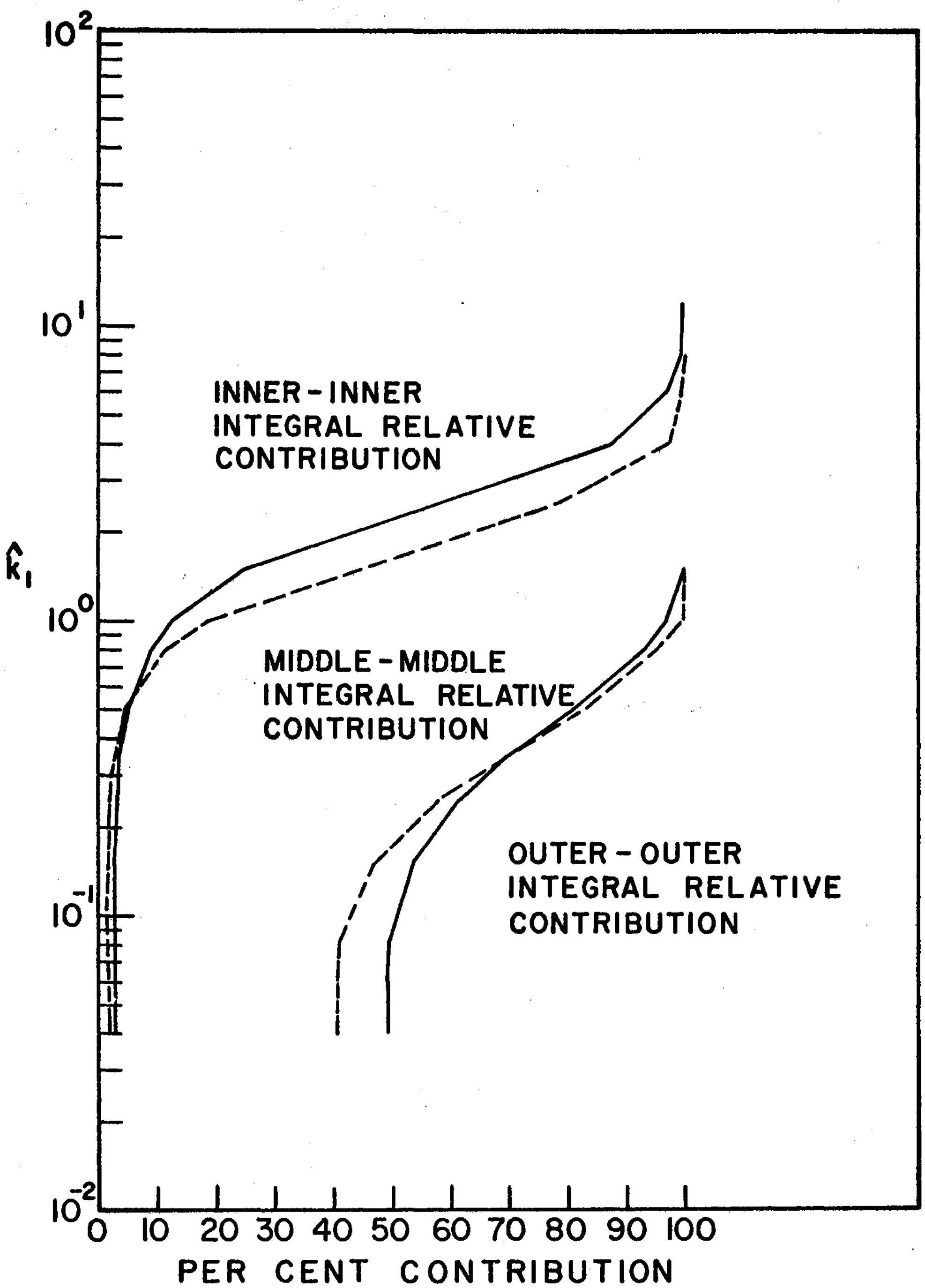

Figure 18. Computed Relative Regional Contributions to the Wave Spectra as a Function of Wave Number. $\alpha = 1.0$, $\alpha = 2.0$. Inner-inner Integral Region: $0 \leq y_2/\delta \leq .025$. Middle-middle Integral Region: $.025 < y_2/\delta < .20$. Outer-outer Integral Region: $.20 \leq y_2/\delta \leq 1.0$. $\tilde{k}_1 = \hat{k}_1 \delta/\delta^*$ Where $\delta/\delta^* = 6.9$.

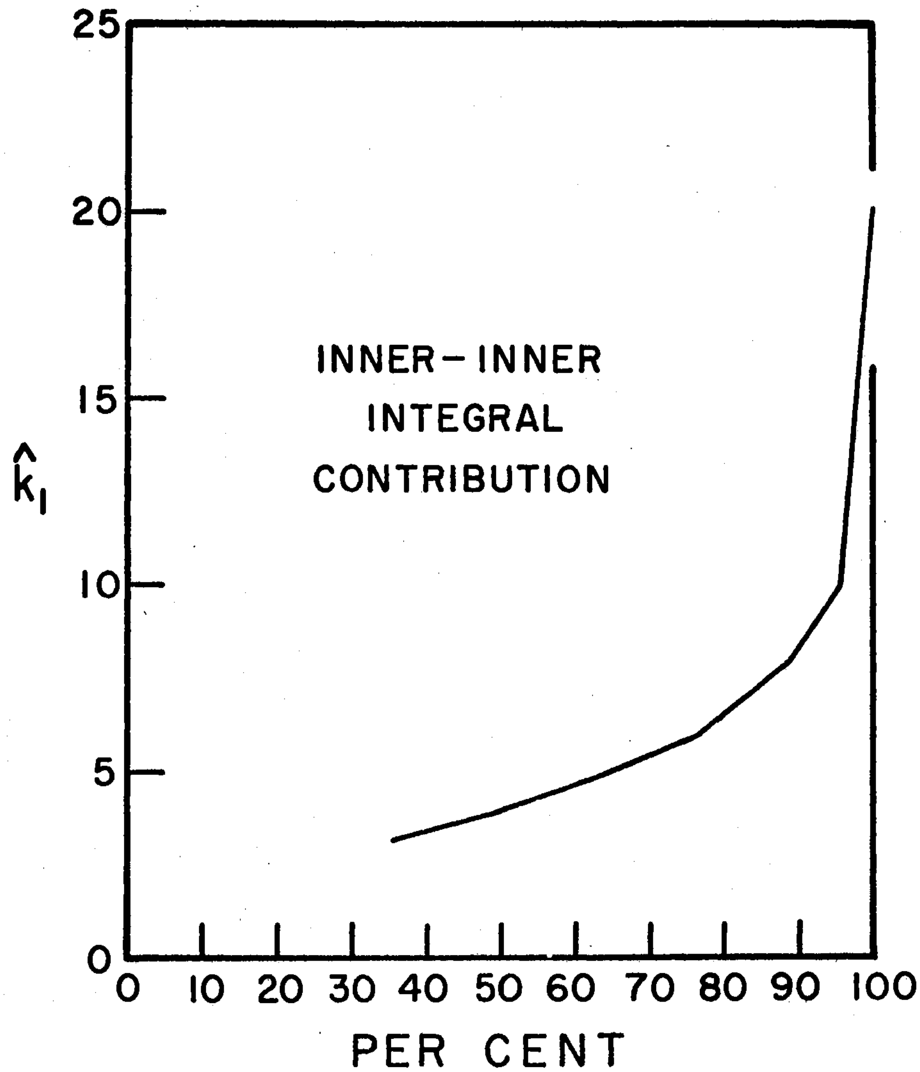

Figure 19. The Inner-inner Region Integral Contribution to the Wave Number Spectrum as a Function of Wave Number. $\alpha = 1.0$. $\tilde{k}_1 = \hat{k}_1 \delta/\delta^*$ Where $\delta/\delta^* = 6.9$.

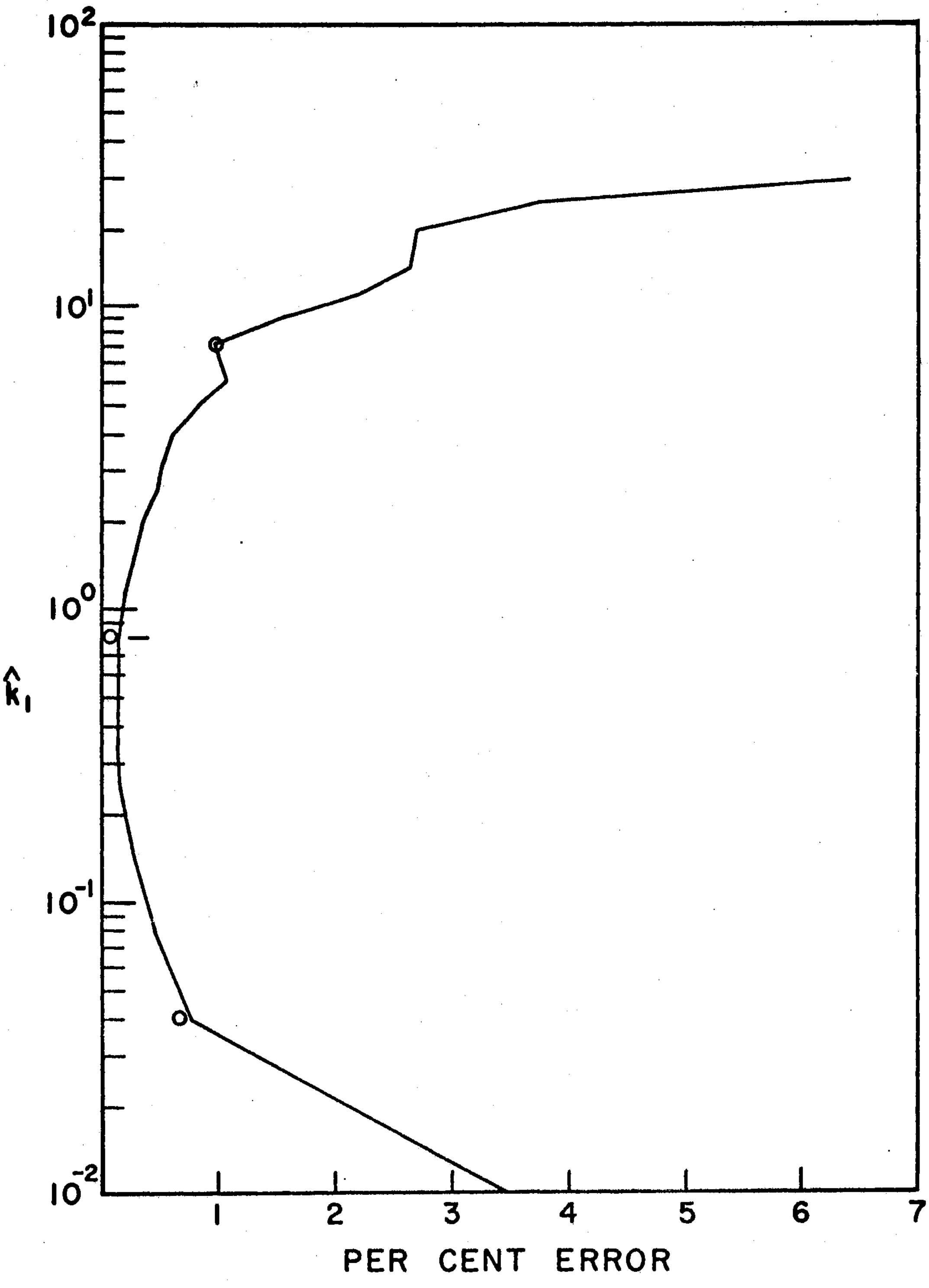

Figure 20. The Monte Carlo Integration Program Statistical Error. $\alpha = 1.0$. ——— Predicted Standard Deviation for 5000 Iterations. o Computed Standard Deviation for 5000 Iterations.

VITA

John H. Linebarger

Candidate for the Degree of

Doctor of Philosophy

Thesis: COMPUTATION OF THE SPECTRA OF TURBULENT BOUNDARY LAYER SURFACE-PRESSURE FLUCTUATIONS

Major Field: Mechanical Engineering

Biographical:

Personal Data: Born in Clarion, Iowa, March 9, 1932, the son of Mr. and Mrs. Warren W. Linebarger.

Education: Graduated from Storm Lake High School, Storm Lake, Iowa in May, 1950; attended Buena Vista College in 1950 and 1951; received the Bachelor of Science degree from the United States Naval Academy in June, 1955, with a major in Engineering; received the Master of Science degree from the Massachusetts Institute of Technology in June, 1961, with a major in Aeronautics and Astronautics; completed the requirements for the Doctor of Philosophy degree at Oklahoma State University in May, 1972.

Professional Experience: Jet Fighter Pilot, U. S. Air Force, 1957-59; Project Officer, High Altitude Vehicle Test Section, Eglin AFB, Florida, 1961; Project Officer, Skybolt Missile System, Eglin AFB, Florida, 1962; Project Officer, Gemini Project Office, NASA Manned Spacecraft Center, Houston, Texas, 1963-65; Assistant Professor of Engineering, LeTourneau College, Longview, Texas, 1965-67.